University of Alberta

Sedimentology, diagenesis, and dolomitization of the Brac Formation (Lower Oligocene), Cayman Brac, British West Indies

by

Breanna Corynne Uzelman

A thesis submitted to the Faculty of Graduate Studies and Research
in partial fulfillment of the requirements for the degree of

Master of Science

Department of Earth & Atmospheric Sciences

Fall 2009
Edmonton, Alberta

Examining Committee

Dr. Brian Jones, Earth & Atmospheric Sciences

Dr. Karlis Muehlenbachs, Earth & Atmospheric Sciences

Dr. George Ball, Biological Sciences

ABSTRACT

The Oligocene Brac Formation is the oldest part of the Bluff Group that is exposed on Cayman Brac. Sediments of the Brac Formation were deposited on a small, open bank in shallow marine waters. Today, the formation is composed of limestone, finely crystalline dolostone, and coarsely crystalline sucrosic dolostone. The Pollard Bay member, defined herein, comprises the sucrosic dolomite that is exposed only on the south coast of Cayman Brac. Changes in sea level and subsequent groundwater chemistry mediated a complex diagenetic evolution that is responsible for the lithological heterogeneity that now characterizes the formation. Field, petrographic, and geochemical analyses indicate that dolomitization was probably mediated by normal to slightly modified seawater. Multiphase dolomite crystals represent different stages of textural and geochemical maturity, and attest to time-transgressive dolomitization processes that evolved in various hydrologic regimes through time.

Acknowledgements

I am indebted to so many people for their assistance in this enormous undertaking. First and foremost, I would sincerely like to thank my supervisor, Dr. Brian Jones, without whom this project would never have been possible. His undeterred patience, encouragement, professionalism, wisdom, and tireless editing skills are most certainly to credit for the evolution of this thesis into a finished product. It has also been a pleasure to get to know and work with various members of the carbonate research group – Alex MacNeil, Sandy Bonny, Rachel Day, Hilary Corlett, Dustin Rainey, and Hongwen Zhao. I hope I've lived up to the high academic standard and camaraderie set by this ever-rotating cast of characters. I would also like to express my gratitude to Dr. Karlis Muehlenbachs for allowing me to run countless isotope samples in his lab and for his valuable feedback on their significance. Hendrik van Genderen of the Cayman Islands Water Authority is thanked for his help collecting samples in the field, and I would like to acknowledge NSERC for the financial support of this project.

My love and appreciation go out to my family – Mom, Dad, Amanda, and CJ – for your constant belief in me coupled with occasional nagging. This thesis would have been a lot more daunting without such a strong support network behind me. Tracye and Mike Davies also deserve much gratitude for allowing their family to become my extended family in Edmonton. Without them, I wouldn't have honed my knitting skills and sarcasm to such a fine degree, nor gone trekking in Nepal for my "Congratulations on finishing your thesis… *almost*" trip. Next, I hope they can teach me about punctuality.

No one deserves more gratitude than James Scott for his limitless understanding, highbrow taste in music, and for being my most ardent supporter through all pursuits, scientific and otherwise. Justin Dodd is sincerely thanked for the lessons in life, for initiating my unabating photography habit, and for the occasional soapbox discourse on stable isotope geochemistry. I have learned and grown so much from knowing both of you.

My colourful group of office mates in the off-brown walls of Tory 3-4 helped to make our mutual internment as enjoyable as possible. I'm very fortunate to have been surrounded by the flawlessly cynical group of Mike and Tracye Davies, Simon Robinson, Melissa Bowerman, Michael Lawson (whose duration was short but legacy is eternal), Sandra Correa, Kristen Kennedy, Katie Smart, and Gideon Lambiv. Roy Coulthard in particular deserves acknowledgement for spending more time inside the walls of that office than most people formally assigned to it. I'd also like to credit the other exceptional people I've had the opportunity to meet through this department, friends who have come and gone but ultimately left an indelible impression. Finally, thanks to the good friends I've made in Calgary – especially Ali Jaafar, Becky Rogala, and Tom Hamilton – who have provided much-needed encouragement and patiently listened to my endless stream of consciousness iterating on "it's almost done – just one more thing." This thesis is undoubtedly the culmination of support I've received from so many people over its duration. Thank you; it hasn't gone unnoticed.

Table of Contents

List of Tables

List of Figures

Chapter One:
Introduction

1.1 Introduction

Caribbean islands have long been recognized as optimal study sites to derive the mode of formation and diagenetic evolution of isolated carbonate systems. The highly altered Tertiary strata of the Cayman Islands are well suited to such investigations because they are geologically young and geographically isolated by surrounding ocean waters. Cayman Brac is a small Caribbean island with an exposed succession of Oligocene to Pleistocene carbonate bank deposits. The Tertiary Bluff Group is composed of the Brac Formation (Lower Oligocene), Cayman Formation (Middle Miocene), and Pedro Castle Formation (Pliocene). These stratigraphic units, distinguished by regional unconformities, form the core of the Cayman Islands (Jones *et al.*, 1994b). The Ironshore Formation (Late Pleistocene) unconformably overlies and onlaps the Bluff Group.

In this study, the depositional and diagenetic features of the Brac Formation on Cayman Brac are examined and interpreted, and it is proposed herein that the existing stratigraphic architecture be revised to reflect the results of this investigation. Strata of the Brac Formation are lithologically unique from overlying units due to their distinctive diagenetic textures – particularly those caused by dolomitization. The irregular geometry and petrography of the Brac Formation distinguishes it from previously described formations in the Bluff Group, and provides an opportunity to further delineate the stratigraphic variability of the Cayman Islands. The purpose of this research is to identify the depositional textures, faunal assemblages, facies architecture, and stages and types of diagenesis in the Brac Formation. These data will be assembled from petrographic, geochemical, and field studies, and then integrated to characterize the geology of the Brac Formation on Cayman Brac.

1.2 Geologic and Geographic Setting

1.2.1 Location and Physiography

The Cayman Islands are an overseas territory of the United Kingdom, located approximately 240 km south of Cuba and 290 km northwest of Jamaica in the western Caribbean Sea (Fig. 1.1). George Town, the country's capital, is located on the western shore of Grand Cayman, the largest island. Cayman Brac and Little Cayman (sometimes called the "Sister Islands" due to their small size) are approximately 130 km northeast of Grand Cayman. Although Cayman Brac lies only 7 km east of Little Cayman, water depths of 900 m separate the islands (Horsfield, 1975).

Cayman Brac (19°43' N, 79°48' W) has a surface area of 36 km^2 and trends in a northeast-southwest direction. The island is 20 km long with a maximum width of 3 km. Cayman Brac boasts the greatest elevation of the Cayman Islands, rising from sea level at its western end to a maximum height of 43 m at its eastern end. Cayman Brac is named after the Gaelic word for "bluff", referring to the island's elevated core that terminates in a sheer cliff face at the east end. Many caves are carved into the bluff around the perimeter of the island; speleothem development is variable and most caves extend no more than 50 m inland from the cliff face (Tarhule-Lips and Ford, 1998). A horizontal marine erosional notch, approximately 6 m above sea level, encircles most of the island (Woodroffe *et al.*, 1983).

Bedrock geology exerts a strong influence on Caymanian topography. Coastline geomorphology on Cayman Brac is typified by nearly vertical cliffs and narrow, fringing coastal plains. The dramatic bluff landscape is composed almost entirely of highly indurated, dolomitic strata. Shorelines are composed of friable

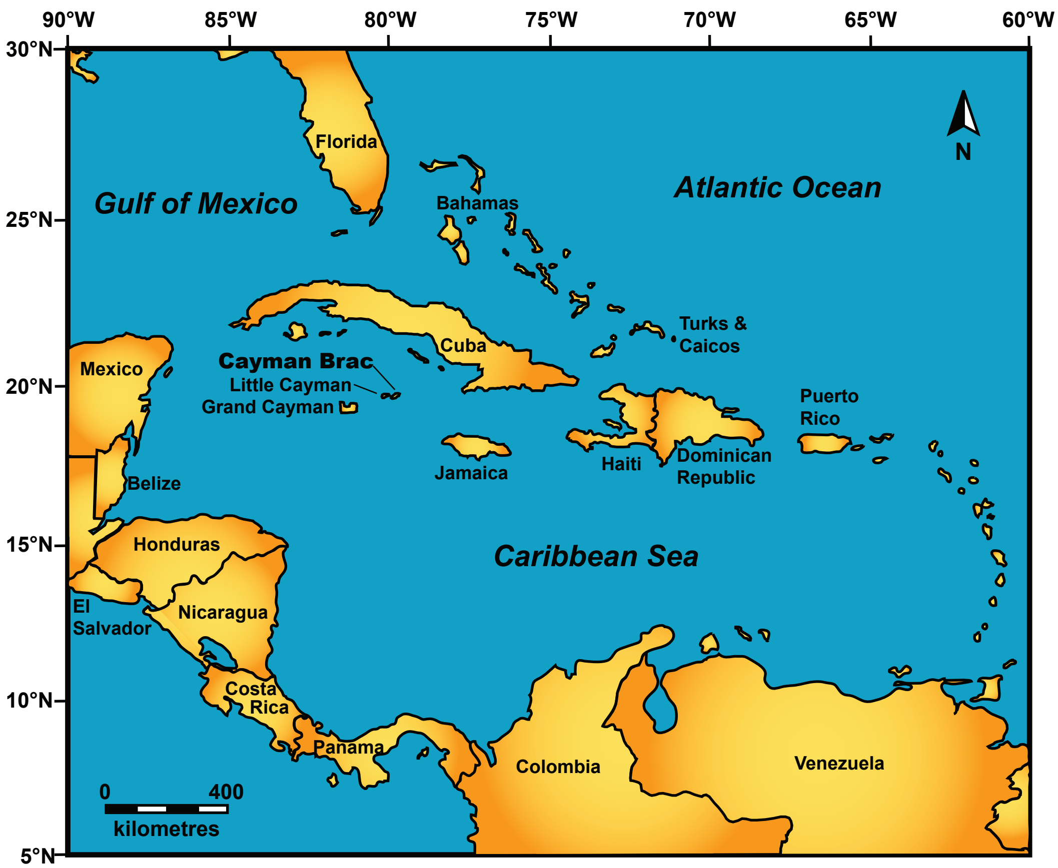

Figure 1.1 Map of the Caribbean area showing the location of the Cayman Islands.

limestone and display subdued karst topography. Sandy carbonate beaches are restricted in area. Exposed rock surfaces are extensively weathered and outcrop can be difficult to access due to its steep-sided nature. Dense, semi-tropical woodland vegetation is rooted in thin terra rossa soils, which overlie sharp phytokarst on most of the island. Shallow salt ponds and marshy wetlands occupy low-lying areas on the western end of the island and provide nesting areas for many tropical bird species. There is no overland runoff on Cayman Brac because precipitation quickly infiltrates the porous bedrock.

The Cayman Islands are renowned as one of the best diving sites in the Caribbean due to the flourishing marine biota and spectacular shelf-edge "walls" around the islands. A fringing reef complex surrounds most of Cayman Brac, but lagoons are rare (Fenner, 1993). On the southwestern shore, however, a small lagoon is enclosed by a boulder rampart. This biodetrital deposit (<5 m depth) is a former reef crest dominated by *Acropora palmata* that formed along the windward margin (Manfrino *et al.*, 2003). Hurricane destruction to Caymanian reefs destroys coral frameworks and deposits storm rubble structures in their place (Blanchon *et al.*, 1997; Riegl, 2001). Two seaward-sloping submarine terraces (8-15 m and 15-20 m depth), divided in most places by a mid-shelf escarpment, surround the Cayman Islands (Rigby and Roberts, 1976; Blanchon and Jones, 1995; Manfrino *et al.*, 2003).

A subhumid, tropical climate moderated by the Northeast Trade Wind System regulates the Cayman Islands, yielding an average annual temperature of 27°C. Rainfall varies seasonally and spatially, with western locations typically receiving more precipitation (Jones *et al.*, 1997). Easterly trade winds prevail during the wet season (May to November), bringing higher temperatures and the risk of hurricanes. Lower temperatures and winds from the northeast to northwest dominate during the dry season (December to April). The Cayman Islands are recovering from major damage caused by Hurricane Ivan in 2004 and Hurricane Gustav in 2008.

1.2.2 Tectonic Setting

The Cayman Islands are emergent carbonate pinnacles situated upon the Cayman Ridge, a submarine rise that extends east-northeast across the Caribbean, from the Sierra Maestra of southeastern Cuba to the Misteriosa Bank off the Gulf of Honduras (Fig. 1.2). Located along the southern margin of the North American Plate, the Cayman Ridge is an uplifted fault block (Fahlquist and Davies, 1971) that formed in a Late Mesozoic to Early Cenozoic island-arc setting (Holcombe *et al.*, 1990). The ridge crest varies in depth from 0 to 3000 m below sea level, and its width ranges from 50 to 80 km. A composite stratigraphy assembled from dredge samples indicates that the Cayman Ridge is composed of a granodiorite foundation overlain by volcanics and capped by carbonate rocks (Perfit and Heezen, 1978; Holcombe *et al.*, 1990). The total thickness of the carbonate succession is unknown, but drilling indicates a minimum depth of 401 m (Emery and Milliman, 1980). Independent tectonic movement experienced by the Cayman Islands implies that each may be positioned on a separate fault block extending above the general elevation of the ridge (Matley, 1926; Horsfield, 1975).

The Cayman Trough (historically named the “Bartlett Trough”) is a narrow, slow-spreading ocean basin bounded by the Cayman Ridge to the north and the Nicaraguan Plateau to the south. With a length of 1200 km, width of 100 km, and reaching depths in excess of 6800 m (Ladd *et al.*, 1990), the Cayman Trough is the deepest feature in the Caribbean Sea (ten Brink *et al.*, 2002). The Mid-Cayman Rise, a 100 km-long active spreading center, bisects the Cayman Trough at 82°W. Left-lateral, strike-slip motion of the North American Plate relative to the Caribbean Plate is accommodated by two offset transform faults:

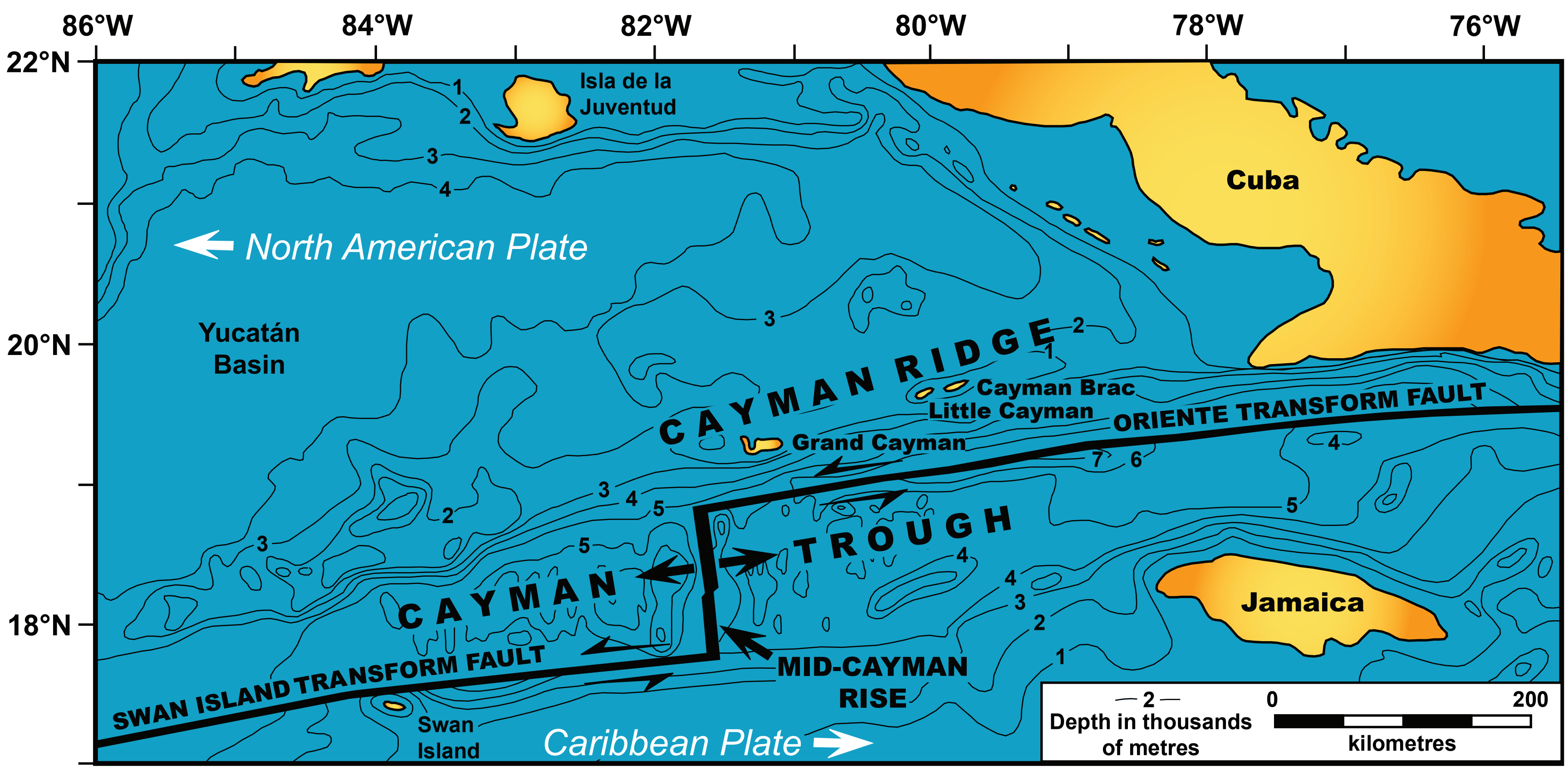

Figure 1.2 Tectonic and bathymetric setting of the northwestern Caribbean showing the location of the Cayman Islands on the Cayman Ridge. Modified from Perfit and Heezen (1978) and MacDonald and Holcombe (1978).

the Oriente Transform Fault to the east of the Mid-Cayman Rise and the Swan Island Transform Fault to its west (MacDonald and Holcombe, 1978). Opening of the Cayman Trough may have begun during the Eocene (Perfit and Heezen, 1978). GPS measurements record a plate motion rate of 20 mm/yr in a direction 070° (Dixon *et al.*, 1998). Crustal thickness varies appreciably along the Cayman Trough; the thinnest oceanic crust (2–3 km) is located proximal to the Mid-Cayman Rise and thickens distally to 7–8 km at the far ends of the trough (ten Brink *et al.*, 2002).

1.3 Stratigraphic Framework of the Cayman Islands

1.3.1 Development of Stratigraphic Nomenclature

The geology of the Cayman Islands was first documented by Matley (1924a, b, 1925a, b, 1926), who conducted a detailed reconnaissance survey for the British government. Based on his investigation, Matley (1926) assigned the name Bluff Limestone to the massive, crystalline, cliff-forming carbonate that makes up the core of the islands. Samples of *Lepidocyclina* (a benthic foraminifer) limestone were sent to T.W. Vaughan for identification, and a Middle Oligocene (Rupelian) age was assigned to the strata (Matley, 1926; Vaughan, 1926). The Pleistocene Ironshore Formation was named after a local term for the rocky limestone shoreline that surrounds the central carbonate platform (Matley, 1926). Subsequent geological investigations (Jones *et al.*, 1984; Jones and Hunter, 1989; Jones *et al.*, 1989; Pleydell *et al.*, 1990) revealed that most of the Bluff Limestone is actually formed of dolostone. In order to remove the lithological connotation, Jones and Hunter (1989) proposed that the succession be called the Bluff Formation. A type section was designated from a quarry near Pedro Castle on Grand Cayman, and the Bluff Formation was divided into the Cayman Member and Pedro Castle Member (Jones and Hunter, 1989).

Caymanian stratigraphy was further refined in 1994 following extensive outcrop analysis on Cayman Brac (Jones *et al.*, 1994a, 1994b). The Brac Formation was defined as the basal 33 m of the succession exposed on the bluff at the east end of the island. It was distinguished from the overlying Cayman Formation by a change in lithology and truncation by an unconformity dipping 0.5° to the southwest (Jones *et al.*, 1994a). The Bluff Formation was successively promoted to group status, with stratigraphic members including the Brac Formation, Cayman Formation, and Pedro Castle Formation (Jones *et al.*, 1994b). Lithological variations and age gaps between the three unconformity-bounded packages of the Bluff Group justify their elevation to formational status. Overall, the succession represents prolonged periods of submarine deposition followed by episodes of emergence and erosion (Jones *et al.*, 1994a).

The Tertiary strata of the Bluff Group are correlative with carbonate successions on neighbouring Caribbean islands. The Brac Formation can be correlated with the San Sebastian Formation of Puerto Rico, the Tinguaro Formation of Cuba, and the Brownstone Formation of Jamaica (Jones *et al.*, 1994a). Erosional unconformities bounding the individual formations of the Bluff Group represent sequence boundaries that developed during eustatic sea level lowstands (Jones and Hunter, 1994a, 1994b).

1.3.2 Present Stratigraphic Architecture

To date, the carbonate succession identified on the Cayman Islands includes the Lower Oligocene Brac Formation, the Middle Miocene Cayman Formation, the Pliocene Pedro Castle Formation, and the onlapping Late Pleistocene Ironshore Formation (Fig. 1.3). Regional unconformities representing eustatic drops in sea level separate the formations (Jones and Hunter, 1994a); however, these erosional contacts are relatively obscure due to the poorly bedded

AGE	LITHOTYPE	UNIT	LITHOLOGY	FAUNA	FOSSIL PRESERVATION
Hol.		Unconformity	Swamp deposits, storm deposits		
Pleist.		IRONSHORE FORMATION Unconformity	Limestone	Corals (VC) Bivalves (VC) Gastropods (C)	Well preserved, shells aragonitic, minor leaching
Plio.		BLUFF GROUP: PEDRO CASTLE FORMATION Cayman Unconformity	Dolostone (fabric retentive) and limestone	Forams (VC) Corals (C) Bivalves (LC) Gastropods (C) Red algae (C) Halimeda (R)	Aragonitic shells leached; other fossils well preserved
M. Mio.		BLUFF GROUP: CAYMAN FORMATION Brac-Cayman Unconformity	Dolostone (fabric retentive)	Corals (VC) Bivalves (LC) Rhodolites (LC) Gastropods (R) Forams (LC) Halimeda (R)	Aragonitic shells leached; other fossils dolomitized
L. Olig.		BLUFF GROUP: BRAC FORMATION	Limestone, partly dolomitized limestone (fabric retentive) and sucrosic dolostone (fabric destructive)	Forams (VC) Red algae (VC) Bivalves (LC) Gastropods (LC) Corals (LC) Halimeda (R)	Aragonitic shells leached; variable preservation in dolostones; good preservation in limestones

VC = very common; C = common; LC = locally common; R = rare

Figure 1.3 Stratigraphic column for the Cayman Islands showing main features of each depositional unit. Modified from Jones *et al.* (1994a).

and highly weathered nature of the strata. Surface exposure and thickness of the units varies between the islands, and much of this data has been collected from subsurface samples that were obtained through drilling.

The Brac Formation is exposed only on the eastern end of Cayman Brac, at the base of vertical to overhanging sea cliffs. The maximum exposed thickness of the formation is 33 m (Jones *et al.*, 1994a). Its total thickness is unknown because the lower boundary is not exposed and has never been reached during drilling. Although the Brac Formation does not crop out on Grand Cayman, it has been recovered from depths between 122 and 155 m below sea level – the maximum depth being constrained only by the depth of the well (Jones and Luth, 2003a). The lithology of the unit varies with location. On the northeast coast of Cayman Brac, bioclastic limestones (wackestones to grainstones) contain abundant *Lepidocyclina* and lesser numbers of other foraminifera, red algae, and echinoid plates. In contrast, coarse, sucrosic dolostone (euhedral rhombs up to 1.5 mm long) containing scattered lenses of bioclastic limestone predominates on the southeast coast. Branching corals are rare, having only been identified in the uppermost outcrop sections (Jones *et al.*, 1994a). The incomplete dolomitization of this formation signifies a lateral lithological transition over a distance of ~ 2 km. Furthermore, subsurface samples recovered during a recent drilling program reveal foraminiferal limestones (wackestones to grainstones), largely devoid of *Lepidocyclina* but rich in other taxa, which have been variably altered to finely crystalline, fabric retentive dolostones. This biotic assemblage and style of alteration have not been encountered in the Brac Formation thus far, and necessitate revision of the current stratigraphic architecture. An upper Lower Oligocene age has been assigned to the Brac Formation based on foraminifera biostratigraphy (Vaughan, 1926) and $^{87}Sr/^{86}Sr$ isotope ratios (average = 0.70808, corresponding to 28 million years) from constituent limestones (Jones *et al.*, 1994a). The uneven topography of the Brac-Cayman disconformity (dipping from 0.5° to 2° southwest, with a relief of 25 m) indicates that subaerial exposure, lithification, and erosion of the Brac Formation predated deposition of the overlying units (Jones *et al.*, 1994a).

The Cayman Formation has the greatest thickness and surface exposure of units in the Bluff Group. On Cayman Brac, the formation attains a maximum thickness of at least 100 m (Jones *et al.*, 1994a) and on Grand Cayman drilling has yielded sections up to 130 m thick (Jones and Luth, 2003a). Microcrystalline dolostones (formed of euhedral crystals 5-100 μm long, average 15-30 μm long) are pervasive throughout the Cayman Formation. Although the dolomite has been subject to extensive diagenetic modification, original depositional textures have been preserved. The Cayman Formation has a diverse biota that includes corals (colonial and branching), bivalves, gastropods, red algae, foraminifera, echinoids, rhodolites, and *Halimeda* (Jones *et al.*, 1994a). Corals grew in isolated thickets, and there is no evidence of reef development (Jones and Hunter, 1994a). Dolomitization has reset the $^{87}Sr/^{86}Sr$ isotope ratios (Pleydell, *et al.*, 1990; Jones and Luth, 2003a) and age-diagnostic fossils are not yet recognized, but a foraminifera fauna corresponding to established Caribbean associations implies a Middle Miocene age for the formation (Jones *et al.*, 1994a). The Cayman Unconformity, which divides the Cayman Formation from the overlying Pedro Castle Formation, is marked by locally variable relief (up to 40 m) that formed as a result of emergence during the Messinian lowstand event, when sea level was ≥40 m lower than present-day sea level (Jones and Hunter, 1994b). Faunal borings and well-developed karst topography on this erosional surface indicate that subaerial exposure and dissolution occurred prior to the deposition of the Pedro Castle Formation (Jones *et al.*, 1994b).

The Pedro Castle Formation ranges in composition from limestone (mudstones to packstones) to dolomitic limestone to dolostone (MacNeil and Jones, 2003). Significant paleorelief on the underlying Cayman Unconformity has produced a unit that ranges from 6 to 10 m thick on Cayman Brac and locally, over 20 m on Grand Cayman. Grain components in the Pedro Castle Formation include foraminifera, red algae, *Halimeda*, molluscs, echinoids, scattered corals (*Stylophora* and *Porites*), and rhodolites (Jones *et al.*, 1994b; MacNeil and Jones, 2003). The style of dolomitization varies from texture preserving but non-mimetic to texture destructive replacive dolomite, and dolostone distribution varies laterally and vertically (MacNeil and Jones, 2003). Most measured sections grade upward from basal dolostone into dolomitic limestone and recrystallized limestone (Jones *et al.*, 1994b; MacNeil and Jones, 2003). Intense diagenesis postdated dolomitization, evidenced by phytokarst, caves, rhizoconcretions, terra rossa, terrestrial oncoids, and meteoric cements (MacNeil and Jones, 2003). The Pedro Castle Formation was deposited during the Pliocene, based on coral biostratigraphy and $^{87}Sr/^{86}Sr$ isotope ratios determined from the limestones (Jones *et al.*, 1994b). The contact between the Pedro Castle Formation and Ironshore Formation is not exposed in outcrop, and is identified in wells by a change in core recovery controlled by the induration of the strata (Jones *et al.*, 1994b). On Grand Cayman, the maximum relief on the Bluff-Ironshore unconformity is 8 m (Jones *et al.*, 1997).

The Ironshore Formation covers much of the western half of Grand Cayman and forms a narrow coastal platform around the Bluff Group on Cayman Brac. Generally less than 9 m thick, it reaches a thickness of 19 m on the northeast coast of Grand Cayman (Vézina *et al.*, 1999). Composed of friable limestones beneath a hard calcrete crust (Matley, 1926), the Ironshore Formation is the only unit on the Cayman Islands that has escaped dolomitization (Jones *et al.*, 1997). Facies of this shallowing-upward sequence include patch reef, subtidal lagoon, and foreshore-backshore deposits (Jones and Hunter, 1990; Hunter and Jones, 1996). Faunal assemblages include bivalves, gastropods, foraminifera, *Halimeda*, and a diverse suite of corals, and trace fossils are well preserved (Pemberton and Jones, 1988). The bathymetry and facies of this sequence were controlled by the development of topography on Grand Cayman following deposition of the Pedro Castle Formation (Jones *et al.*, 1997). The textural heterogeneity preserved in this unit (including mudstones, oolitic grainstones, and coral framestones) reflects a diverse depositional environment. The Ironshore Formation can be divided into six unconformity-bounded units (A through F) that were deposited during sea level highstands at >400 ka, ~346 ka, ~229 ka, ~125 ka, ~104 ka, and ~84 ka, respectively (Vézina *et al.*, 1999; Coyne *et al.*, 2007). The present day erosional surface forms the upper boundary of the Ironshore Formation.

1.4 Study Area

The only outcrop of the Brac Formation is a vertical section exposed at North East Point on Cayman Brac (Fig. 1.4). Access to this exposure can be gained on the south coast from South Side Road, and on the north coast from North East Bay Road. From the end of both roads, a short traverse over the karstified shoreline leads to the bluff. Outcrops on the cliff can be followed laterally for a few hundred meters until the coastal terrace pinches out, but ascent is impossible due to the vertical to overhanging cliff face. Boulder rubble fallen to the base of the cliff allows limited access to higher sections. Although the maximum elevation of the Brac Formation is 33 m above sea level (asl) on the east end of the island, it slopes sharply down to sea level and becomes buried beneath coastal deposits to the west due to dipping relief on its upper boundary. The unconformity overlying the Brac Formation is viewed most clearly on the north shore but is difficult to distinguish on the south shore due

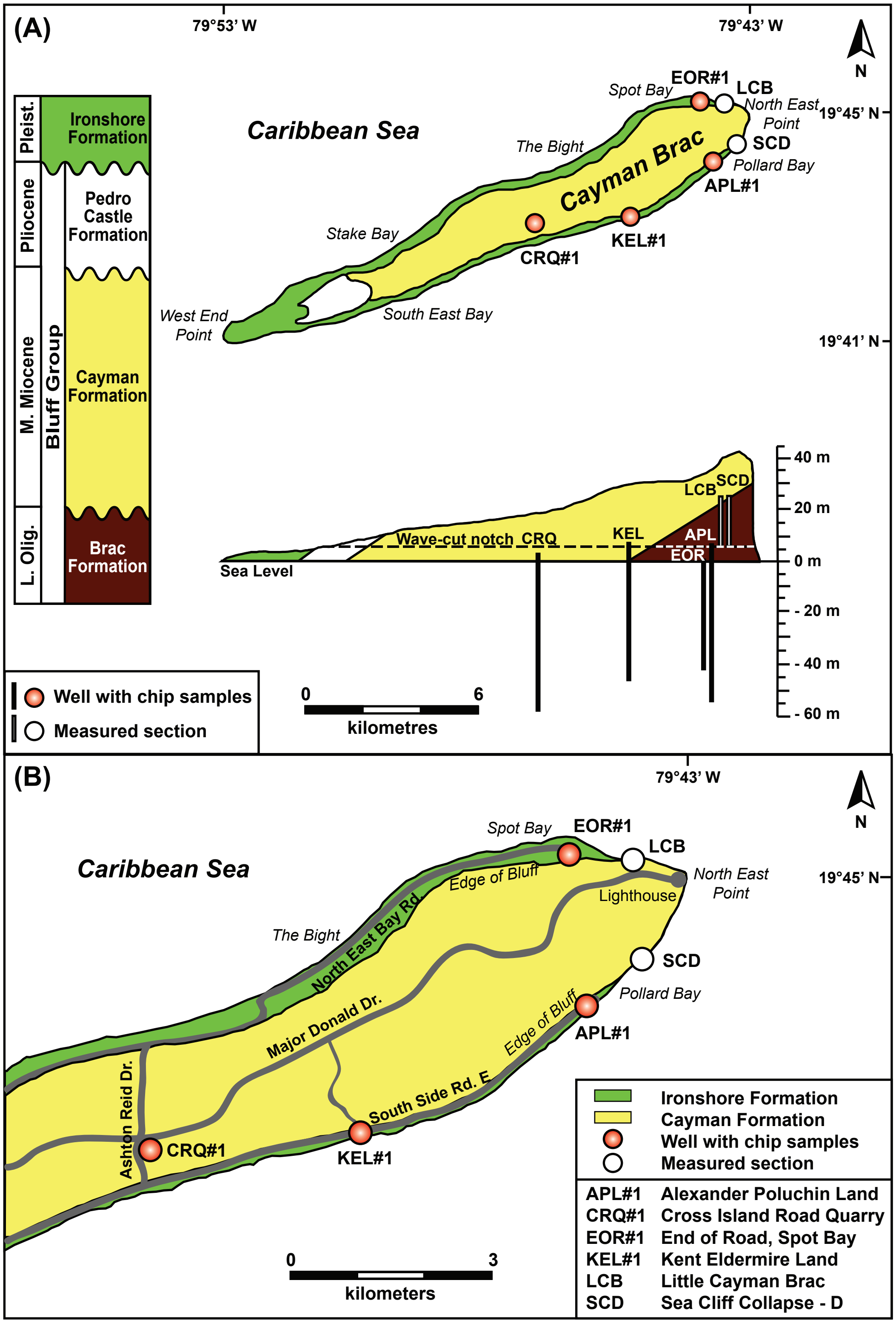

Figure 1.4 **(A)** Stratigraphic column, map, and cross section through Cayman Brac showing location of measured sections and wells from which cuttings were obtained. Modified from Jones *et al.* (1994a).
(B) Detail map of well sites and stratigraphic sections on Cayman Brac.

to severe weathering. Inactive springs and small caves with flats roofs mark the unconformity, formed by a permeability contrast between units. A wave-cut notch in the cliff, ~6 m asl, formed during the Sangamon Highstand (Jones and Hunter, 1990).

Cuttings from four wells drilled on the eastern end of Cayman Brac in 2002-2003 constitute the majority of material collected for this study (Fig. 1.5). Two wells drilled at the easternmost end of the island (EOR#1 on the north coast and APL#1 on the south coast) were positioned as close to the bluff as possible to ensure continuity with corresponding sections measured on the cliff and to recover a maximum thickness of the Brac Formation. Well KEL#1, located ~ 4 km west of APL#1 on South Side Road, was sited in a similar fashion. Well CRQ#1 was drilled in the central part of the island, on the floor of the Cross Island Road Quarry, and a corresponding section was measured on the quarry's west wall. Some portion of the Brac Formation was recovered from each well, ranging from 11 to 53 m; this amount varied depending on the depth of the well, its location, and the thickness of overlying strata.

Data collected from stratigraphic sections measured on the bluff are integrated with well data to gain a comprehensive understanding of the Brac Formation in outcrop and subsurface. Sections LCB on the northeast coast and SCD on the southeast coast (cf. Jones *et al.*, 1994a) are proximal to wells EOR#1 and APL#1, respectively. Samples from these sections are combined with well cuttings to maximize the sampled interval and to characterize the Brac Formation using all available data.

1.5 Objectives

The genesis and post-depositional evolution of the Cayman Formation, Pedro Castle Formation, and Ironshore Formation have been meticulously studied

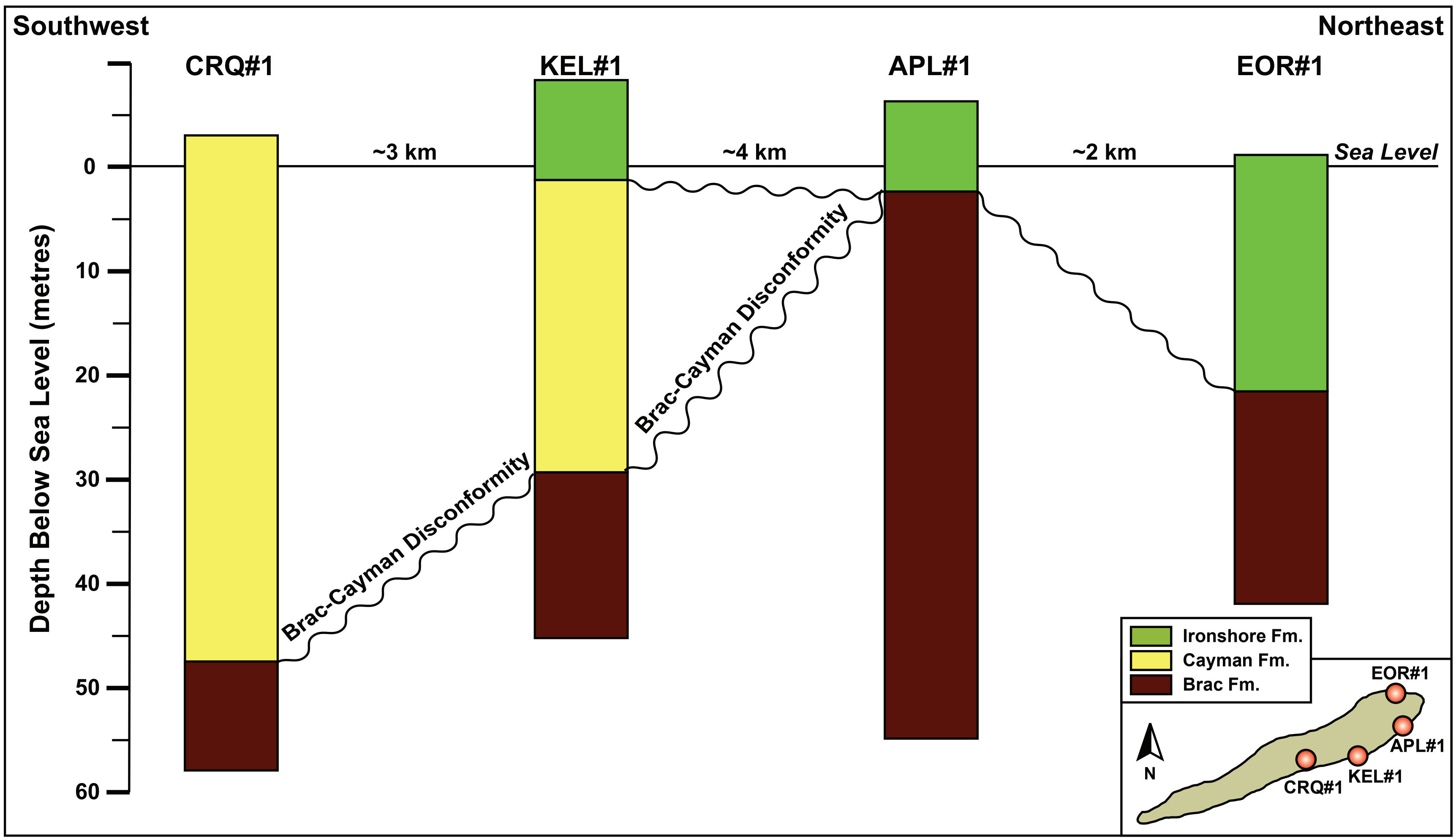

Figure 1.5 Stratigraphic units found in wells CRQ#1, KEL#1, APL#1 and EOR#1 on Cayman Brac.

and documented (Jones *et al.*, 1984; Jones, 1989; Jones and Hunter, 1989; Jones *et al.*, 1989; Pleydell *et al*., 1990; Jones, 1992a; 1992b; Wignall, 1995; Willson, 1998; Vézina *et al.*, 1999; Arts, 2000; Jones and Luth, 2002; Jones and Luth, 2003a,b; MacNeil and Jones, 2003; Etherington, 2004; Jones, 2004; Jones, 2005; Coyne *et al.*, 2007; Jones, 2007). The Brac Formation, however, has only been described and interpreted at a cursory level (Jones *et al*., 1994a; Jones and Hunter, 1994a). Herein, the first detailed study of the Brac Formation is conducted with the intention of further refining Caymanian stratigraphy.

Until recently, minimal surface exposure, inaccessible outcrop, extensive weathering, and a transition from limestone to dolostone concealed in the middle of the island have hindered thorough characterization of the Brac Formation. A recent drilling program centered on east-central Cayman Brac, however, has yielded the first extensive sections of the Brac Formation from subsurface (CRQ#1, KEL#1, APL#1, EOR#1), which may provide new insight into its sedimentological character. Cuttings from these wells greatly supplement the physical database from the Brac Formation, and their evaluation in combination with outcrop material provides an unrivalled opportunity to delineate the spatial extent and variability of the Brac Formation.

The objective of this study is to describe and characterize the sedimentologic, stratigraphic, and diagenetic features of the Brac Formation on Cayman Brac. The petrography, geochemistry, and geometry of dolomitization are analyzed in well cuttings and samples collected from outcrop to meet the following goals.

i. To describe the sedimentology of the Brac Formation, with emphasis on the pre-diagenetic lithology and paleontology, in order to define the depositional facies and facies architecture.
ii. To propose amendment to Bluff Group stratigraphy in order to reconcile

inconsistencies in the current definition of the Brac Formation.

iii. To integrate the observed sedimentary features, stratigraphy, and facies definitions to infer paleoenvironmental conditions and develop a depositional model for the Brac Formation.

iv. To identify diagenetic features and patterns in order to determine the stages and mechanisms of diagenesis – specifically, dolomitization – that affected the Brac Formation.

1.6 Methodology

1.6.1 Outcrop Analysis and Drilling Program

Fieldwork on Cayman Brac was essential to survey outcrops of the Brac Formation, assess its lithological and spatial variability, and place it in a stratigraphic context. Observations made in previous field seasons (Jones *et al.*, 1994a) were corroborated with measured sections on the north and south coasts of the bluff, and representative hand-sized samples were collected for analysis. The sites of wells EOR#1, APL#1, KEL#1, and CRQ#1 (all drilled between 2002 and 2003) were located in order to relate the well cuttings to their geological setting. This information was used to determine the spatial distribution of facies and geometry of dolomitization, and in turn, establish a depositional and diagenetic model for the Brac Formation.

The wells described in this study were drilled in 2003 and 2004 using a truck-mounted rig system. Mechanical limitations of the drilling equipment determined the maximum depths that the wells could be drilled to. Well cuttings were collected over 2.5 to 3 foot intervals (~0.75 to 0.9 m) by Dr. Brian Jones and Hendrik van Genderen. Chip samples (5 to 20 mm diameter) were washed up to surface with drilling fluids and collected on mesh gathering screens. Representative samples from each well interval were packaged and shipped back to the University of Alberta for petrographic analysis. Well cuttings were sampled for thin section and SEM petrography every ~ 1.5m, and measured outcrop sections were sampled for thin sections at finer intervals. In total, 56 thin sections were prepared from well samples, and 62 from outcrop samples. SEM photomicrographs were collected from every second well interval.

1.6.2 Thin Section Petrography

Hand samples and well cuttings were studied petrographically using a polarizing light microscope (25-500x magnification) and standard thin sections (1”x2” and 2”x3”). Sample intervals ranged from 1.5 to 3 m, and represent limestone- and dolostone-dominated regions. Thin sections were stained with Alizarin Red S to facilitate differentiation between calcite and dolomite, and blue stain was added to the epoxy to emphasize original porosity. A petrographic guide (Scholle and Ulmer-Scholle, 2003) aided in grain identification and textural classification. Matrix and allochems that escaped dolomitization were used to develop a facies classification. The size, packing, and textures of dolomite crystals were documented to characterize replacive dolomites.

1.6.3 Scanning Electron Microscopy

Microscopic allochems and cements beyond the resolution of conventional polarizing light microscopy were identified using scanning electron microscopy (SEM). Samples were prepared and analyzed by Dr. Brian Jones and George Braybrook at the University of Alberta using a Jeol SM-6301 FXV SEM. Dolostone samples were polished and lightly etched in 30% HCl, then sputter coated with gold. Crystal boundaries were thus accentuated to reveal the size and shape of constituent dolomite crystals. Partially dolomitized limestones were examined for fabric retentivity and selective replacement of matrix or allochem components. Well cuttings were selected from the same intervals as thin sections, where possible, to facilitate comparison between thin section and SEM data.

1.6.4 X-Ray Diffraction

X-ray diffraction (XRD) was employed to determine the mineralogical composition of the carbonate samples. Analyses were run at 40 kV and 35 mA in a Rigaku Geigerflex sealed-tube X-ray generator with a Co tube. Samples were mixed with an internal quartz standard and scans ran from 29° to 38° 2θ. The peak-fitting X-ray diffraction (PF-XRD) technique of Jones *et al*. (2001) was used to determine the percent of calcite and dolomite in the samples, and to calculate the percent calcium (%Ca) in the dolostones. Heterogeneous samples composed of multiple populations of dolomite crystals could thus be identified based on %Ca content. XRD analysis also served as a method to back-check lithological observations made from thin section and SEM petrography.

1.6.5 Electron Microprobe Analysis

Backscatter electron imaging on the electron microprobe supplemented XRD analyses by indicating, on a micron scale, the spatial distribution of dolomite crystal populations based on differences in %Ca. Five samples with the largest dolomite crystals (determined from SEM) were selected for analysis from APL#1. Thin sections ground to ~ 60 μm thick were double polished and carbon coated, and spot analyses were made with a 3 μm diameter beam. Individual dolomite crystals (replacive and cements) were probed for Mg/Ca zoning representing discrete growth phases, identified by relative brightness caused by differences in atomic weight. Quantitative measurements also recorded the variability in other elements (Sr, Mn) within the dolomite.

1.6.6 Stable Isotope Analysis

Well cuttings and selected outcrop samples were analyzed for oxygen and carbon isotope ratios in the stable isotope laboratory of Dr. Karlis Muehlenbachs at the Department of Earth and Atmospheric Sciences, University of Alberta. Calcite and dolomite $\delta^{18}O$ and $\delta^{13}C$ were analyzed in 167 samples (EOR#1: n=26; APL#1: n=68; KEL#1: n=21; CRQ#1: n=15; LCB: n=26; SCD: n=11) by differential phosphoric acid extraction (modified procedure of Epstein *et al.,* 1963). Variable amounts of calcite and dolomite were contained in most samples, with compositions ranging from pure calcite to pure dolomite.

Samples were powdered with an agate mortar and pestle, and single large chip samples were selected rather than combining several small pieces to avoid averaging isotope values. Samples were crushed to a uniform grain size (75-150 μm) to ensure homogeneity and provide a uniform surface area for reaction (cf. Walters *et al.*, 1972). SEM analysis indicated that dolomitic and calcitic fractions were intimately mixed, making physical separation of the minerals and cement populations impossible. Chemical separation was thus required to analyze carbonate mineral fractions independently.

40-50 mg of carbonate powder and 3 ml of anhydrous phosphoric acid (H_3PO_4) were measured into glass reaction vessels and evacuated on a vacuum line to remove atmospheric components. Samples were reacted at 25°C for one hour according to:

$$3CaCO_3 + 2H_3PO_4 \rightarrow 3CO_2 + 3H_2O + Ca_3(PO_4)_2.$$

CO_2 evolved after one hour's time formed principally from the reaction of acid with the calcite in the samples (Epstein *et al.*, 1963, their Fig. 1). This CO_2 was purified by distillation through a dry ice trap, condensed in a sample collection tube immersed in liquid nitrogen, and analyzed for calcite $\delta^{18}O$ and $\delta^{13}C$ values. CO_2 gas formed between the first and fourth hour of reaction was pumped away to avoid contamination. The vessel was then placed in a hot water bath at 50°C; the reaction was thus sustained for another 24 hours. CO_2 formed during the remainder of the reaction was extracted in a similar manner and analyzed for $\delta^{18}O$ and $\delta^{13}C$ of the dolomite component.

All stable isotopes were analyzed on a Finnigan-MAT 252 Mass Spectrometer in the Stable Isotope Laboratory at the University of Alberta. $\delta^{18}O$ and $\delta^{13}C$ ratios were reported using δ notation:

$$\delta_{sample} = (R_{sample}/R_{standard} - 1) \times 1000$$

where R = $^{18}O/^{16}O$ for oxygen isotopes and R = $^{13}C/^{12}C$ for carbon isotopes. All results are reported relative to the PeeDee Belemnite (PDB) standard normalized to NBS-18 in per mil (‰) notation. Dolomite $\delta^{18}O$ values have not been corrected for any fractionation factor with phosphoric acid. Total analytical error for the preparation and isotope ratio measurement is ±0.3‰, based on reproducibility.

1.6.7 Sr Isotope Analysis

Limestones and dolostones from the Brac Formation were dated by strontium isotope stratigraphy. Samples of pure calcite or pure dolomite were selected, where possible, from evenly spaced intervals spanning the length of each well. 23 samples were analyzed in the Radiogenic Isotope Laboratory at the University of Alberta (EOR#1: n=4; APL#1: n=8; KEL#1: n=7; CRQ#1: n=4), and repeat analyses were carried out for samples suspected of contamination by mixed lithology. $^{87}Sr/^{86}Sr$ values were Rb-corrected and normalized against the NIST SRM 987 Sr isotope standard value of 0.710245. Measured $^{87}Sr/^{86}Sr$ values were compared with a high-resolution curve of seawater $^{87}Sr/^{86}Sr$ through time (McArthur *et al.*, 2001) to assign a numerical age to the samples.

Chapter Two: Stratigraphy & Facies of the Brac Formation

2.1 Introduction

A full understanding of the internal stratigraphy of the Brac Formation is complicated because outcrops are limited to vertical sea cliff exposures at the east end of Cayman Brac (Fig. 2.1A), rendering the internal stratigraphy and overall geometry difficult to assess. Reconnaissance surveys of the Brac Formation yielded preliminary data from outcrop (Jones *et al.*, 1994a; Jones and Hunter, 1994a), but early interpretations were constrained by exposure and accessibility. The dip of the formation is unknown due to an absence of identifiable bedding planes, and its thickness cannot be determined because the lower boundary is not exposed. The lithology of the Brac Formation varies laterally, from limestone to sucrosic dolomite, between outcrops less than 2 km apart. Vertical trends in lithology are difficult to identify because the sheer cliff face limits access to the outcrop. The addition of new well data to the existing dataset is therefore critical to refining the internal stratigraphy of the Brac Formation. Thus, analyses of strata in wells CRQ#1, KEL#1, APL#1, and EOR#1 are coupled with stratigraphic sections LCB and SCD (Jones *et al.*, 1994a) to further elucidate the internal stratigraphy of the Brac Formation.

2.2 Stratigraphy

2.2.1 Existing Stratigraphy

Section LCB, located on the north coast, was designated as the type section because it is formed of limestone, whereas section SCD, located on the south coast, was named as a reference section because it represents the part of the formation that has been replaced by dolomite (Jones *et al.*, 1994a).

Figure 2.1 **(A)** Field photograph of the bluff on Cayman Brac, looking south from North East Point. The white arrow marks the unconformity between the Brac Formation at the base of the cliff and the overlying Cayman Formation. The top of the cliff is 43 metres asl. Section LCB is shown for reference. **(B)** Thin section photograph of *Lepidocyclina* packstone from section LCB on the north coast of Cayman Brac. *Lepidocylina* (L) surrounded by a matrix of mud and various smaller foraminifera (*WOJ1-5066*). **(C)** Thin section photograph of sucrosic dolomite from section SCD on the south coast of Cayman Brac (*WOJ7-5157*).

The lower boundary of the Brac Formation is located below the base of the measured sections, and therefore remained undefined. The upper boundary is an unconformity that separates the Brac Formation from the overlying Cayman Formation. The maximum exposed thickness of the Brac Formation at North East Point is 33 m (Jones *et al.*, 1994a).

On the north coast of Cayman Brac, bioclastic limestones (wackestones to grainstones) of the Brac Formation contain abundant *Lepidocyclina* (up to 32 mm diameter; Fig. 2.1B) and lesser numbers of other foraminifera (rotalids, miliolids, small encrusting foraminifera, *Carpenteria*), red algae, and echinoid plates (Jones *et al.*, 1994a). Large bivalve and gastropod shells are restricted to the uppermost part of the formation, and corals (*Porites porites*) are rare. On the south coast, the Brac Formation is formed of coarse, sucrosic dolostone that contains isolated lenses of bioclastic limestone. The textures and biota of the limestone in these lenses are identical to the limestone on the northeast coast. The massive dolostone is formed of interlocking, subhedral to euhedral dolomite crystals (up to 1.5 mm long) that have dark, inclusion-rich cores surrounded by clear rims (Fig. 2.1C). Original limestone textures have been largely destroyed with only rare ghosts of foraminifera and red algae evident. Fossil mouldic to vuggy porosity, formed by the dissolution of *Lepidocyclina* and other bioclasts, ranges from 5 to 40% and averages ~30%. Fabric retentive microcrystalline dolostone is restricted to small lenses in the uppermost part of the formation. The location, geometry, and nature of the lithological transition between the limestones on the north coast and the dolostones on the south coast are unknown.

Lepidocyclina collected from the base of the cliffs on the north coast by Matley (1926) were identified and dated by T. W. Vaughan (1926). The strata were assigned a Middle Oligocene (Rupelian) age based on the presence of *Lepidocyclina (Lepidocyclina) yurnagunensis* Cushman, *Lepidocyclina*

(Nephrolepidina) undosa Cushman, *Lepidocyclina (Nephrolepidina) undosa* var. *tumida* nov. Vaughan, *Lepidocyclina gigas* Cushman, *Lepidocyclina* sp. cf. *L. marginata* (Michelotti), *Lepidocyclina* sp. indet., and *Carpenteria americana* Cushman (Matley, 1926; Vaughan, 1926). Matley (1926) correlated the *Lepidocyclina undosa* zone on Cayman Brac with the White Limestone of Jamaica.

Limestones from the Brac Formation have an average $^{87}Sr/^{86}Sr$ ratio of 0.708122 (Jones and Luth, 2003a). Interpretation of this value indicates that the limestones are ~26 million years old (late Oligocene) if the $^{87}Sr/^{86}Sr$-time curve developed by McArthur *et al.* (2001; Look-Up Table Version 4: 08/03) is used, or ~27 million years old using the $^{87}Sr/^{86}Sr$-time curve of Oslick *et al.* (1994). Age-diagnostic *Lepidocyclina* preserved in Brac Formation limestones are consistent with the age derived by the $^{87}Sr/^{86}Sr$ geochronometer (Jones *et al.*, 1994a; Jones and Luth, 2003a). Dolostones in the Brac Formation yield an average $^{87}Sr/^{86}Sr$ ratio of 0.708939, indicating that dolomitization took place ~8 Ma, during the late Miocene (Jones and Luth, 2003a).

2.2.2 Revised Stratigraphy

Cuttings recovered from the basal parts of wells CRQ#1, KEL#1, APL#1, and EOR#1 are assigned to the Brac Formation because (1) they lie below the unconformity at the top of the Brac Formation and (2) their lithology is consistent with the limestones in the type section (LCB) of the Brac Formation. The strata in these wells represent the deepest, most continuous sections of the Brac Formation. The top of each well is located slightly above sea level on the coastal platform surrounding the bluff, with the maximum depth reached being 58 m below sea level (bsl). Thus, the Brac Formation on Cayman Brac is now known to be at least 91 m thick. The lower boundary of the Brac Formation is still unknown because it has not yet been encountered in well cuttings.

On Cayman Brac, the Brac Formation is formed of limestone, finely crystalline dolostone, and sucrosic dolostone. The sucrosic dolostone succession found on the south coast of Cayman Brac (east of Great Cave, including section SCD) is lithologically distinct from the limestone and finely crystalline dolostone succession exposed on the north coast (section LCB) and found in wells EOR#1, APL#1, KEL#1, and CRQ#1 (Fig. 2.2).

The Brac Formation was defined, by necessity, on the limestones found in section LCB and the sucrosic dolostones found in section SCD. Although originally thought to be dominated by sucrosic dolostones, it is now apparent that limestones and finely crystalline dolostones dominate the Brac Formation in wells CRQ #1, KEL #1, APL #1, and EOR #1. Thus, it is necessary to revise the definition of the Brac Formation to reflect the fact that: (1) limestone, dolomitic limestone, and finely crystalline dolostone dominate the succession; and (2) the sucrosic dolostone is restricted in aerial extent. Discrepancies within the existing stratigraphy may be resolved by: (1) maintaining the current definition of the Brac Formation as limestone represented by type section LCB, and defining the sucrosic dolostone in section SCD as a new member within the Brac Formation; or (2) defining a new formation wherein the existing Brac Formation is demoted to member status and the dolostone is defined as a second member.

Of the two possibilities for amending the stratigraphy of the basal part of the Bluff Group, the first option is considered the most viable. The second option would involve the adoption of excessive terminology that would ultimately cause confusion. It is now apparent that the sucrosic dolostone is restricted to the south coast of Cayman Brac, and hence forms only a small part of the succession. The simplest solution is to maintain section LCB as the type section of the Brac Formation, and designate section SCD as the type section for the sucrosic

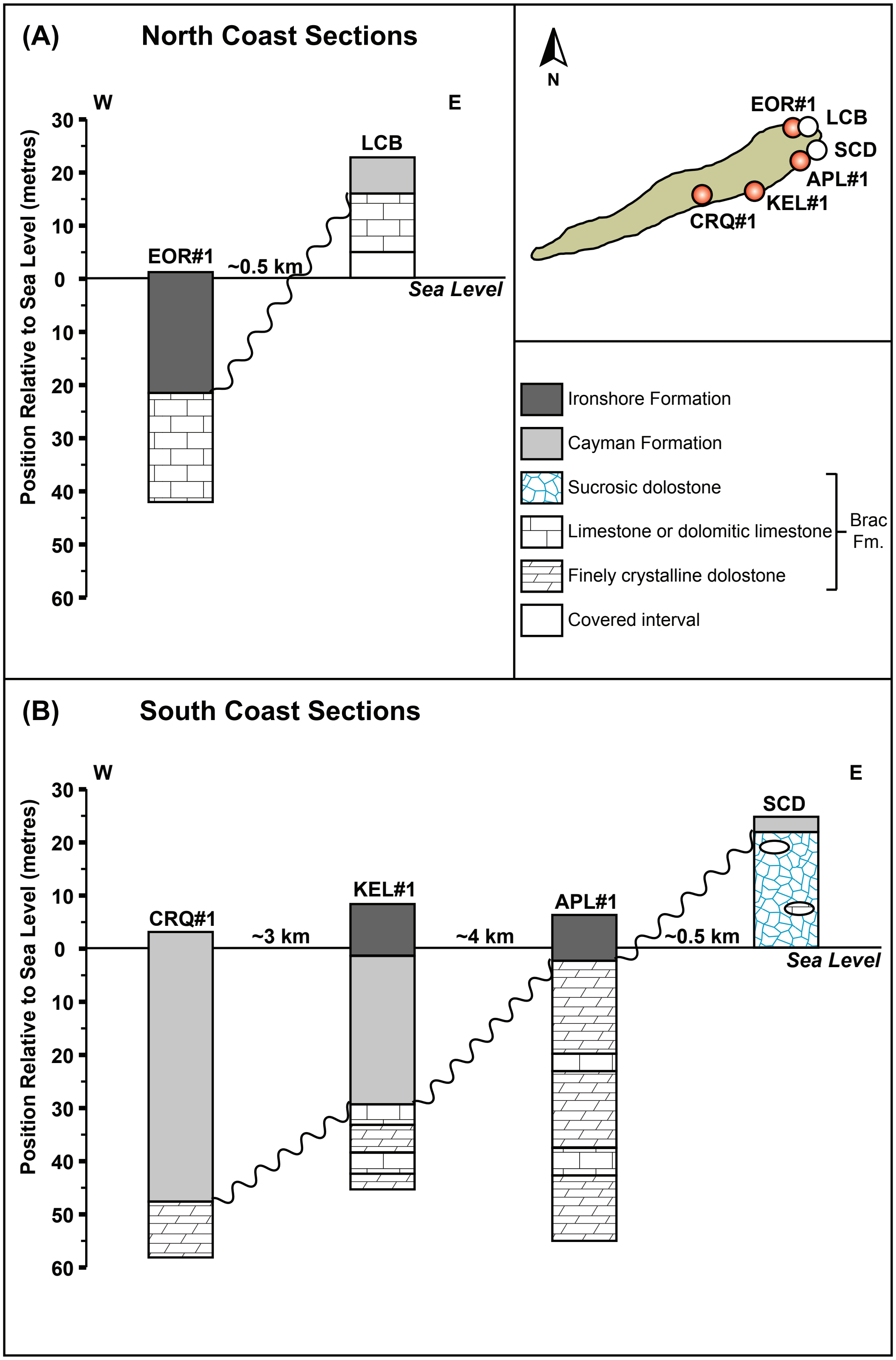

Figure 2.2 Lithological sections of **(A)** well EOR#1 and measured section LCB on the north coast, and **(B)** wells CRQ#1, KEL#1, APL#1 and measured section SCD on the south coast of Cayman Brac.

dolostone member of the succession. Due to the restricted scale of type section LCB in outcrop, a new reference section, well APL#1, is assigned to represent the Brac Formation in subsurface.

Herein, the definition of the Brac Formation is expanded to include all of the strata found below the base of the Cayman Formation in wells EOR#1, APL#1, KEL#1, and CRQ#1, in addition to the strata already identified by Jones *et al.* (1994a) in outcrop at the east end of Cayman Brac. Defined in this manner, the Brac Formation is dominated by limestones, dolomitic limestones, and finely crystalline dolostones. The sucrosic dolostone, represented in section SCD, is herein defined informally as the “Pollard Bay member” of the Brac Formation (Fig. 2.3).

2.2.2.1 Sedimentology of the Brac Formation

Most limestones in the Brac Formation are found on the north coast of Cayman Brac, in section LCB and well EOR#1. Dolomitization is localized and primary structures are commonly retained. Limestone and partially dolomitized limestone from EOR#1 is lithologically similar to that exposed in LCB. Most well cuttings contain less than 25% dolomite, which has selectively replaced matrix and less commonly fossils (e.g., red algae, echinoids, foraminifera). Where present, dolomite is finely crystalline (crystals up to 30 μm long) and fabric retentive, but replacement is predominantly non-mimetic. *Lepidocyclina*, common in the limestones exposed in LCB, are conspicuously absent in EOR#1. The wackestones to grainstones in EOR#1 include a diverse array of foraminifera (rotalids, miliolids, *Carpenteria*, encrusting and planktonic forams) and red algae. *Halimeda*, echinoids, ostracods, and corals (*Porites porites*, *Siderastrea radians*) are locally common, whereas bivalves and gastropods are rare. Fossil mouldic porosity is 10 to 45% (average 30%) in EOR#1 and pores are lined by thin (5-

AGE	STRATIGRAPHIC UNIT				LITHOLOGY
Pleistocene	Bluff Group	Ironshore Formation		Unconformity	Limestone
Pliocene		Pedro Castle Formation		Unconformity	Limestone, dolomitic limestone, finely crystalline dolostone
Miocene		Cayman Formation		Unconformity	Finely crystalline dolostone
Oligocene		Brac Formation	Pollard Bay member		Sucrosic dolostone
					Limestone, dolomitic limestone, finely crystalline dolostone

Figure 2.3 Revised stratigraphy for Cayman Brac, denoting the addition of the Pollard Bay member to the Brac Formation to account for its disparate lithology.

10 μm) isopachous dolomite cement that is commonly postdated by isopachous, sparry calcite cement (crystals up to 50 μm long).

Wells CRQ#1, KEL#1, and APL#1 represent the more pervasively dolomitized parts of the Brac Formation. These wells contain an assortment of rock types not evident in surface exposures. Well cuttings are composed predominantly of dolomitic limestone and dolostone, but are petrographically disparate from the dolostones exposed in section SCD on the south coast. Microsucrosic dolostone (euhedral rhombs up to 50 μm long embedded in a fine-grained, inclusion-rich matrix) comprises < 5% of dolostone found in these wells. Dolomite, which varies from fabric retentive to fabric destructive, replaces matrix and allochems indiscriminately. Most precursor limestones are packstones that contain a biota similar to that found in EOR#1. Outlines of leached fossils (*Halimeda*, foraminifera, echinoids, bivalves) and allochem ghost structures are common. *Lepidocyclina* are present only in the foraminiferal packstones from KEL#1. Porosity is predominantly fossil mouldic, but varies from vuggy to intercrystalline depending on crystal size and the extent of dissolution (5 to 50%; average 25%). Isopachous, limpid dolomite cement (crystals up to 100 μm long) lines voids, and is postdated by bladed to sparry calcite cement (crystals up to 150 μm long). The overall fine-grained, fabric retentive nature of dolostones found in these wells is distinct from the coarsely crystalline, sucrosic dolostones exposed in section SCD.

2.2.2.2 Sedimentology of the Pollard Bay Member

Sucrosic dolostones from the Brac Formation have been described by Jones *et al.* (1994a). The Pollard Bay member is distinguished from the remainder of the Brac Formation by its abundance of coarsely crystalline, fabric destructive, sucrosic dolostones relative to other lithologies. Though locally pervasive, the sucrosic dolostones of the Pollard Bay member have been identified only on the sea cliffs on the south coast of Cayman Brac.

2.3 Brac Formation – Cayman Formation Contacts

Delineating the stratigraphy of the Brac Formation is hindered by the lack of exposed contacts. Although the lower boundary of the Pollard Bay member has not been found in outcrop or in the wells, it must be located between the base of the cliffs on the south coast of Cayman Brac and the top of the finely crystalline dolostone in APL#1, at a depth near sea level (Fig 2.4). The lateral contact and the width of the transition between the Pollard Bay member and the rest of the Brac Formation remains unknown due to the inaccessibility of the vertical to overhanging sea cliffs between sections SCD and LCB at North East Point. The Pollard Bay member is probably a wedge-shaped unit that passes laterally into the limestones of the Brac Formation.

On the south coast of Cayman Brac, the unconformity between the Brac Formation and the Cayman Formation separates the sucrosic dolostones of the Pollard Bay member from the finely crystalline, fabric retentive dolostones of the overlying Cayman Formation. Extensive tropical weathering has caused staining and dissolution on outcrop surfaces that partially conceal the location of the unconformity. Small, inactive springs on the cliff face, evident from flowstone deposits, indicate a permeability contrast between the two formations. This unconformity commonly forms the roofs of caves (including Great Cave) in the upper part of the Brac Formation (Jones *et al.*, 1994a), providing further evidence for a difference in permeability. The dip of the unconformity along the south coast is approximately 0.5° to the west. Tubular structures (10 cm long, 2 cm in diameter) found near section SCD appear to be borings formed at the unconformity between the Brac Formation and the Cayman Formation, suggesting

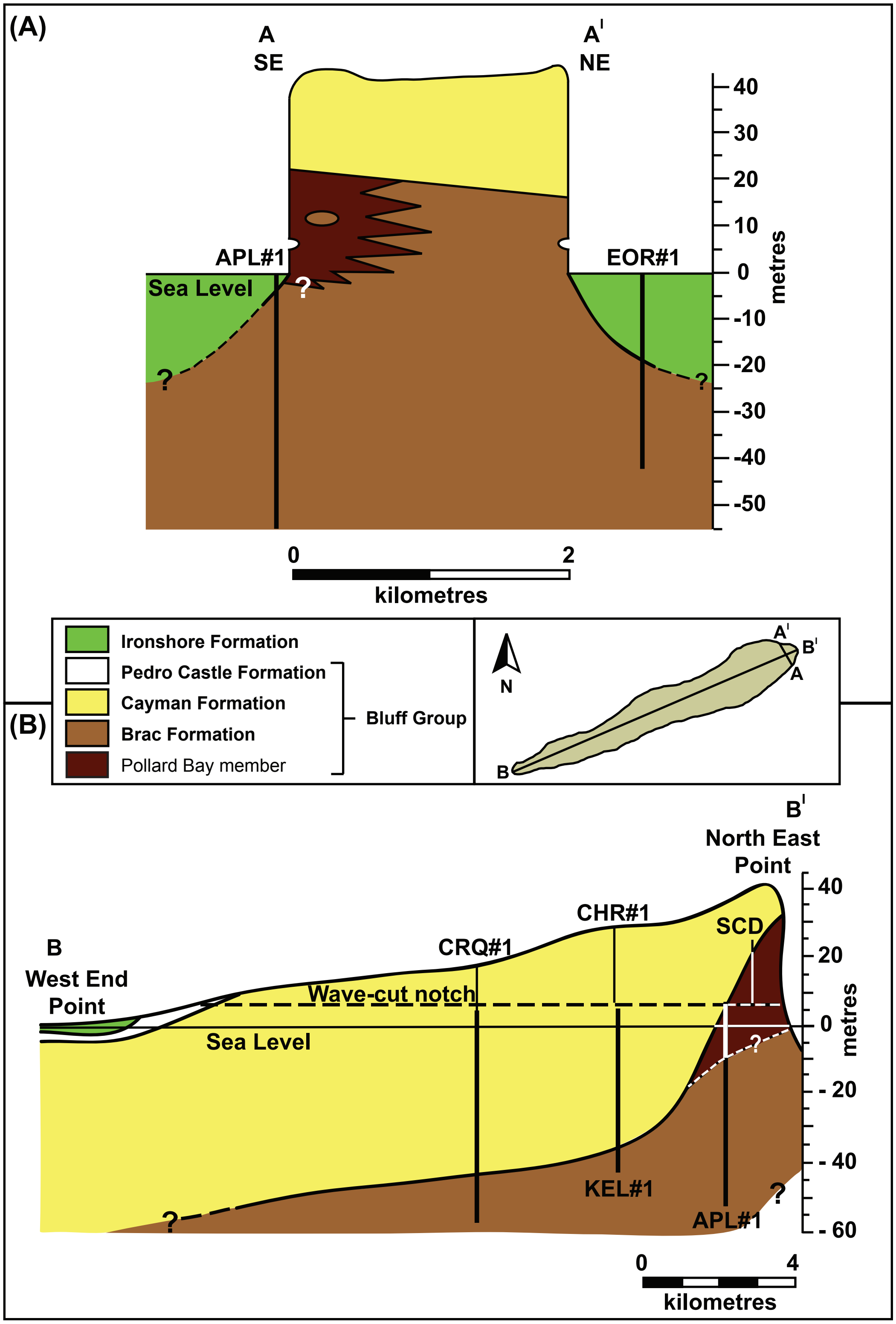

Figure 2.4 Proposed modification to Bluff Group stratigraphy, demonstrated in perpendicular cross sections, on Cayman Brac. (**A**) Transect from southeast to northeast. (**B**) Transect from west to east. Modified from Jones (2005).

that subaerial exposure, lithification and erosion of the Brac Formation took place before deposition of the Cayman Formation (Jones and Hunter, 1994a).

On the north coast, the unconformity is clearly visible at North East Point, where it stands out from the comparatively featureless cliff face. There, the unconformity separates the *Lepidocyclina*-rich limestones of the Brac Formation from the mimetically replaced dolostones of the Cayman Formation. There are no caves below the unconformity on the north coast; however, the floor of a cave marks the unconformity in this location, also pointing to a permeability difference between formations. The dip of the unconformity varies laterally along the north coast, ranging between 0.4 and 2° to the west (Jones *et al.*, 1994a). Topographic variations on the disconformity imply that the Brac Formation underwent substantial erosion prior to the deposition of the Cayman Formation (Jones and Hunter, 1994a).

2.4 Facies

Facies descriptions of the Brac Formation summarize the lithologic and paleontologic features of the strata with no genetic connotation. Lithology in the Brac Formation varies from pure calcite to pure dolomite; therefore, rocks composed primarily of calcite are herein defined as limestone (0 to 15% dolomite) or dolomitic limestone (15 to 50% dolomite). Rocks that contain more dolomite than calcite are defined as calcareous dolostone (50 to 85% dolomite) or dolostone (85 to 100% dolomite). Within this system, facies are defined primarily on lithology (lithofacies), and where possible, on fossil content (biofacies).

Six different facies are defined for the Brac Formation on Cayman Brac (Table 2.1). Limestones and dolomitic limestones are classified and described according to Dunham's (1962) limestone classification scheme. Biofacies and depositional fabrics in the limestones are defined by the presence and relative

Table 2.1 Facies in the Brac Formation on Cayman Brac. VC = Very common, C = common, LC = locally common, R = rare.

	Facies	Fabric	Major Allochems	Minor Allochems	Porosity	Cement	Cavity Fills
Limestone and Dolomitic Limestone (>50% Calcite)	*Lepidocyclina*	Wackestone - Grainstone	*Lepidocyclina* Miliolids Rotalids Encrusting Forams *Carpenteria*	Red Algae Echinoids *Porites*	Fossil mouldic (0 to 20%)	Bladed to sparry calcite cement (up to 100 μm)	Caymanite Terra Rossa Speleothems
	Mollusc	Wackestone - Packstone	Bivalves, Gastropods *Lepidocyclina* Miliolids, Rotalids Encrusting Forams *Carpenteria*	Red Algae Echinoids *Porites*	Fossil mouldic (10 to 40%)	Bladed to sparry calcite cement (up to 100 μm)	Caymanite Speleothems
	Foraminifera	Wackestone - Grainstone	Rotalids, Miliolids Globigerinids Globorotalids Encrusting Forams Red Algae	*Porites, Siderastrea* *Carpenteria, Homotrema* *Halimeda* Echinoids, Ostracods Bivalves	Fossil mouldic (0 to 20%)	Dolomite rim cement (5 to 20 μm) Bladed calcite cement (up to 50 μm)	Not apparent
	Facies	**Fabric**	**Crystal Length**	**Porosity**	**Cement**	**Biota**	**Fossil Preservation**
Dolostone and Calcareous Dolostone (>50% Dolomite)	Fabric Retentive Finely Crystalline Dolomite	Wackestone - Packstone (fabric retentive but non-mimetic)	10 to 100 μm (average 50 μm)	Fossil mouldic (10 to 30%)	Isopachous, limpid dolomite cement (up to 100 μm); Bladed to sparry calcite cement (up to 150 μm)	Rotalids (VC) Miliolids (VC) Encrusting Forams (C) Red Algae (C) Echinoids (R), *Porites* (R) Bivalves (VR)	Fossils leached or replaced by dolomite Red algae, echinoids mimetically replaced
	Fabric Destructive Finely Crystalline Dolomite	Matrix dolomite (fabric destructive)	20 to 100 μm (average 70 μm)	Not apparent	Limpid dolomite cement (rare) (up to 300 μm)	None preserved	N/A
	Sucrosic Dolomite	Sucrosic dolomite (fabric destructive)	0.5 to 1.5 mm	Fossil mouldic - Intercrystalline - Vuggy (5 to 40%)	Microstalactitic - pendant cement (mixed mineralogy) (up to 500 μm)	*Lepidocyclina* (VC) Bivalves (LC) Gastropods (LC) *Porites* (LC)	Fossil mouldic porosity Allochem ghosts

abundance of foraminifera, red algae, molluscs, corals, echinoids, *Halimeda*, ostracods, and mud content. Dolostones are divided into lithofacies based on the type of dolomite present (e.g., finely crystalline or sucrosic), and if the original fabric has been preserved or destroyed. Allochem preservation varies between facies and is determined by the amount and type of dolomite present.

2.4.1 Lepidocyclina *Facies*

Lepidocyclinid foraminifera are the dominant faunal elements in the wackestones to grainstones of this facies (Fig. 2.5A). Preservation of *Lepidocyclina* (up to 4 mm in diameter) is variable; many are intact and aligned parallel to each other, whereas others are fragmented and abraded. Miliolids, rotalids, small encrusting foraminifera, and *Carpenteria* are also common. Abraded fragments of coralline red algae (<0.5 mm in diameter) are locally common and have been partially replaced by mimetic dolomite. Echinoid plates and *Porites* branches are rare. Mud content is variable, but most typically comprises <15% of samples.

2.4.2 Mollusc Facies

A local abundance of bivalves and gastropods distinguishes the Mollusc Facies from the *Lepidocyclina* facies. The relative abundances and style of preservation of *Lepidocyclina*, miliolids, rotalids, encrusting foraminifera, *Carpenteria*, coralline red algae, echinoids, and *Porites* are similar in the mollusc facies and the *Lepidocyclina* facies. Bivalves and gastropods are commonly leached, but can be identified by their distinctively shaped fossil mouldic vugs surrounded by micrite envelopes (Fig. 2.5B).

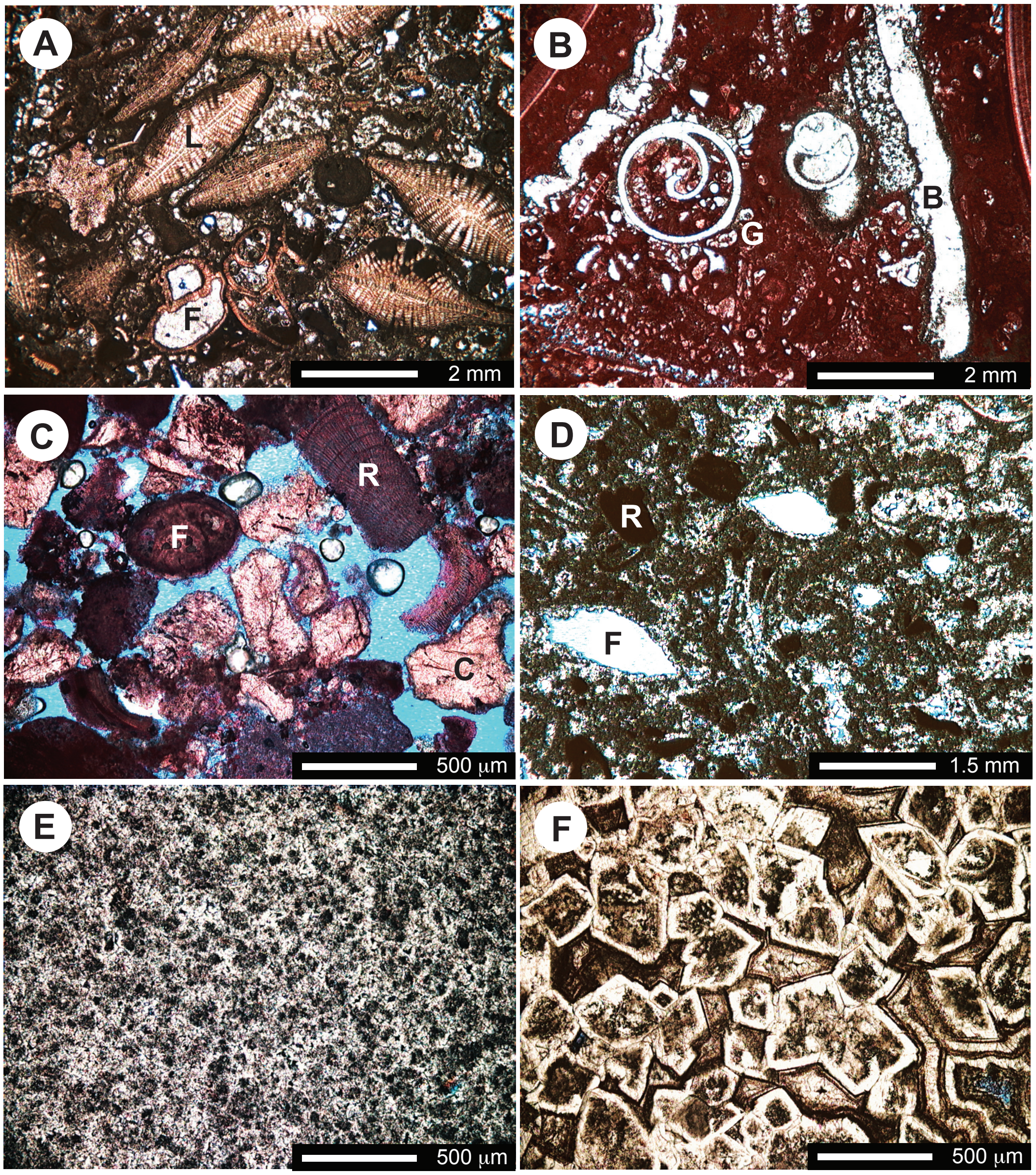

Figure 2.5 Facies in the Brac Formation on Cayman Brac. Plane polarized light; L = *Lepidocyclina*; G = gastropod mold; B = bivalve mold; F = foraminifera fragment/mold; R = red algae fragment; C = coral fragment. **(A)** *Lepidocyclina* Facies. Packstone matrix composed of smaller foraminifera (*WOJ1-5121*). **(B)** Mollusc Facies. Gastropods and bivalves represented by fossil moldic pores (*WOJ2-5126*). **(C)** Foraminifera Facies. Note high diversity of grain types (*EOR#1-137.5 ft.*). **(D)** Fabric Retentive Finely Crystalline Dolomite Facies. Fossils replaced by dolomite or represented by fossil moldic pores (*APL#1 - 171.25 ft.*). **(E)** Fabric Destructive Finely Crystalline Dolomite Facies (*CRQ#1 - 181.25 ft.*). **(F)** Sucrosic Dolomite Facies (*WOJ11-5197*).

2.4.3 Foraminifera Facies

Wackestones to grainstones of the Foraminifera Facies comprise the most diverse suite of allochems within the study (Fig. 2.5C). Benthic foraminifera are the dominant component of this facies and include rotalids, miliolids, and encrusting foraminifera. Planktonic foraminifera species are dominated by the Globigerinidae and Globorotaliidae families. Preservation of the foraminifera is variable; most chambers are lined by isopachous dolomite cement (5 to 10 μm thick), whereas some tests are replaced entirely by fabric retentive dolomite. Fragments of coralline red algae are abundant, and cellular structures are well preserved due to replacement by mimetic dolomite. *Porites* and *Siderastrea* are locally common, and are preserved as both colonial skeletons and abraded grains (<0.5 mm in diameter) within grainstones. *Halimeda* is locally common; aragonitic plate walls are commonly leached, and utricles are surrounded by micrite envelopes and filled with sparry calcite cement. Ostracods are less common, and shells are lined by isopachous dolomite cement (5 to 10 μm thick) and filled with sparry calcite cement (crystals 20 to 50 μm long). Echinoid spines are relatively rare, and are leached or replaced by dolomite. *Carpenteria* and *Homotrema rubrum* are rare. Bivalves, commonly leached, are very rare, and are identified by the shape of their outlines. Bioclast abundances and mud content vary on a local scale.

2.4.4 Fabric Retentive Finely Crystalline Dolomite Facies

Many dolostones in the Brac Formation on Cayman Brac partially preserve the fabric of their limestone precursors. Wackestones to packstones are texturally dominant in this facies, although some detail has been lost as a result of dolomitization. Dolomite is finely crystalline (crystals 10 to 100 μm long, average 50 μm) and fabric retentive, but allochem replacement is largely non-mimetic (Fig. 2.5D). Dolomite has replaced matrix and fossils, and is present as an isopachous, limpid cement (crystals <100 μm long) that lines fossil mouldic pores. Selected skeletal allochems including coralline red algae, rotalids, miliolids, encrusting foraminifera, and echinoid spines have been replaced and their cellular structures preserved by fabric retentive dolomite. Other skeletal grains, such as *Porites*, bivalves, ostracods, and *Halimeda* have been leached, but are identifiable due to their distinctively shaped molds and micrite envelopes. *Lepidocyclina* is absent in this facies. Porosity is predominantly fossil mouldic and ranges from 10 to 30%.

2.4.5 Fabric Destructive Finely Crystalline Dolomite Facies

The depositional fabrics of the original limestones in this facies have been completely obliterated by dolomitization. Matrix dolomite has a uniform appearance due to the destruction of all textural details and allochems (Fig. 2.5E). Dolomite is finely crystalline (crystals 20 to 100 μm long, average 70 μm) and limpid dolomite cement (crystals <300 μm long) is rare, filling only small fractures and voids. This facies is almost completely dolomitic; no calcite is apparent in thin section or SEM samples. The type and degree of porosity development are minimal, and not evident from available samples.

2.4.6 Sucrosic Dolomite Facies

The sucrosic dolomite in this facies is largely fabric destructive. Original limestone textures, where apparent, were *Lepidocyclina* packstones to grainstones. Dolomite crystals are large (0.5 to 1.5 mm), euhedral, and consist of dark, inclusion-rich cores surrounded by clear, limpid rims (Fig. 2.5F). Hollow dolomite rhombs are rare. Porosity (5 to 40%) transitions between fossil mouldic, vuggy, and intercrystalline forms depending on the size of the dolomite crystals and pores. Allochem ghost structures of *Lepidocyclina* are very common, and *Porites* ghosts are rare. Bivalves and gastropods have been leached, but are identified as fossil moldic vugs. A microstalactitic/pendant cement of mixed calcite/dolomite mineralogy (acicular crystals <500 μm long) has precipitated in larger vugs in the sucrosic dolomite matrix.

2.5 Facies Architecture

Most facies in the Brac Formation on Cayman Brac are isolated to a single locality (Fig. 2.6). This distribution may, however, be attributed in part to the limited accessibility of outcrops and availability of sampling sites for the Brac Formation. The distribution of lithology (i.e., limestone vs. dolostone) is dependent on location, as facies composed primarily of limestone and dolomitic limestone are largely restricted to the north coast of Cayman Brac, whereas facies composed of calcareous dolostone and dolostone are concentrated on the south coast. Facies are typically continuous in vertical sections, but vary markedly over short lateral distances. Lateral contacts between facies cannot be identified using available data because they are concealed between wells or inaccessible in outcrop.

The *Lepidocyclina* facies is most apparent on the north coast of Cayman Brac (section LCB), where it forms most of the bluff outcrop. This facies is apparent in large boulders at the base of the cliffs, which were incorrectly identified by Matley (1926) as having fallen from the top of the bluff. In this location, the *Lepidocyclina* facies extends from the base of the bluff to approximately two meters below the Brac-Cayman unconformity, where it is overlain by a thin bed of the Mollusc facies. The *Lepidocyclina* facies is also present in well KEL#1 on the south coast of Cayman Brac, though in this location it contains a greater proportion of dolomite than on the north coast.

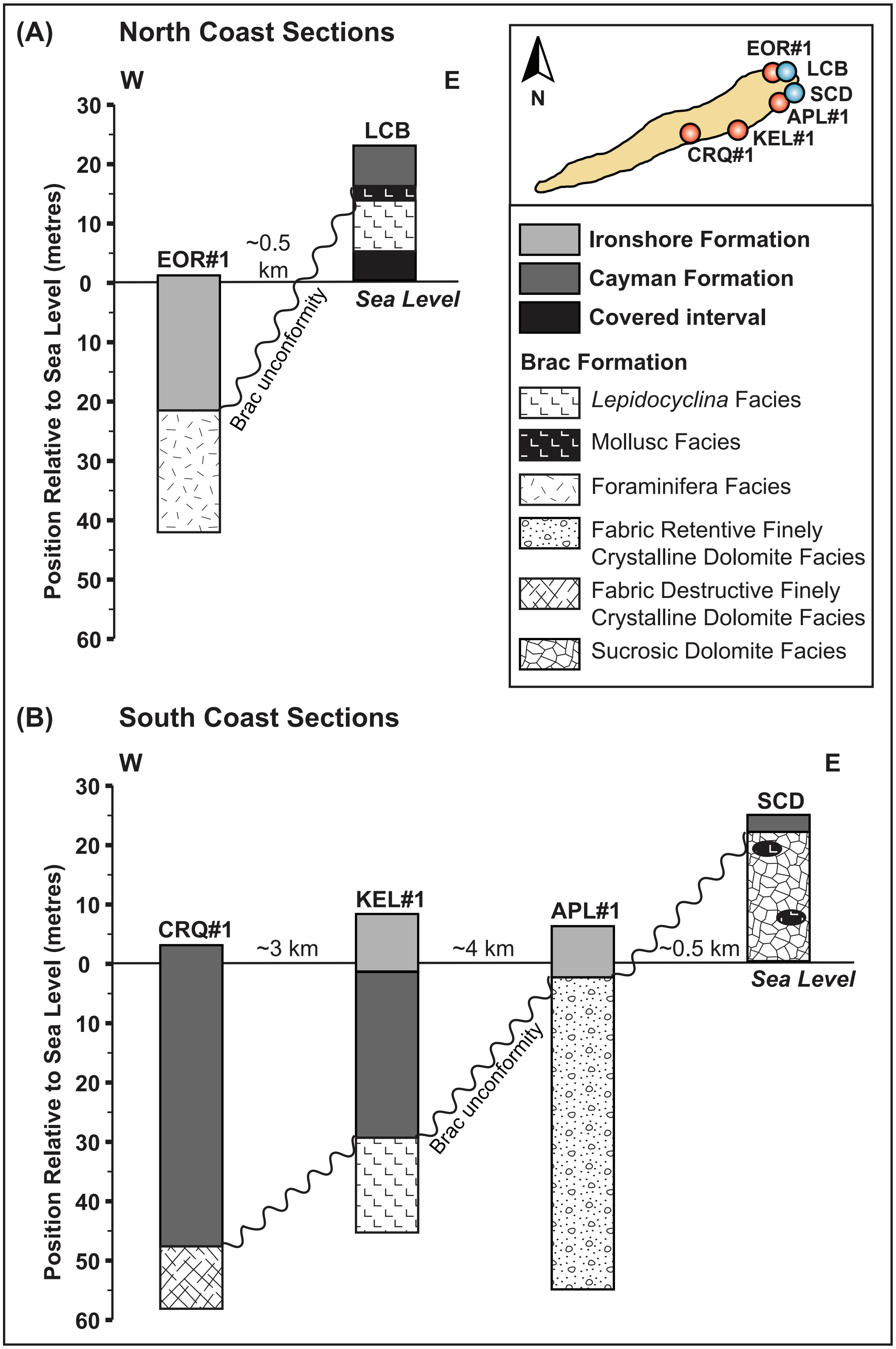

Figure 2.6 Facies distribution in **(A)** well EOR#1 and measured section LCB on the north coast, and **(B)** wells CRQ#1, KEL#1, APL#1 and measured section SCD on the south coast of Cayman Brac.

In section LCB on the north coast of Cayman Brac, the Mollusc Facies is limited to the uppermost 2 m of the Brac Formation. This facies is also present in section SCD on the south coast, where it forms the top 8 m of the Brac Formation below the unconformity (Jones and Hunter, 1994a). The relic limestone lenses contained in the sucrosic dolostone on the south coast are composed of the Mollusc Facies, and allochem ghosts from this facies are evident in the surrounding dolomitized strata.

The Foraminifera Facies is found primarily on the north coast of Cayman Brac and forms all of the Brac Formation in well EOR#1. Similar in lithology to the *Lepidocyclina* Facies but for the notable absence of *Lepidocyclina*, the Foraminifera Facies is found at a stratigraphically lower position than the former. The Foraminifera Facies is also present in thin limestone intervals (<2 m thick) in well APL#1 on the south coast, ~2 km south of EOR#1.

The Fabric Retentive Finely Crystalline Dolomite Facies is found only in well APL#1, but forms most (~90%) of the strata in that well. Intervals in APL#1 that have been less pervasively replaced by dolomite are composed of the Foraminifera Facies and exhibit gradational contacts with the fabric retentive dolostone.

Well CRQ#1 is the only locality where the Fabric Destructive Finely Crystalline Dolomite Facies exists. This facies spans the length of the well below the Cayman Formation and demonstrates the greatest lithologic homogeneity in all of the wells and sections surveyed in this study. No contacts between this facies and any others in the Brac Formation have been identified.

Though initially believed to be a dominant component of the Brac Formation, the Sucrosic Dolomite Facies is, in fact, restricted to the cliffs on the south coast of Cayman Brac. This facies is found only in the Pollard Bay member. Its lower and lateral contacts with other facies remain unidentified, and it is truncated upsection by the disconformity with the overlying Cayman Formation. The limestone lenses bounded by the sucrosic dolomite are composed of the Mollusc and *Lepidocyclina* Facies, and allochem ghost structures from both facies are evident in the Sucrosic Dolomite Facies. Localized occurrences of microsucrosic dolostone are evident in APL#1, but the small crystal size (<100 μm diameter) and limited vertical continuity (detectable only in single well cuttings) precludes extending this to the Sucrosic Dolomite Facies. Similarly, minute amounts of sucrosic dolomite exist in CRQ#1 amongst the fabric destructive finely crystalline dolomite, but its rarity again bars the extension of the Sucrosic Dolomite Facies to this well.

2.6 Facies Interpretation

Isolated carbonate banks are offshelf shoals separated from a continental shelf by water at least 200 m deep and tens of kilometers wide (Vecsei, 2000). The Brac Formation on Cayman Brac was deposited in such a setting, evidenced by its lack of terrigenous sediments, the restricted pinnacle geomorphology of the island, and its paleogeographic position during the Oligocene (Perfit and Heezen, 1978). Cayman Brac is a small, elongate (20 km long by 3 km wide), steep sided bank, and the Brac Formation shows no evidence of fringing reef or patch reef development. Instead, it is dominated by bioclastic sands and some mud. This contrasts sharply with the Cayman Formation and Pedro Castle Formation, which contain isolated coral thickets, and thus indicates that conditions were unfavourable for coral growth during deposition of the Brac Formation. The interaction between temperature, water depth, salinity, storm events, and relative changes in sea level influenced the development of various facies in the Brac Formation.

Interpretation of the depositional environment is based on the fossil assemblages and mud content (i.e., depositional fabrics) that characterize the different facies. Benthic foraminifera are especially useful as facies indicators in modern and ancient carbonate environments (Frost and Langenheim, 1974; Chaproniere, 1975; Hallock and Glenn, 1986; Banerjee et al, 2000; Geel, 2000; Gischler *et al.*, 2003), and are thus significant to the paleoenvironmental interpretation for the Brac Formation. Distribution of larger foraminifers is regulated by substrate and light conditions; thus, their value lies in their ability to be correlated with specific environments and record environmental changes (e.g., shallowing or deepening trends) in carbonate platform settings (Geel, 2000).

Determining the paleoecology of the Brac Formation is complicated by the fact that *Lepidocyclina*, the most abundant benthic foraminifer in many of the facies, is now extinct. Comparisons to modern carbonate bank environments are thus limited, and must rely on indirect evidence such as distributions of analogous modern large benthic foraminifers and assemblages containing extant species. Despite the abundance of *Lepidocyclina* in Oligocene strata of the Caribbean, there exists little consensus on its paleoecology. It is thus used in conjunction with the remaining faunal elements in the Brac Formation to determine the paleoenvironmental setting.

The greatest source of uncertainty in interpreting the paleoenvironment of *Lepidocyclina* is determining the optimal depth at which it flourished. In general, large, flat, perforate foraminifera tend to be located in deeper parts of the habitat, probably due to their dependence on symbiotic algae (Hallock and Glenn, 1986; Geel, 2000). Indeed, *Lepidocyclina* have been interpreted to occupy a forereef setting (~100 m deep) in packstones from Puerto Rico (Frost *et al.*, 1983), and an outer ramp setting in Tethyan carbonate ramp sequences, where flatter forms were proposed to dominate softer substrates and deeper habitats (Buxton and Pedley, 1989). Haig (1985) interpreted *Lepidocyclina*-bearing mudstones from

Papua New Guinea to be deposited at depths in excess of 400 m, although it was noted that *Lepidocyclina* were likely transported downslope from the photic zone (depth <150 m). Cole (1961), however, observed that lepidocyclinids with robust test walls could be found in warm, shallow environments in contrast with more delicate individuals from cooler, deeper environments. Whereas Amirshahkarami *et al.* (2007) proposed that *Lepidocyclina* packstones to grainstones of the Asmari Formation in southwest Iran were deposited in a middle ramp to open marine environment, Vaziri-Moghaddam *et al.* (2006) suggested that they could have been deposited anywhere from the outer slope to shallow, high-energy shoals along the platform margin. Oligocene *Lepidocyclina* associations from western Australia were interpreted by Chaproniere (1975) to originate in sea grass communities in water less than 12 m deep with normal marine salinity. Similarly, Bosellini and Russo (1992) interpreted lepidocyclinid-bearing grainstones from the Castro Limestone in southern Italy as a shallow reef flat facies, analogous to sand flats in modern reefs stabilized by the sea grass *Thalassia*, *Halimeda*, and scattered corals. Western European lepidocyclinids were interpreted by Geel (2000) to occupy shallow, high-energy environments with normal marine salinity, such as the reef crest, backreef shoals with coral thickets, and reef front. By modelling foraminiferal distributions in Philippine cores, Hallock and Glenn (1986) interpreted red algae-lepidocyclinid packstones to have formed on an algal-stabilized open platform at depths shallower than 5 m. Previous work on the Brac Formation indicates that it was deposited on an isolated bank in water 5 to 10 m deep (Jones and Hunter, 1994a). Clearly, paleoecological interpretations of *Lepidocyclina* can vary widely, and paleoenvironmental interpretation of the Brac Formation must therefore be inferred from associations with other benthic foraminifera and biota.

Miliolid and rotalid foraminifera are numerically the next most abundant constituents of wackestones to grainstones in the Brac Formation. Miliolids predominate in shallow water environments with low turbulence, and their presence often indicates a restricted lagoonal or nutrient-rich backreef environment (Geel, 2000). Although they are capable of tolerating high salinity, the abundance of miliolids around reef environments at normal salinities means that they do not necessarily indicate hypersaline conditions (Hallock and Glenn, 1986). Rotalids are found in very shallow, turbulent reef environments at depths between 0 and 40 m (Chaproniere, 1975; Geel, 2000). Unlike miliolids, however, rotalids are commonly stenohaline with tolerance limits between 30 and 45‰ (Hallock and Glenn, 1986). The encrusting rotalid *Homotrema rubrum* is similarly found in shallow, high-energy, reef margin environments (Gischler *et al.*, 2003). *Carpenteria* is typical of shallow water conditions (water depths <30 m), and may be affixed to a solid substrate (Chaproniere, 1975). Planktonic foraminifera (e.g., globigerinids and globorotalids), though relatively rare in the Brac Formation, typically indicate open marine (basinal) conditions with increasing abundance seaward (Chaproniere, 1975; Geel, 2000). However, storm-generated waves can homogenize sediments by transporting constituent foraminifera across a reef crest, thereby introducing forereef species (i.e., planktonic forms) into lagoonal environments (Li and Jones, 1997; Li *et al.*, 1998).

Assemblages of the most abundant benthic foraminifera are integrated to determine the environment of deposition for the Brac Formation. By mapping the distribution of Paleogene foraminifera, Geel (2000; his Fig. 2) demonstrated that lepidocyclinids, rotalids, and miliolids overlapped in backreef shoals with coral thickets – i.e., a moderate to high-energy setting. Likewise, Hallock and Glenn (1986) interpreted their Red Algal-Larger Foraminiferal Packstone Facies (with similar biota and textures to the *Lepidocyclina* Facies described herein) to have formed on an algal-stabilized open platform (<5m depth) subject to winnowing by waves and tides. In such a setting, carbonate muds could settle among the grains during periods of low wave activity, or become resuspended and carried away during winnowing periods to produce fabrics characteristic of the Brac Formation. It must be noted, however, that an open platform should exhibit a more diverse assemblage of benthic foraminifera than a restricted platform due to fluctuations in circulation and salinity (Gischler *et al.*, 2003). The relatively restricted foraminiferal assemblage in the Brac Formation might therefore indicate some type of environmental stress (though by which parameter is not apparent), or it may simply be a function of post-mortem taphonomic processes (cf. Li and Jones, 1997). Based on the foraminiferal evidence then, it seems probable that the Brac Formation was deposited on a shallow, moderate- to high-energy carbonate bank that may have been partially restricted from normal marine circulation.

The depositional fabrics and faunal content of all facies in the Brac Formation support the paleoenvironmental interpretation suggested by the foraminiferal assemblage. Jones and Hunter (1994a) conducted a facies analysis of the Brac Formation from outcrop and proposed that it was deposited in a low-energy, shallow water environment. This conclusion was based on the restricted foraminiferal assemblage and paucity of evidence for reef development. Data obtained from the four wells in this study, however, indicate that energy levels were higher than previously suggested, due to the fact that robust and encrusting organisms are more common in the well samples than they are in outcrop. Coral rubble and abraded coralline red algae fragments compose a significant part of the Foraminifera Facies (~50% of biota volumetrically), indicating that small coral heads may have developed and contributed sediment to the Brac Formation. The abraded coral and red algal fragments, well-sorted foraminiferal grains, and relatively small amount of mud matrix in the wackestones to grainstones of the Brac Formation collectively indicate that deposition occurred in a shallow (probably less than 10 m deep), moderate-energy carbonate bank setting (cf. Vaziri-Moghaddam *et al.*, 2006).

Variations in fabrics and biota between facies in the Brac Formation may indicate small-scale heterogeneities in bank morphology during deposition. Relief exists on each of the unconformities that separate the various formations in the Bluff Group; it might therefore be plausible to infer some amount of preexisting topography on the bank during deposition. In a shallow setting, even small changes in depth due to topographic variations or slight fluctuations in sea level may be enough to create ecological niches favourable to certain organisms. Cay Sal Bank, a submerged platform in the Bahamas, may be considered a modern analogue for the Brac Formation based on its biotic structure. With a lagoonal surface 9 to 16 m below sea level and only rare patch reefs at least 30 m below the surface on deeper margins, the biological poverty of Cay Sal Bank is maintained through stresses caused by an open, poorly developed rim (Goldberg, 1983). The establishment of four major biotic zones on the surface of the bank (including a *Thalassia* zone) is interpreted to reflect control by wind-induced stress and periodic storm events (Goldberg, 1983). The Brac Formation may have been deposited in such a setting, where various facies could have developed in close proximity but physical control by shallow water processes prohibited coral reef growth. Serranilla Bank, a 10 to 40 m deep carbonate bank located on the Nicaraguan Rise, also lacks coral reefs and has only a thin sediment cover due to unfavorable environmental conditions (Triffleman *et al.*, 1992). It may thus serve as another modern analogue for the Brac Formation. Sorting trends in the type and size of sediments can also be caused by a physical energy flux between the windward and leeward margins on a carbonate platform (Triffleman *et al.*, 1992). Such a relationship could account for the preferential accumulation of coarse-grained molluscs and corals along the south coast of Cayman Brac. The appearance of coral debris and molluscs in the upper part of the Brac Formation may represent a period when carbonate productivity surpassed the creation of accommodation space (possibly triggered by a fall in sea level).

Collectively, all available information gathered from the biotic assemblages, depositional textures, and comparisons with modern bank environments indicates that the Brac Formation was deposited in a shallow, moderate-energy bank setting. The *Lepidocylina*, Mollusc, and Foraminifera Facies probably formed in depths less than 10 m, evidenced by shallow water foraminiferal assemblages and well-sorted packstones and grainstones produced by winnowing currents. The environment of deposition may have been subject to physical stress, resulting in a restricted foraminiferal assemblage and barring significant development of coral reefs beyond small patch reefs located on submerged margins.

2.7 Synopsis

The addition of subsurface well data to known surface exposures of the Brac Formation has facilitated a more detailed classification of its internal architecture. The sedimentology of the new well samples has been integrated with previous sedimentological descriptions from outcrop to refine the stratigraphy of the formation, provide a facies analysis, and interpret its depositional environment. Specifically:

- The Brac Formation is dominated by limestone, dolomitic limestone, and finely crystalline dolostone in wells CRQ#1, KEL#1, APL#1, EOR#1, and section LCB.
- Coarsely crystalline sucrosic dolostone is only found on the south coast of Cayman Brac, in section SCD.
- The sucrosic dolostone is herein defined as the Pollard Bay member of the

Brac Formation due to its local pervasiveness and restricted extent.

- Six different facies have been defined in the Brac Formation based on lithology (i.e., limestone vs. dolostone) and fossil content. These include:
  a. *Lepidocyclina* Facies
  b. Mollusc Facies
  c. Foraminifera Facies
  d. Fabric Retentive Finely Crystalline Dolomite Facies
  e. Fabric Destructive Finely Crystalline Dolomite Facies
  f. Sucrosic Dolomite Facies
- Most facies in the Brac Formation are restricted to a single locality
- Limestone facies are located primarily on the north coast of Cayman Brac, whereas dolomitic facies tend to be concentrated on the south coast.
- The paleoecology of the Brac Formation was determined by analyzing fossil assemblages (with particular emphasis on benthic foraminifera), depositional fabrics (i.e., mud content), and comparisons with modern bank environments.
- The Brac Formation was deposited on a shallow (<10 m), moderate-energy carbonate bank with no evidence for reef development. It is dominated by shallow water foraminiferal assembles and well-sorted packstones produced by winnowing currents.

Chapter Three: Isotope Geochemistry

3.1 Introduction

The rocks of the Brac Formation are comprised of limestones, dolomitic limestones, and dolostones that have undergone several stages of diagenesis. Where present, calcite in the Brac Formation is derived from a number of sources including micritic matrix, bioclasts, and sparry and microstalactitic meteoric cements. Each of these sources may be present in varying amounts in a given sample interval or well, imparting a high degree of heterogeneity to the sample suite.

Dolomite of the Brac Formation is typically crystalline (< 20 μm) and is commonly intermixed with calcite on a micrometer scale. As such, physical separation of calcite and dolomite for isotopic analyses was impossible. It was therefore necessary to isolate dolomite and calcite chemically through a differential phosphoric acid extraction process, possibly imparting additional error to the subsequent analyses.

Unsorted bulk samples of the rock chips were prepared for isotopic analyses from selected well cuttings; thus $\delta^{18}O$ and $\delta^{13}C$ values of analyzed minerals represent an average isotopic composition of the sample from each given interval (cf. MacNeil, 2001).

3.2 Calcite Isotopes

3.2.1 Results of Calcite Isotope Analyses

Results of oxygen, carbon, and strontium isotope analyses of calcite in the Brac Formation are presented in Appendix 1. $\delta^{18}O$ values of calcite (n=138) range from -6.11‰ to +1.24‰ and $\delta^{13}C$ values range from -10.68‰

to +1.16‰. The average $\delta^{18}O$ composition of calcite in all wells and sections in the Brac Formation is -1.82‰ and the average $\delta^{13}C$ value is -2.34‰. The average strontium isotope ratio of calcite (n=12), measured from samples from EOR#1, APL#1, and KEL#1, is 0.708569 ± 0.000022. $^{87}Sr/^{86}Sr$ values range from 0.708033 ± 0.000010 to 0.709144 ± 0.000025.

A cross-plot of $\delta^{18}O$ and $\delta^{13}C$ values (Fig. 3.1) displays a variable carbon signature, a relatively more constant oxygen signature, and a positive covariant trend. The average $\delta^{18}O$ and $\delta^{13}C$ values of calcite vary slightly between wells and sections (Fig. 3.2). $\delta^{18}O$ and $\delta^{13}C$ values are most variable in WOJ-2 (equivalent to the upper part of SCD) and the upper half of APL#1 (at depths less than 27 m). WOJ-2 is characterized by the lowest $\delta^{13}C$ values whereas KEL#1 contains the highest $\delta^{18}O$ and $\delta^{13}C$ values. In APL#1, there is a trend toward more positive $\delta^{18}O$ and $\delta^{13}C$ values with depth. Trends in $\delta^{18}O$ and $\delta^{13}C$ values cannot be correlated between sequences.

3.2.2 Interpretation of Calcite Isotopes

The isotopic signature of calcite in the Brac Formation represents the average of original sediment components and various stages of diagenesis. The $\delta^{18}O$ and $\delta^{13}C$ values obtained from the calcite reflect compositional averages of at least four types of calcite: micrite, bioclasts, sparry cement, and microstalactitic cement. The total volumetric abundance of the latter type of cement is small (< 1% of samples) and is present only in section SCD. It is thus likely that the microstalactitic cement contributes only minimally to the average $\delta^{18}O$ and $\delta^{13}C$ values. Despite the variety of calcite populations identified in the samples, XRD analyses reveal that all of the calcite is low magnesium-calcite (mean $MgCO_3$ = 1.5 to 3.5%). It is therefore likely that the original marine calcite was stabilized through isotopic exchange with diagenetic fluids in the meteoric phreatic zone

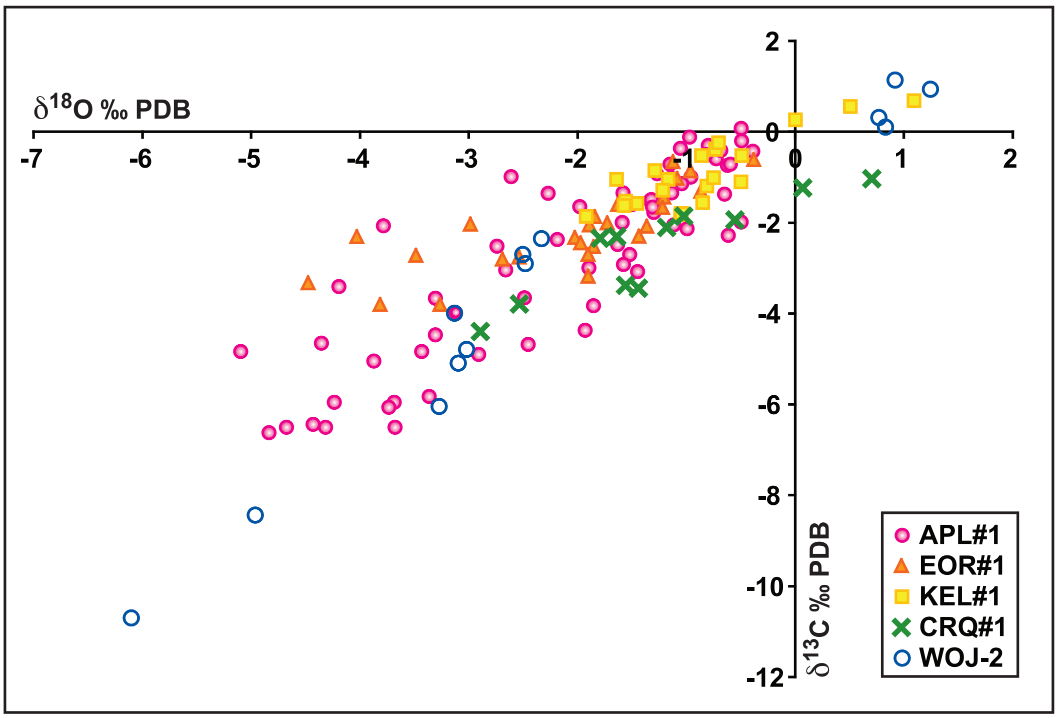

Figure 3.1 $\delta^{18}O$ and $\delta^{13}C$ isotope signatures of calcite in the Brac Formation on Cayman Brac (n = 138). WOJ-2 is equivalent to the upper part of section SCD.

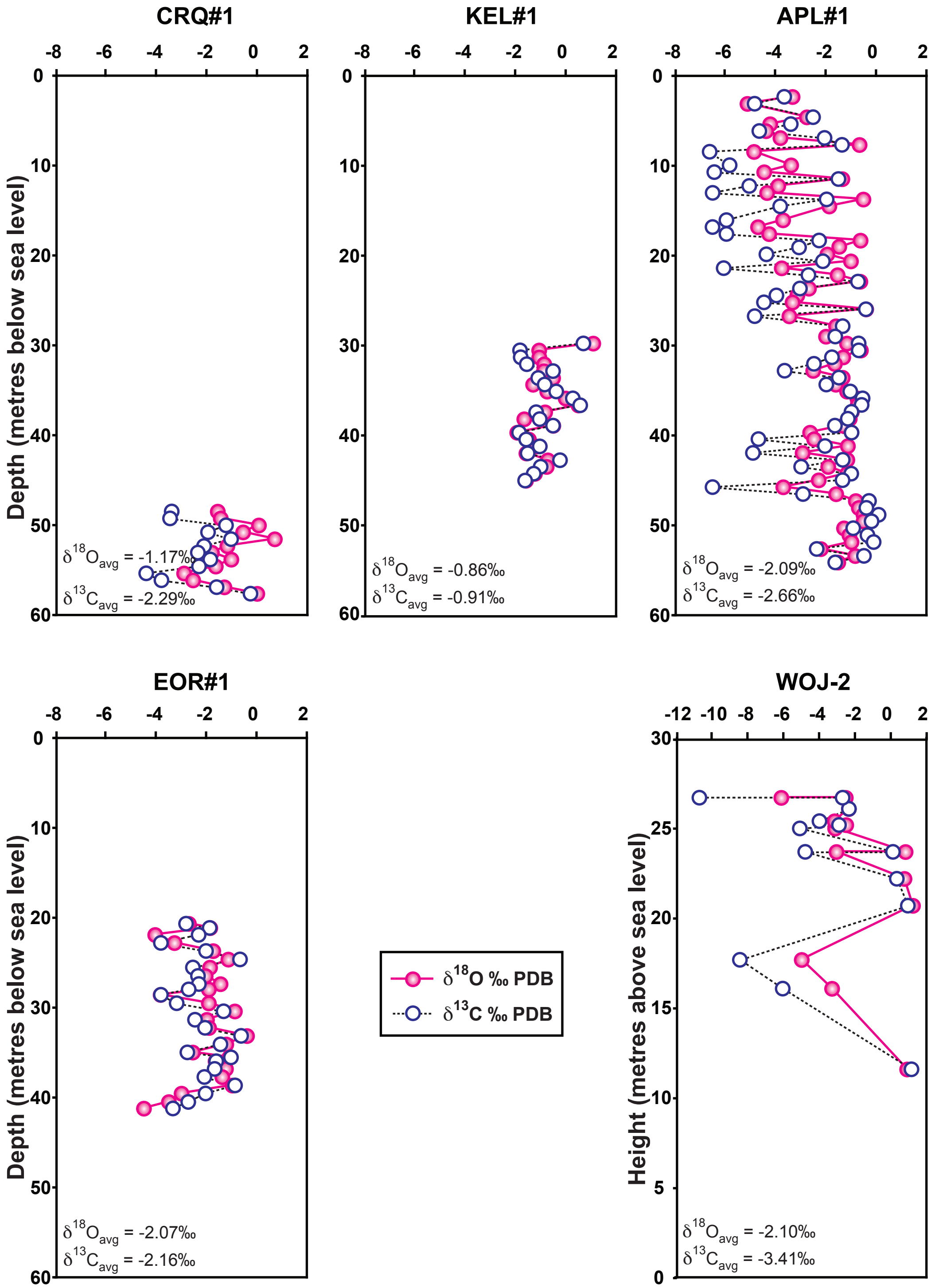

Figure 3.2 Depth profiles of $\delta^{18}O$ and $\delta^{13}C$ values of calcite in the Brac Formation. WOJ-2 is equivalent to the upper part of section SCD. $\delta^{18}O$ and $\delta^{13}C$ signatures are most variable in WOJ-2 and in the upper half of APL#1.

(e.g., Allan and Matthews, 1982; Quinn, 1991; MacNeil, 2001). Pore-occluding calcite spar, pervasive in all locations and representing a late stage of diagenesis, probably precipitated in the meteoric phreatic environment (cf. Jones *et al.*, 1984). It is thus assumed that the various calcite populations in the Brac Formation have similar $\delta^{18}O$ and $\delta^{13}C$ signatures because they were formed or stabilized by comparable fluids in a common diagenetic environment (cf. MacNeil, 2001).

Assuming that the mean $\delta^{18}O$ accurately represents the calcite in the Brac Formation, paleotemperatures were calculated using the low temperature oxygen isotope fractionation equation between calcite and water of Kim and O'Neil (1997):

$$1000 \ln \alpha_{calcite\text{-}water} = 18.03 \times 10^{3}T^{-1} - 32.42 \qquad [1]$$

where the fractionation factor $\alpha = (1000+\delta^{18}O_{calcite}‰SMOW)/(1000+\delta^{18}O_{water}‰SMOW)$, and temperature (T) is measured in kelvins. Conversions between SMOW and PDB standards are expressed by the following equations (Kyser, 1987):

$$\delta^{18}O_{V\text{-}SMOW} = (1.03091)(\delta^{18}O_{PDB}) + 30.91 \qquad [2a]$$

$$\delta^{18}O_{PDB} = (0.097002)(\delta^{18}O_{V\text{-}SMOW}) - 29.98 \qquad [2b]$$

in which the standards Vienna Standard Mean Oceanic Water (V-SMOW) and SMOW are considered identical (Kyser, 1987).

Groundwater temperatures in the Cayman Islands are relatively constant year round, averaging 27-30°C in the shallow zone and 25-27°C in the deeper saline zone (Ng, 1990). The paleotemperatures (PT) calculated for calcite formation (Table 3.1) indicate that the $\delta^{18}O$ of calcite was in equilibrium with seawater (calculated PT = 28.9°C) or saline water (PT = 25.3°C), concordant with modern measured temperatures. The paleotemperatures calculated for calcite formation based on highly brackish water (PT = 13.7°C), lightly brackish water (PT = 3.4°C), and fresh ground water (PT = 1.8°C) are unreasonably low for a

Table 3.1 Calculated (using the mean $\delta^{18}O_{calcite}$ in the Brac Formation) temperature of calcite diagenesis, using data collected from different types of water in the Cayman Islands (Ng, 1990). Oxygen isotope fractionation equation for calcite from Kim and O'Neil (1997). Mean $\delta^{18}O_{calcite}$ = -1.82‰ PDB or +29.03‰ SMOW.

Water Type	Average $\delta^{18}O$ composition (‰ SMOW)	Salinity	Calculated temperature of calcite formation (ºC)
Fresh ground water	-4.54	<1.01 ‰	1.8
Lightly brackish water	-4.16	<15% seawater	3.4
Highly brackish water	-1.82	>15% seawater	13.7
Saline water	0.63	~35 ‰	25.3
Normal seawater	1.34	~35 ‰	28.9

tropical climate.

Although the calculated paleotemperatures seem to suggest that marine-derived fluids mediated calcite alteration and precipitation in the Brac Formation, numerous studies have suggested that such calcite was typically formed in the meteoric phreatic zone (e.g., Allan and Matthews, 1982; James and Choquette, 1984; Jones *et al.*, 1984; Quinn, 1991; MacNeil, 2001). Before accepting that the calculated paleotemperatures for calcite stabilization are accurate, potential limitations to this method must be considered. The fundamental issue is that the paleotemperatures derived from "old" calcite are being compared with modern day hydrological systems.

Paleoclimate studies of ancient meteoric systems are hindered by secular variations in the isotopic composition of seawater, thereby causing uncertainty about the $\delta^{18}O$ values of paleometeoric waters (Lohmann, 1988). Furthermore, because the $\delta^{18}O$ values of meteoric water reflect numerous variables including altitude, latitude, orographic (land) effect, temperature, weather patterns, and isotopic composition of coeval marine water, it is not possible to identify meteoric diagenesis in ancient carbonate sequences based on an absolute calcite $\delta^{18}O$ value alone (Lohmann, 1988). Orographic effects caused by Rayleigh fractionation are probably minimal on Cayman Brac, however, and likely do not cause additional fractionation of meteoric water. Additionally, laboratory error (i.e., contamination of calcite CO_2 by simultaneous dissolution of calcian dolomite) may skew $\delta^{18}O_{calcite}$ toward artificially positive values. In light of these observations, it is obvious that the calculated paleotemperature of calcite stabilization should be used only as a guide in the interpretation of the diagenetic environment.

If the relatively positive calcite $\delta^{18}O$ signature and accordingly cold paleotemperature calculated for calcite stabilization are indeed accurate, a number of environmental factors could possibly explain these anomalous values.

(a) The calcite was geochemically stabilized in saline water with a composition similar to normal seawater or that modified only slightly by rock-water interaction. The saline water would have been enriched in ^{18}O relative to fresh water, contributing to more positive $\delta^{18}O$ values.

(b) The water temperature may have been higher than typical modern Caribbean values. Higher water temperatures would cause increased evaporation and oxygen isotope fractionation, resulting in a concentration of ^{18}O in surrounding fluids and precipitating calcite with higher $\delta^{18}O$ values.

(c) Hurricanes cause significant $\delta^{18}O$ depletion in storm precipitation, to values of 10 to 30‰ lower than source seawater (Lawrence, 1998; Lawrence *et al.*, 2002; Miller *et al.*, 2006). These tropical storm events may reduce meteoric $\delta^{18}O$ values and yield artificially cool calculated temperatures of calcite stabilization.

(d) The calcite $\delta^{18}O$ value is not in equilibrium with $\delta^{18}O$ values of modern groundwaters. Relatively positive calcite $\delta^{18}O$ values may reflect equilibrium with previous fluids that had different $\delta^{18}O$ compositions than those present today.

(e) Recrystallization or alteration of calcite in the meteoric-marine, mixed water zone resulted in the covariance of calcite $\delta^{18}O$ and $\delta^{13}C$ values. Variations in water chemistry are reflected by a mixed calcite $\delta^{18}O$ signal.

The first three possibilities proposed to explain the unusual calcite $\delta^{18}O$ values can be eliminated based on assorted lines of evidence. First, coarse calcite cements, such as those prevalent in the Brac Formation, are generally considered indicative of precipitation in the meteoric phreatic zone (James and Choquette, 1984; Jones *et al.*, 1984; Quinn, 1991; Humphrey, 2000). Given the abundance of these cements and corresponding absence of marine cements, saline water can probably be eliminated as a fluid responsible for mediating calcite diagenesis.

Second, the possibility that warm oceanic waters circulated through the Brac Formation is in contrast with the widely recognized, long-term, unidirectional Cenozoic cooling trend (Zachos *et al.*, 2001). Although tectonically driven circulation of magmatic-hydrothermal solutions through Grand Cayman has been postulated on the basis of Sr isotope data (Machel, 2000), the validity of this claim has been debated (Jones and Luth, 2003a). Additionally, there is no evidence for upward movement of heated fluids from the basement rocks. Finally, it is unlikely that hurricanes are capable of altering $\delta^{18}O$ compositions of groundwaters in the Cayman Islands for any considerable length of time. Given the high porosity and groundwater recharge rates in the Cayman Islands (Ng *et al.*, 1992), it seems improbable that the calcite $\delta^{18}O$ signatures record the isotopic effects of secular storm events.

The complex hydrogeology of the Cayman Islands is consistent with the possibility of chemical disequilibrium between calcite $\delta^{18}O$ values and modern groundwaters. The highly variable hydrologic system is the product of a severely karsted terrain characterized by extensive secondary porosity and complex fracture systems. Fluctuations in groundwater composition can be attributed to low water table elevations, limited storage capacity of fresh water lenses, rapid recharge and discharge rates, and a tenuous balance between rainwater recharge and evapotranspiration (Ng *et al.*, 1992). Given the instability of the hydrologic system, it is probable that the $\delta^{18}O$ values of groundwater vary considerably with location and time. Consequently, the isotopic composition of ancient diagenetic fluids was probably different than that of modern groundwaters. It is therefore likely that calcite $\delta^{18}O$ values are in disequilibrium with modern groundwaters, and instead reflect equilibrium with a paleohydrologic system.

Physical and chemical alteration of calcite in a mixed water zone is supported by petrographic and isotopic evidence. Grain contacts between micrite crystals indicate that the original calcite has undergone at least one phase of recrystallization (B. Jones, pers. comm.). It is probable that this alteration from the original depositional fabric was accompanied by a chemical re-equilibration with fluids in the meteoric-marine mixing zone, evidenced by the covariant trend in $\delta^{18}O$ and $\delta^{13}C$ values. Recrystallization must have involved at least some component of meteoric water, as depleted $\delta^{13}C$ values reflect introduction of soil CO_2 during periods of emergence and negative $\delta^{18}O$ values indicate modification of the original marine isotope signal by meteoric water (Lohmann, 1988). Despite the inconclusive nature of the paleotemperature calculation, the overall $\delta^{18}O$ signature of calcite in the Brac Formation probably reflects recrystallization in an active hydrologic system by a mixed water solution.

Mixed meteoric and marine solutions are generally considered unfavourable for carbonate mineral stabilization due to rapid changes in water chemistry. Ng (1990) and MacNeil (2001), however, also concluded that calcite in the Cayman Formation and Pedro Castle Formation was probably stabilized in the presence of mixed fluids. Simple groundwater-seawater mixing models fail to incorporate the variety of fluid interactions possible and their effects on the chemical equilibrium conditions of complicated natural water-rock systems (Ng, 1990). Additionally, problems with the sampling method may be at issue, as whole-rock sampling causes physical mixing of compositional end members (Budd, 1997; Jones *et al.*, 2001). As a result, the mean $\delta^{18}O_{calcite}$ value may actually represent an intermediate signal between true marine and meteoric fluid end members that variably influenced calcite diagenesis (MacNeil, 2001). It can be concluded that calcite in the Brac Formation underwent multiple stages of diagenesis in a zone characterized by fluctuating water chemistry, and that $\delta^{18}O_{calcite}$ values are in disequilibrium with modern groundwaters.

3.3 Dolomite Isotopes

3.3.1 Results of Dolomite Isotope Analyses

$\delta^{18}O$, $\delta^{13}C$, and $^{87}Sr/^{86}Sr$ analyses of dolomite in the Brac Formation are tabulated in Appendix 1. $\delta^{18}O$ and $\delta^{13}C$ values (n=156) range from -4.64‰ to +4.73‰ and -4.53‰ to +3.80‰, respectively. The average $\delta^{18}O$ value in all sequences is +1.39‰, and the average $\delta^{13}C$ value is +1.36‰. Strontium isotope ratios of dolomite (n=11) range from 0.708605 ± 0.000016 to 0.709155 ± 0.000025. The average $^{87}Sr/^{86}Sr$ ratio, determined from samples from APL#1, KEL#1, and CRQ#1, is 0.708900 ± 0.000017.

Cross-plotting dolomite $\delta^{18}O$ and $\delta^{13}C$ values reveals a scattered to positive covariant trend in EOR#1 and APL#1 – the only wells that contain negative oxygen and carbon isotope values (Fig. 3.3). Samples from WOJ-2 and WOJ-7 (the combined equivalent of SCD), KEL#1, and CRQ#1 are clustered in a field from $\delta^{18}O$ +1‰ to +3‰ and from $\delta^{13}C$ 0‰ to +3‰. Plotting $\delta^{18}O$ and $\delta^{13}C$ against depth (Fig. 3.4) reveals highly variable isotope signatures in EOR#1 and APL#1. In contrast, $\delta^{18}O$ and $\delta^{13}C$ compositions in CRQ#1, KEL#1, WOJ-2, and WOJ-7 remain relatively constant with depth. Trends in $\delta^{18}O$ and $\delta^{13}C$ signatures are not correlative between wells and sections.

3.3.2 Interpretation of Dolomite Isotopes

Isotopic analyses of $\delta^{18}O$ and $\delta^{13}C$ from dolomite in the Brac Formation were completed in order to determine the source of the diagenetic fluids. This was possible because seawater, being many times saturated with respect to Mg^{2+}, is the only fluid generally considered capable of supplying enough magnesium to permit carbonate island dolomitization (Land, 1985; Budd, 1997). Therefore, seawater, or a mixture of other fluids (e.g., fresh or evaporated hypersaline water) with seawater must be regarded as a potential solution in which carbonate island

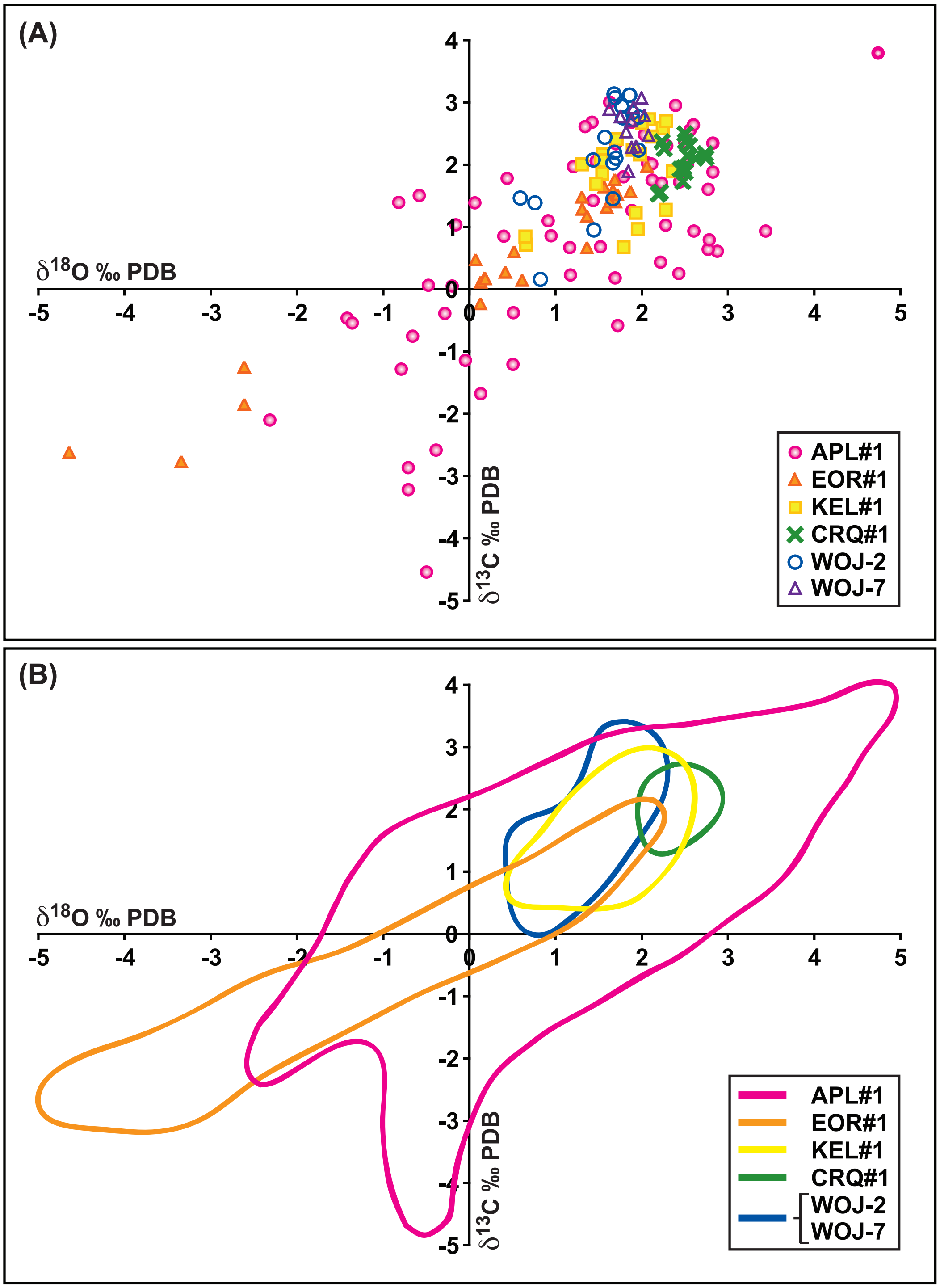

Figure 3.3 (A) $\delta^{18}O$ and $\delta^{13}C$ isotope compositions of dolomite in the Brac Formation on Cayman Brac (n = 156). WOJ-2 and WOJ-7 are the combined equivalent of section SCD. **(B)** Data fields of wells and sections plotted in **A**. APL#1 and EOR#1 are the only wells with negative $\delta^{18}O$ and $\delta^{13}C$ values. KEL#1, CRQ#1, WOJ-2 and WOJ-7 are characterized by positive $\delta^{18}O$ and $\delta^{13}C$ values in overlapping fields.

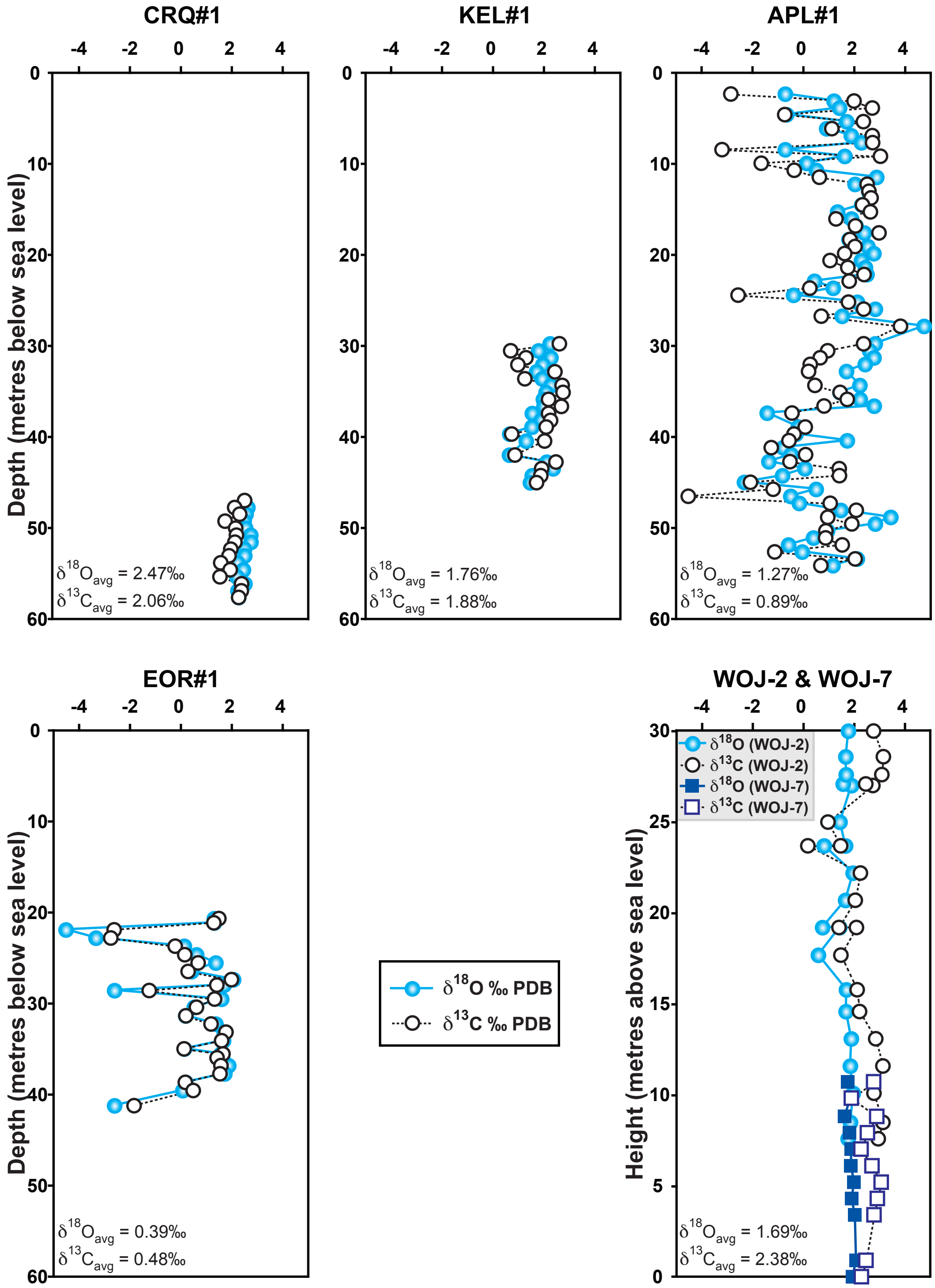

Figure 3.4 Depth profiles of $\delta^{18}O$ and $\delta^{13}C$ values of dolomite in the Brac Formation. WOJ-2 and WOJ-7 are equivalent to section SCD. $\delta^{18}O$ and $\delta^{13}C$ signatures are most variable in APL#1 and EOR#1, but remain relatively unchanged with depth in CRQ#1, KEL#1, WOJ-2, and WOJ-7.

dolomites may form. Fresh and marine waters possess distinctive oxygen and carbon isotope ratios due to the depletion of ^{18}O (Epstein and Mayeda, 1953) and ^{13}C (Allan and Matthews, 1982) in fresh water relative to marine water. Similarly, evaporated seawater is enriched in ^{18}O and ^{13}C relative to normal marine and fresh waters. These relationships are significant because carbonate minerals precipitate at isotopic equilibrium with surrounding fluids (McCrea, 1950; Epstein et al., 1953; Emiliani, 1955; Clayton and Degens, 1959). Analysis of $\delta^{18}O$ and $\delta^{13}C$ in diagenetic dolomite may therefore help to "fingerprint" the fluids that mediated diagenesis and identify the dolomitization regime that affected the Brac Formation.

Oxygen isotope analyses are fundamental to the interpretation of conditions affecting dolomite formation. This is because the large volumes of Mg-bearing fluids required to alter limestone to dolostone buffer the oxygen isotope composition of the resultant dolomite, causing the $\delta^{18}O$ of the dolomite to be in equilibrium with the surrounding fluids (Land, 1980, 1983). Furthermore, due to the temperature dependence of oxygen isotope fractionation between dolomite and water (Schmidt et al., 2005; Vasconcelos et al., 2005), dolomite $\delta^{18}O$ values can also be used as a paleothermometer to determine the temperature at which dolomitization took place. The practical use of dolomite $\delta^{18}O$ values, however, remains limited by the high degree of uncertainty regarding the assumptions made in any interpretive model (cf. Budd, 1997).

Carbon isotope analyses provide another means by which the source of diagenetic fluids in island dolomites may be identified. It is generally understood that the $\delta^{13}C$ compositions of such dolomites are positive because they have inherited a marine carbon signature from the precursor sediment or rock (Land, 1992). Due to the enrichment of carbon in limestones relative to water, it is unlikely that the $\delta^{13}C$ value of dolomite will be significantly altered from its precursor (Land, 1992). In vertical stratigraphic profiles, excursions of $\delta^{13}C$ toward 0‰ may be found near subaerial exposure surfaces (paleokarst horizons) and reflect inheritance from soil-zone derived carbon (Allan and Matthews, 1982; Vahrenkamp and Swart, 1994). Negative $\delta^{13}C$ values that are unrelated to subaerial exposure horizons may reflect admixing of oxidized organic carbon during dolomitization, and can possibly indicate a fresh water component in the dolomitizing solution (Budd, 1997). Covarying $\delta^{18}O$ and $\delta^{13}C$ values in dolomites may reflect precipitation in a fresh water-seawater mixing zone (Lohmann, 1988). To date, however, examples of dolomites with covariant $\delta^{18}O$ and $\delta^{13}C$ and supporting petrographic evidence are rare (e.g., Ward and Halley, 1985).

Interpreting the geochemistry of a dolomite body requires knowledge of the number of compositional populations of dolomite in the dolostones (Budd, 1997; Jones *et al.*, 2001). Most isotopic analyses of dolostones, however, are based on whole-rock analysis. For heterogeneous dolostones then, analytical results are average values of multiple compositional populations of dolomite crystals (Budd, 1997). By microsampling dolomite populations at a finer resolution, the interpretation of geochemical data might be improved (e.g., Banner and Hanson, 1990; Wheeler *et al.*, 1999). In the Brac Formation, however, individual crystals are commonly < 20μm long and the calcite and dolomite zones are thinner than the spot size of many analytical techniques. Therefore, microsampling is not possible in this formation and interpretation of results from carbon and oxygen isotope data remains limited.

Petrographically, dolostone in the Brac Formation consists of three types of replacement dolomite (finely crystalline fabric destructive, finely crystalline fabric retentive, and sucrosic) and one type of dolomite cement (limpid, isopachous cement). XRD analyses of these dolostones, however, indicate that they are compositionally unimodal (Fig. 3.5). The mol % $CaCO_3$ (%Ca) of

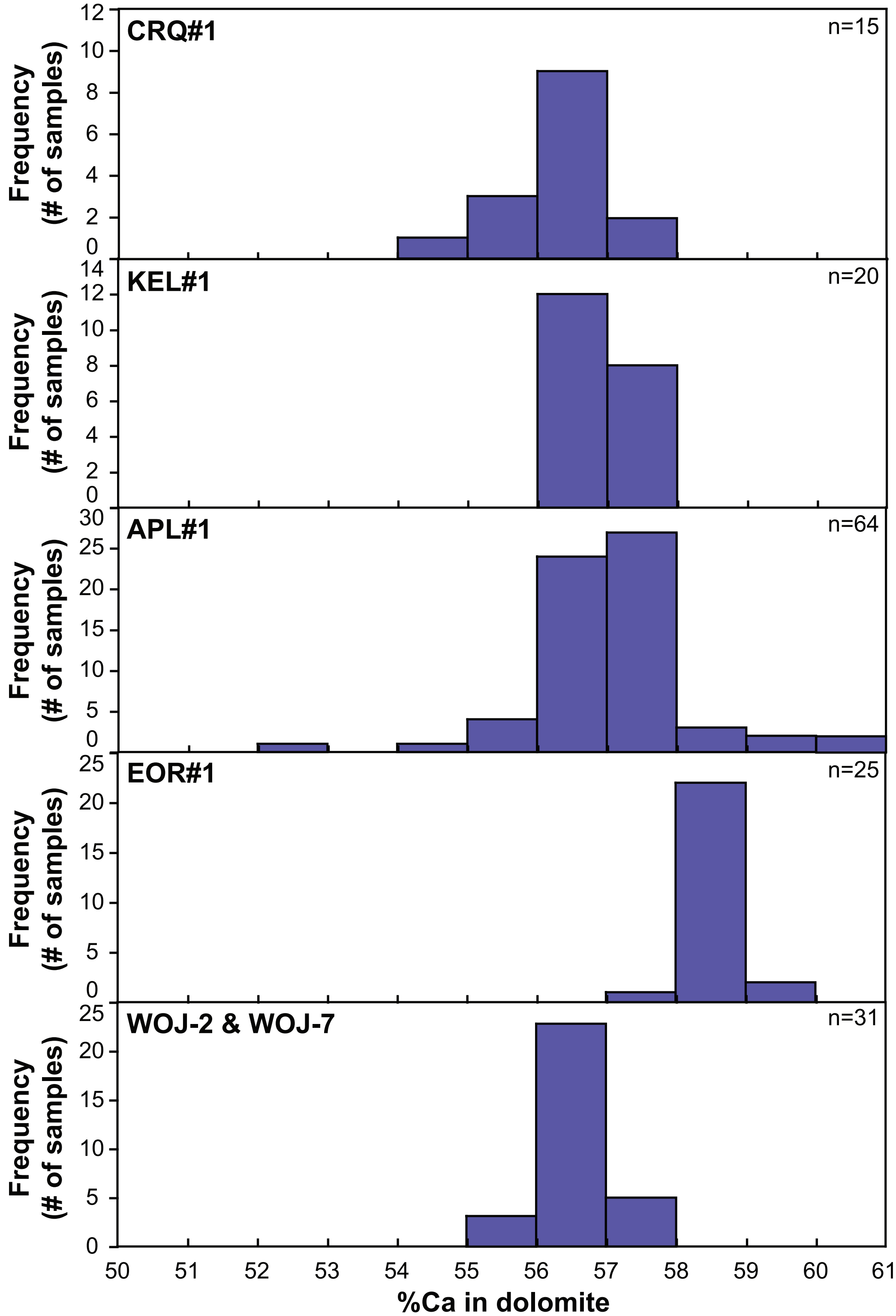

Figure 3.5 Frequency histograms of percent calcium (%Ca) in dolomite in the Brac Formation, demonstrating the unimodal composition of dolomite populations. Note that %Ca is approximately 1.5% higher in EOR#1 than in the remaining wells and sections.

dolomite in CRQ#1 (n=15) ranges from 51.7% to 57.5%, with a mean of 56.4%. KEL#1 (n=20) is characterized by %Ca values between 56.3% and 57.5%, with a mean of 56.9%. In EOR#1 (n = 25), the %Ca ranges from 57.6% to 59.1%, with a mean of 58.6%. The %Ca in APL#1 (n = 64) ranges from 52.2% to 60.7%, with a mean of 57.1%. The %Ca in WOJ-2 and WOJ-7 (n=31) ranges from 51.8% to 57.5%, with a mean of 56.6%. Overall, dolostones in the Brac Formation are composed of high calcium dolomite (contain >55 mol% Ca; cf. Jones *et al.*, 2001), with an average %Ca of 57.1% (i.e., $Ca_{57.12}Mg_{42.88}$) and Ca/Mg ratios comparable to other island dolomites.

Dolomite is enriched in $\delta^{18}O$ compared to coprecipitated calcite, though the magnitude of the enrichment is not clearly understood (Tarutani *et al.*, 1969). Calcian dolomites should thus have lower $\delta^{18}O$ values than stoichiometric (i.e., $Ca_{50}Mg_{50}$) dolomites (Vahrenkamp and Swart, 1994; Budd, 1997). However, cross-plotting %Ca and $\delta^{18}O$ of dolomites in the Brac Formation yields an R-squared value of 0.46, indicating only weak correlation between these variables (Fig. 3.6).

The range in dolomite $\delta^{18}O$ compositions between different locations may be controlled by the dominant type(s) of dolomite contained in the samples (i.e., replacive vs. cement) and the extent of dolomitization. APL#1 and EOR#1 are characterized by a significantly larger spread in $\delta^{18}O$ values than those in CRQ#1, KEL#1, and SCD (Figs. 3.7, 3.8). Dolomitization is variable in APL#1 and EOR#1, consisting of partially dolomitized limestones, finely crystalline, fabric retentive replacive dolomite and limpid dolomite cement. Most of the dolomite in EOR#1 exists as sparry, pore-lining cement. In contrast, CRQ#1, KEL#1, and SCD are more pervasively dolomitized (finely crystalline and sucrosic dolomite), and dolomite, where present, has destroyed the fabric of the precursor limestones. Although all of the dolomite in the Brac Formation is composed of

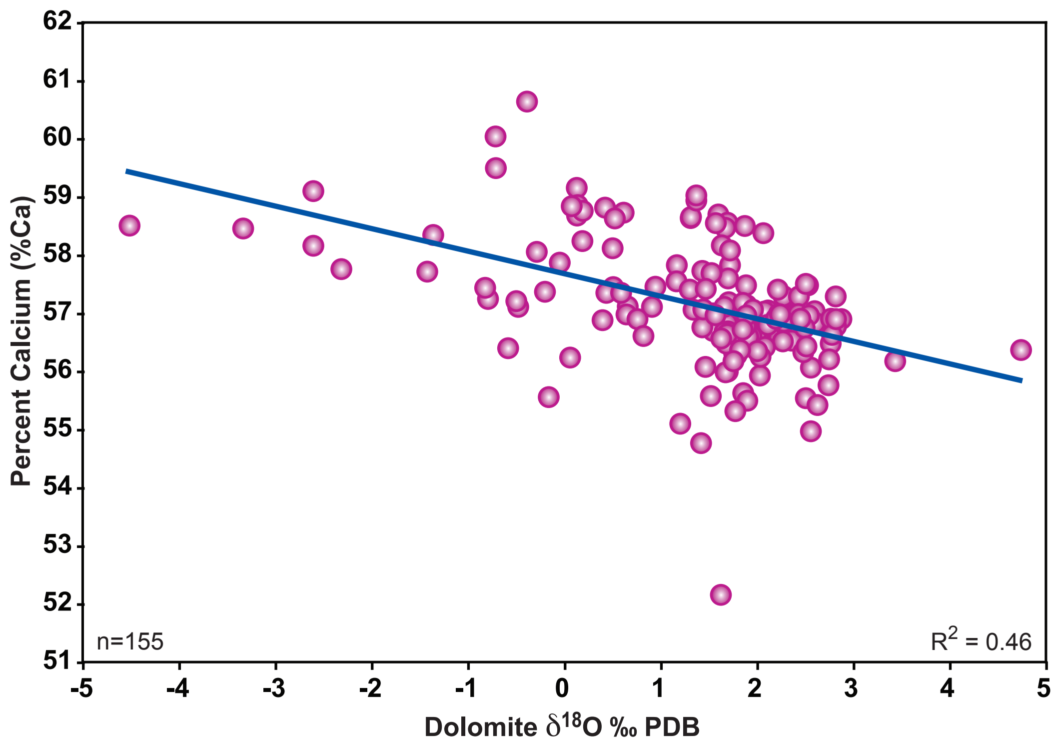

Figure 3.6 Percent calcium plotted against $\delta^{18}O$ for all dolomite analyzed from the Brac Formation. An R-squared value of 0.46 indicates that there is only minimal correlation between these variables.

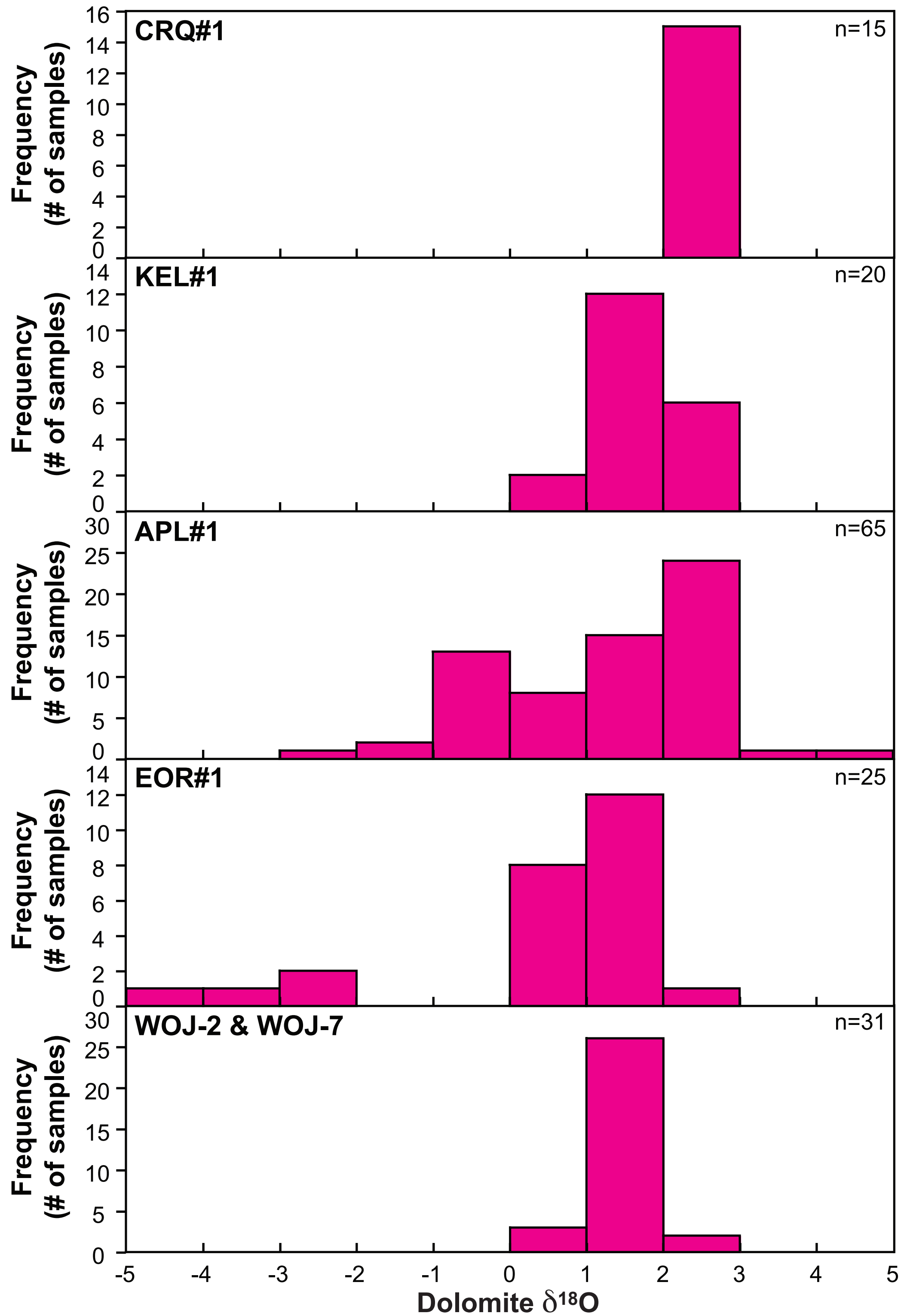

Figure 3.7 Frequency histograms of oxygen isotope values of dolomite in the Brac Formation. Note that isolated $\delta^{18}O$ values in EOR#1 are lower than in the remaining wells and sections. Only this well and APL#1 contain dolomite samples with negative $\delta^{18}O$ values.

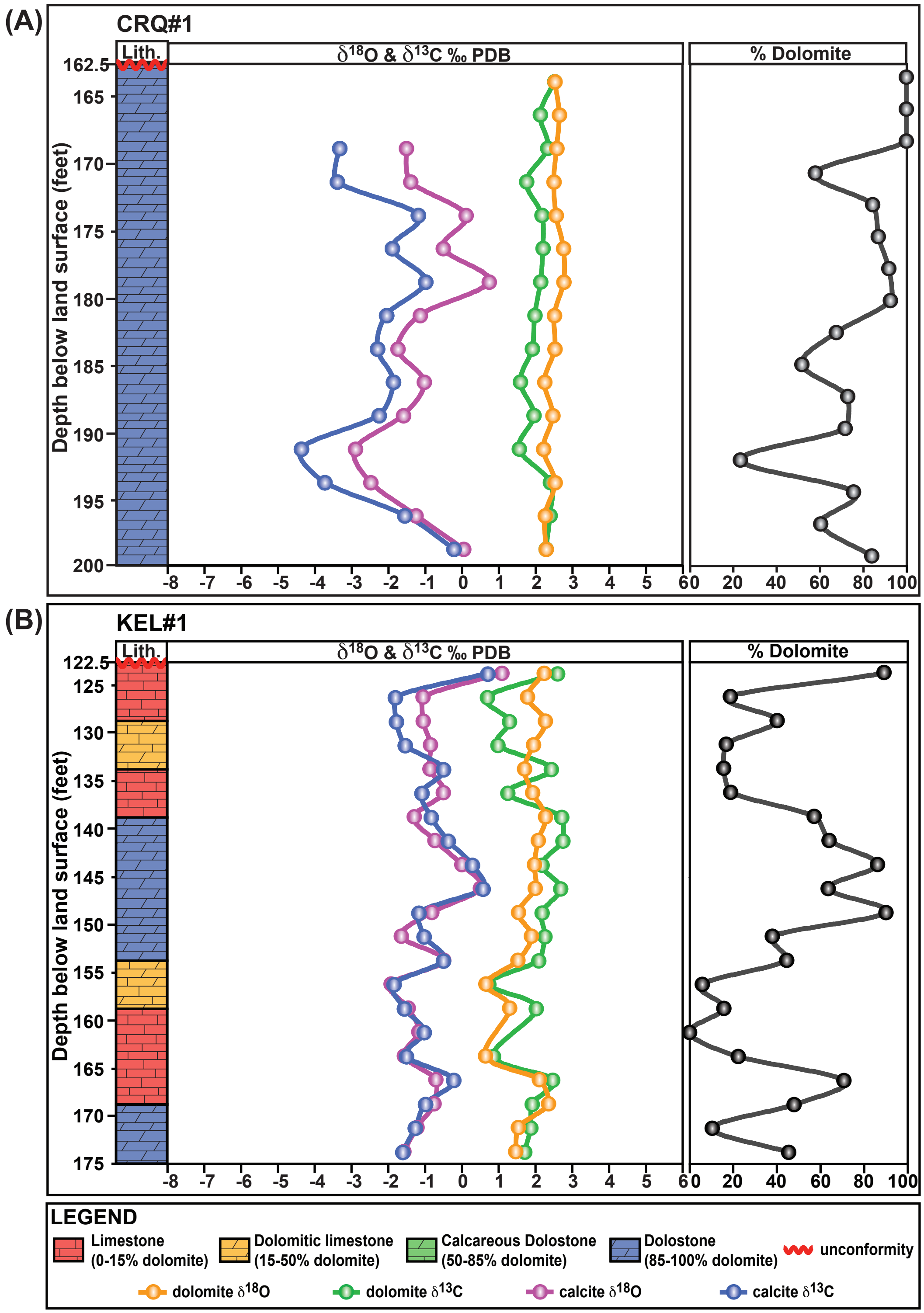

Figure 3.8 Depth profiles of lithology, $\delta^{18}O$ and $\delta^{13}C$ values, and percent dolomite in CRQ#1 **(A)** and KEL#1 **(B)**. Note the correlation of lower isotope values with calcite-rich intervals (apparent in KEL#1) and relatively invariable, higher isotope values in more pervasively dolomitized sections (e.g., CRQ#1).

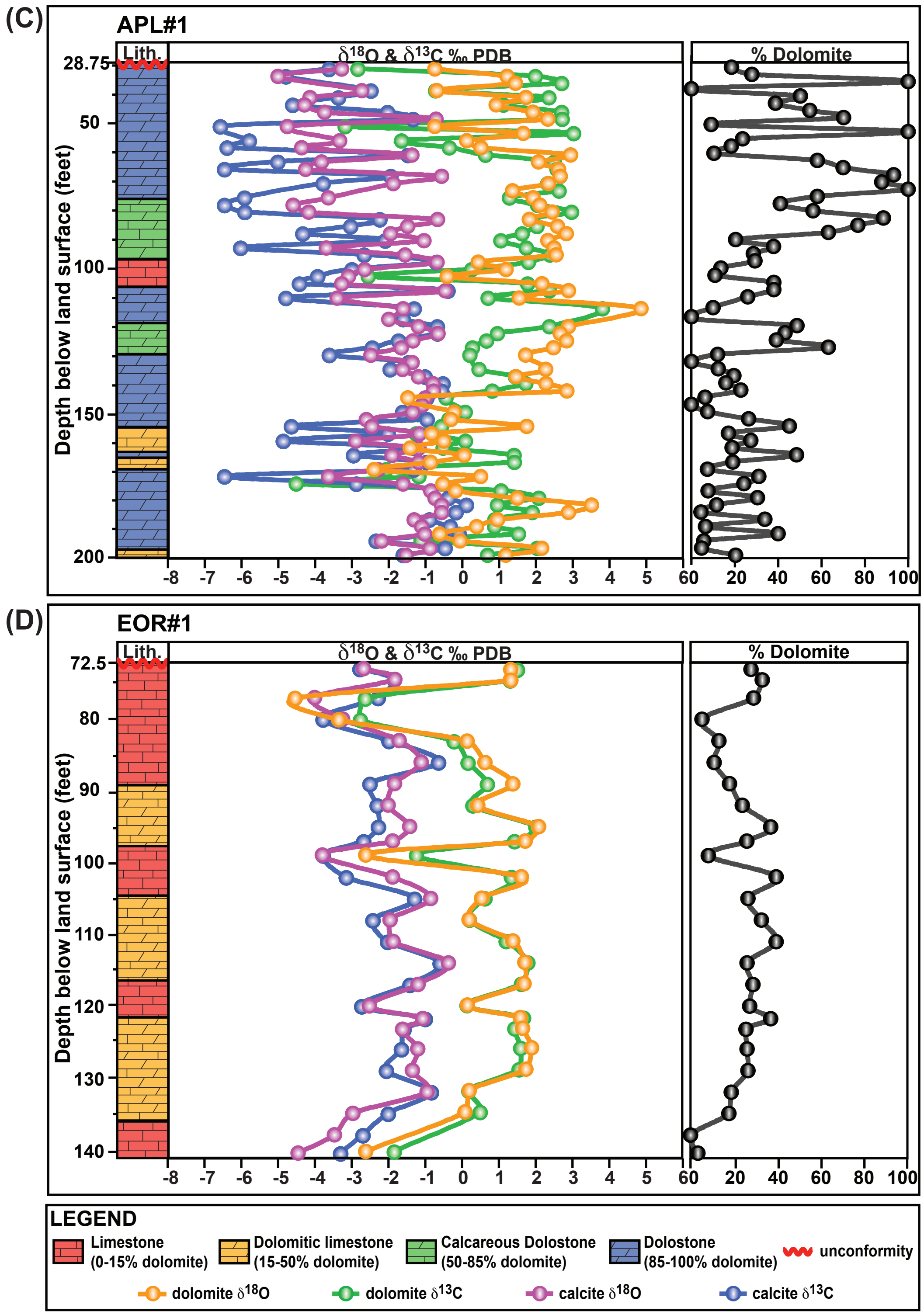

Figure 3.8 Depth profiles of lithology, $\delta^{18}O$ and $\delta^{13}C$ values, and percent dolomite in APL#1 **(C)** and EOR#1 **(D)**. Note the correlation of lower isotope values with calcite-rich intervals (evident in EOR#1) and relatively invariable, higher isotope values in more pervasively dolomitized sections.

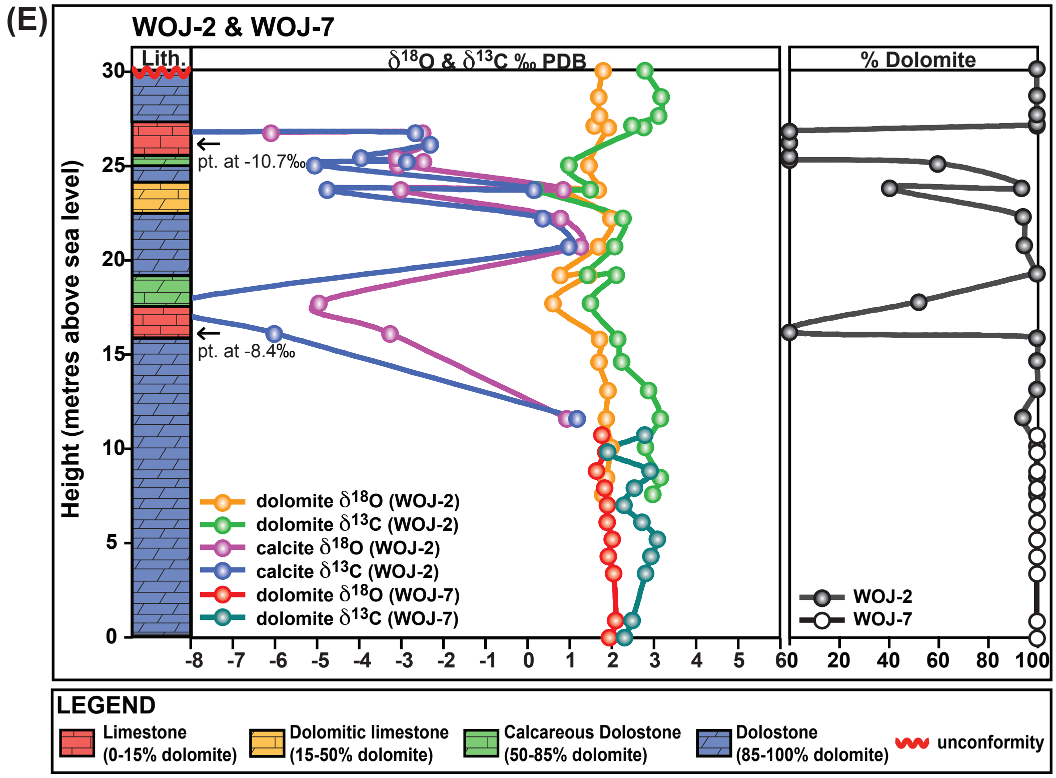

Figure 3.8 (E) Depth profiles of lithology, $\delta^{18}O$ and $\delta^{13}C$ values, and percent dolomite in WOJ-2 and WOJ-7 (combined equivalent of SCD). Calcite $\delta^{13}C$ values are -8.4‰ and -10.7‰ at 17.7 and 26.7 metres above sea level, respectively (data points not shown on diagram). Note the correlation of lower isotope values with intervals that contain more calcite.

high calcium dolomite (i.e., %Ca > 55 mol%; Fig. 3.5), the mean %Ca in EOR#1 is approximately 1.5% higher than in other wells and sections. The dominant type of dolomite present might thus affect the %Ca in the sample and consequently determine the $\delta^{18}O$ value.

The composition of the fluid that mediated dolomitization in the Brac Formation can be approximated with the aid of a dolomite-water fractionation equation (Table 3.2). Several equations have been developed to define the temperature dependence of oxygen isotope fractionation during dolomite precipitation. Due to the difficulty of precipitating dolomite at low (i.e., sedimentary) temperatures, most oxygen isotope fractionation equations are derived from extrapolation of high temperature experiments (e.g., Northrop and Clayton, 1966; O'Neil and Epstein, 1966; Sheppard and Schwarcz, 1970; Fritz and Smith, 1970; Matthews and Katz, 1977). Recent investigation of the role of bacteria in mediating dolomite precipitation has yielded the first dolomite-water oxygen isotope fractionation equation developed at low temperatures (Vasconcelos *et al.*, 2005). This equation yields results consistent with the high temperature equations of Fritz and Smith (1970) and Matthews and Katz (1977), lending validity to all three calculations. Herein, the equation of Vasconcelos *et al.* (2005) is used to derive the temperature of dolomite formation:

$$1000 \ln \alpha_{\text{dolomite-water}} = 2.73 \times 10^6 T^{-2} + 0.26 \qquad [3]$$

where $\alpha = (1000+\delta^{18}O_{dolomite}‰SMOW)/(1000+\delta^{18}O_{water}‰SMOW)$ and temperature is in kelvins.

Temperatures measured in modern groundwater zones on Grand Cayman (Ng, 1990) are compared with the theoretical temperatures calculated from oxygen isotope data to determine the likelihood of dolomite precipitation from various mixtures of seawater and fresh water (cf. MacNeil and Jones, 2003). Calculated temperatures of dolomite formation are based on the assumption that

Table 3.2 Temperature calculations from $\delta^{18}O$ for dolomite formation in different types of water in the Cayman Islands, based on water data collected by Ng (1990). Oxygen isotope fractionation equation for dolomite from Vasconcelos *et al.* (2005). Mean $\delta^{18}O_{dolomite}$ = +1.39‰ PDB or +32.34‰ SMOW.

Water Type	Average $\delta^{18}O$ composition (‰ SMOW)	Salinity	Calculated temperature of dolomite formation (ºC)
Fresh ground water	-4.54	<1.01 ‰	1.8
Lightly brackish water	-4.16	<15% seawater	3.2
Highly brackish water	-1.82	>15% seawater	12.8
Saline water	0.63	~35 ‰	23.9
Normal seawater	1.34	~35 ‰	27.4

the measured temperatures of various water zones in the Cayman Islands are comparable to those at the time of dolomitization. Using an average weighted mean $\delta^{18}O$ value of +1.39‰ for all dolomite populations analyzed, the oxygen isotope signature of dolomite in the Brac Formation is consistent with that of dolomite formed from normal seawater or saline water (i.e., seawater altered by rock-water interaction).

Temperatures calculated from brackish and fresh ground water produce unacceptably low temperatures of dolomite formation for a tropical island, even at depth (e.g. Saller, 1984). Therefore, these types of water may be discounted as possible sources for dolomitizing fluids. For example, the value of 12.8°C calculated for dolomite precipitated in highly brackish water is significantly cooler than measured modern mixing-zone temperatures, and is thus inconsistent with dolomitization by mixed seawater and meteoric water. Temperatures calculated for dolomite precipitated by saline water or seawater (23.9 and 27.4°C, respectively) are therefore closest in agreement with modern temperatures in the deep saline zone of Grand Cayman (25 - 27ºC) measured by Ng (1990), and thus the $\delta^{18}O$ results indicate that these are the most likely fluids responsible for mediating dolomitization.

As noted previously, sample preparation methods may introduce some degree of error in the reported isotopic compositions (see methods, p. 21). Specifically, when mixtures of calcite and dolomite react with phosphoric acid, some CO_2 is evolved from both phases simultaneously; thus the reliability of $\delta^{18}O$ values derived from coexisting calcite and dolomite may be called into question (Walters *et al.*, 1972). Selective phosphoric acid decomposition yields less accurate results when mixtures contain a relatively large amount of one carbonate mineral relative to the other (Epstein *et al.*, 1963). This effect is most apparent in limestone intervals (i.e., those containing <15% dolomite) in

EOR#1, where the small ratio of dolomite to calcite permits CO_2 evolved from dolomite to be contaminated by CO_2 evolved from calcite. These intervals are characterized by significantly reduced dolomite $\delta^{18}O$ values that are nearly identical to corresponding calcite $\delta^{18}O$ values (Fig. 3.8d). CRQ#1, KEL#1, APL#1, WOJ-2 and WOJ-7 contain relatively higher ratios of dolomite to calcite, and are therefore less affected by CO_2 contamination of dolomite $\delta^{18}O$ values (Fig. 3.8a,b,c,e). This effect appears to be limited to intervals that contain only a minimal amount of dolomite; therefore a threshold of 15% is suggested here, below which the reliability of dolomite $\delta^{18}O$ values is questionable.

The carbon isotope signature of dolomite in the Brac Formation (mean +1.36‰) is consistent with $\delta^{13}C$ values of most island dolomites (cf. Budd, 1997) and likely reflects inheritance of marine carbon from the precursor limestone. Excursions in $\delta^{13}C$ toward 0‰ do not appear to be related to subaerial exposure surfaces; however, the petrographic limitations of well cuttings make this difficult to ascertain.

Negative excursions in $\delta^{13}C$, like those of $\delta^{18}O$, are associated primarily with limestone-rich intervals. These excursions are thus interpreted to represent $\delta^{13}C$ values of dolomite that have been partially masked by calcite $\delta^{13}C$ values. There is no evidence that negative $\delta^{13}C$ values were produced by admixing of oxidized organic carbon during dolomitization, nor that there was a fresh water component in the dolomitizing solution. Covariance of negative $\delta^{18}O$ and $\delta^{13}C$ excursions in dolomite in the Brac Formation is thus attributed to muting of the oxygen and carbon isotope signatures of dolomite in samples that contain appreciably more calcite. Depletion of $\delta^{13}C$ values in Brac Formation dolomites is most likely a result of diagenetic stabilization of precursor limestones by mixed meteoric and marine fluids before the onset of dolomitization. The covariant relationship of $\delta^{18}O$ and $\delta^{13}C$ in dolomite is therefore not accepted as conclusive evidence for a mixing-zone origin, as any negative isotope values were likely inherited from the precursor limestones rather than meteoric water. Based on the isotopic evidence, dolomitization could have been mediated by a solution composed primarily of seawater.

No correlation of dolomite $\delta^{18}O$ and $\delta^{13}C$ can be made between the various localities analyzed in the Brac Formation (Fig. 3.4). This may be due to the varying degree of dolomitization that has affected each well, or the predominance of different types of dolomite in the wells. Although a correlation of $\delta^{18}O$ and $\delta^{13}C$ values has not yet been established, the mean isotopic values are comparable between the wells and suggest a common dolomitizing solution.

A lateral change in the dominant lithology, from limestone to dolostone, is discernable over a relatively short distance (< 2 km) between sections LCB and SCD on Cayman Brac. The nature of dolomitization in the Brac Formation varies from the micrometre scale to the kilometre scale; a single dolomite body may therefore display lateral variations in petrography and geochemistry at any scale of investigation. The magnitude of geochemical variability in a dolomitized bed might be too great to assume that a spot sample is representative of an entire formation, and could thus be insufficient to accurately infer ancient geological conditions (Budd *et al.*, 2006).

3.4 Relationship Between Calcite and Dolomite Isotopes

A cross plot of $\delta^{18}O$ and $\delta^{13}C$ compositions of calcite and dolomite in the Brac Formation reveals a classic mixing trend between isotopic end members (Fig. 3.9). Dolomite isotopes occupy the positive area of the linear mixing trend, whereas calcite isotopes comprise the negative end of the mixing line. Approximately 25% of calcite and dolomite $\delta^{18}O$ and $\delta^{13}C$ values overlap between -2 and +2 per mil. This type of positive covariant isotopic mixing trend

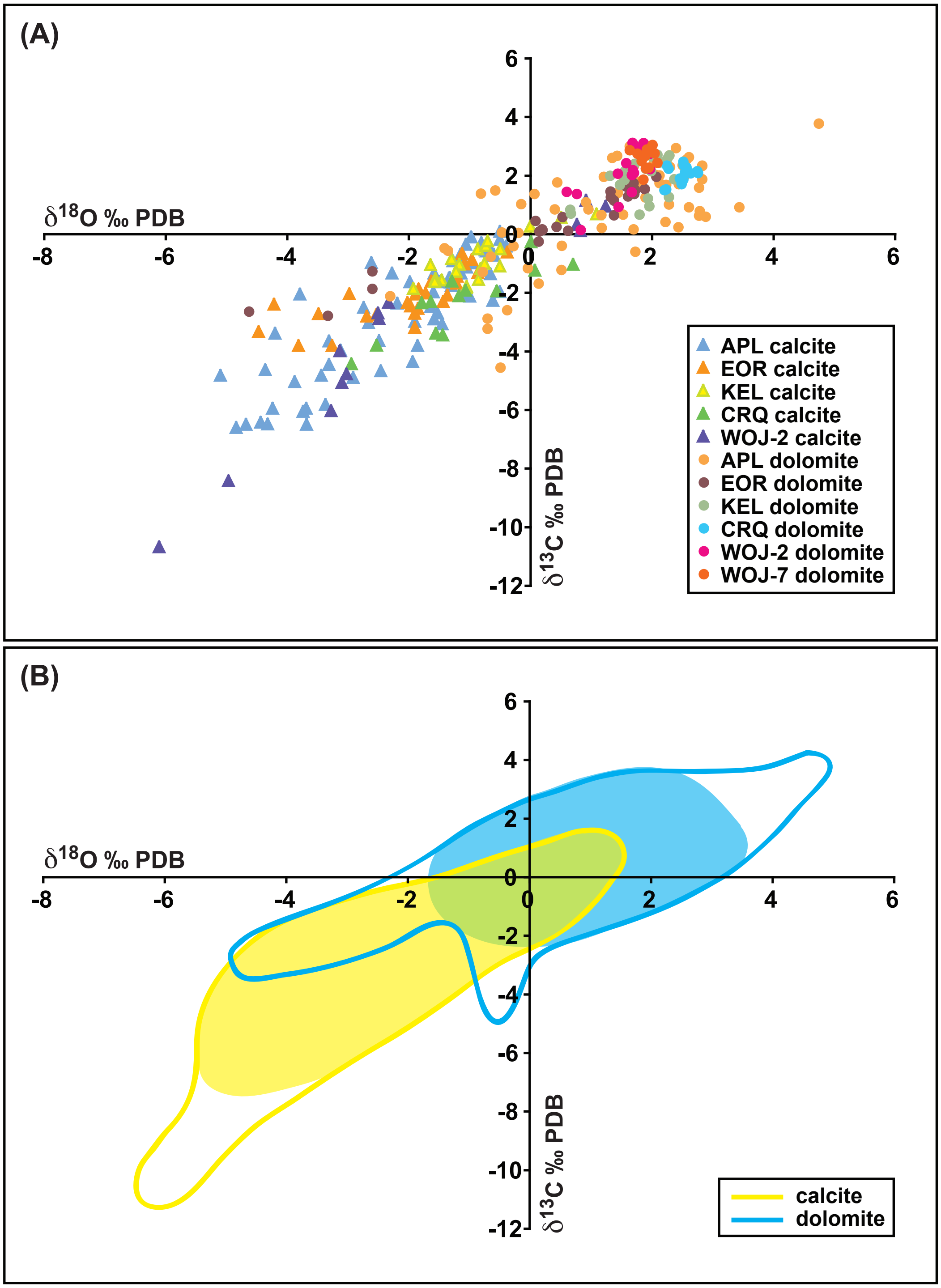

Figure 3.9 **(A)** Cross plot of $\delta^{18}O$ and $\delta^{13}C$ compositions of calcite and dolomite in the Brac Formation. **(B)** Data fields of oxygen and carbon isotopes from **A** indicate a clear mixing trend between calcite and dolomite end members. Shaded areas exclude outlying data points.

is generally taken as evidence for alteration of carbonates in a meteoric-marine mixing zone (Allan and Matthews, 1982; Ward and Halley, 1985; Lohmann, 1988; Gonzalez *et al.*, 1997), in which the positive values are attributed to diagenetic alteration in normal seawater and negative values reflect a meteoric fluid component.

The subject of mixing zone dolomitization has been one of considerable controversy (cf. Land, 1985; Machel and Mountjoy, 1986; Hardie, 1987; Budd, 1997; Machel, 2004). Examples of dolomites formed in the mixing zone that have positive covariant isotopic trends similar to those in the Brac Formation are few; it has been suggested that such dolomites form in isolated regions of limited extent (Humphrey, 1988, 2000; Ward and Halley, 1985; Gonzalez *et al.*, 1997). Melim *et al.* (2004) proposed that dolomites characterized by such covariant isotopic mixing trends are actually formed by marine dolomitization that extends into the mixing zone, continuing despite (rather than because of) dilution by meteoric water. Although the mixing zone has largely been regarded as insufficient for promoting platform-wide dolomitization, Gaswirth *et al.* (2007) resolved the movement of multiple mixing zones through various stratigraphic units in the proto Floridan Aquifer. This finding demonstrates that the repeated establishment of mixing zones through a dolomite body can form regionally significant amounts of secondary dolomite.

By accepting that the freshwater-seawater mixing zone is a potentially significant site of dolomite formation, it becomes critical to establish if the mixed isotopic signature of Brac Formation carbonates is the end product of multistage dolomitization processes or the result of one discrete diagenetic event. Covariant $\delta^{18}O$ and $\delta^{13}C$ values indicate that carbonates formed in a mixing zone only if a single generation of cement is analyzed; a multi-generational carbonate system yielding this type of isotopic signature probably reflects movement of various diagenetic environments through the rock at different times (Allan and Matthews, 1982). The method of whole rock sampling used for isotopic analyses in this study precluded the isolation of separate carbonate populations for individual analysis. Given the limitations of this method, the covariant isotopic mixing trend in limestones and dolostones of the Brac Formation is not unequivocal evidence for stabilization in the mixing zone. Rather, the multi-generational nature of this carbonate system probably records overprinting of the original isotopic signatures by successive stages of alteration in superimposed diagenetic environments. Indeed, Jones and Luth (2003a) identified three discrete phases of dolomitization on Grand Cayman, arguing that dolomites were formed in a time-transgressive process driven by major changes in sea level. The covariant isotopic trend observed in the Brac Formation may be the result of movement of various freshwater-seawater mixing zones throughout the rock; however, this effect can probably be attributed to a superimposed isotopic signal in a multi-generational carbonate system.

3.5 Synopsis

Analysis of $\delta^{18}O$ and $\delta^{13}C$ signatures of calcite and dolomite in the Brac Formation yields the following information.

Calcite:

- Whole-rock analysis of calcite produces an average $\delta^{18}O$ value that is unrepresentative of individual calcite populations.
- Calculated paleotemperatures of calcite formation are unreasonably low because $\delta^{18}O_{calcite}$ values are in disequilibrium with modern groundwaters.
- Calcite was recrystallized/altered in meteoric water during periods of emergence, indicated by a covariant $\delta^{18}O/\delta^{13}C$ trend.

- Calcite diagenesis was mediated in fluctuating groundwater zones.

Dolomite:

- Dolomite $\delta^{18}O$ values indicate that dolomitization was mediated by seawater or saline water modified slightly by rock-water interaction.
- Dolomite $\delta^{13}C$ values were inherited from the precursor limestone.
- $\delta^{18}O$ and $\delta^{13}C$ signatures are related to degree of dolomitization (i.e., the more dolomite is present, the higher and more consistent the isotope ratios)
- Negative excursions of $\delta^{18}O$ and $\delta^{13}C$ in dolomite correlate with limestone-dominated intervals. Covariance of $\delta^{18}O_{dolomite}$ and $\delta^{18}O_{calcite}$ from these intervals points to contamination of $CO_{2\text{-dolomite}}$ by the more abundant $CO_{2\text{-calcite}}$ and highlights problems inherent to the chemical separation method.
- Correlation of the wells is not possible based on dolomite $\delta^{18}O$ and $\delta^{13}C$ values, due to lateral shifts in the geochemical character of the dolomitized body.

Relationship Between Calcite and Dolomite Isotopes:

- A cross plot of $\delta^{18}O$ and $\delta^{13}C$ compositions of calcite and dolomite reveals a positive covariant isotopic signal.
- The mixing trend between end member compositions is attributed to overprinting of original $\delta^{18}O$ and $\delta^{13}C$ values by successive diagenetic environments.

Chapter Four: Discussion and Conclusions

4.1 Introduction

Cayman Brac was a small, isolated bank when sediments of the Brac Formation were deposited during the Oligocene. The absence of fringing reef development in the Brac Formation indicates that the island was an open bank at the time of deposition (Jones and Hunter, 1994a). Water depth, energy levels, temperature, and salinity were the primary controls on original sedimentation patterns. There is no evidence to suggest that these controls deviated from normal marine values. Following deposition, the diagenetic evolution of the Brac Formation was controlled mainly by fluctuations in sea level and the influence of meteoric waters during periods of subaerial exposure. Dolomitization significantly altered the appearance and chemical composition of the formation, destroying many of the original depositional textures and producing the replacive and cementation features that characterize the rocks today.

The geological history of the Brac Formation can be reconstructed through analysis of its sedimentologic, stratigraphic, geochemical, and diagenetic features, with an emphasis on dolomitization. The results of petrographic and geochemical analyses are integrated herein to better characterize the physical and chemical effects of diagenesis on the Brac Formation. By synthesizing the data acquired through field and lab studies, a model is developed to summarize the geological evolution of the Brac Formation on Cayman Brac.

4.2 Tectonic Setting of Cayman Brac in the Oligocene

The growth of carbonate platforms is controlled by the accommodation space that is available during sedimentation (Paterson *et al.*, 2006). Relative accommodation for carbonate banks such as Cayman Brac is influenced by complex interactions between tectonic subsidence, glacioeustatic changes in sea level driven by climate, sediment production and compaction rates, and surface dissolution during periods of subaerial exposure. The small size of this isolated bank makes it especially susceptible to fluctuations in any of these variables. The standalone effect of tectonic subsidence on Cayman Brac during deposition of the Brac Formation is difficult to distinguish from associated factors that simultaneously influence relative sea level. The prevailing tectonic regime during the Oligocene, however, undoubtedly promoted sedimentation as it provided requisite accommodation space and enabled growth of the carbonate bank.

Cayman Brac slopes from a maximum elevation of 43 m on its east end down to sea level on its west end. Similarly, the Brac Formation and the Cayman Formation dip approximately 0.5º to the west (Jones and Hunter, 1994a). Cayman Brac thus assumed its westerly dipping orientation following deposition of these sediments (i.e., post-Miocene). It is unresolved whether the island's present inclination pre-dates or post-dates deposition of the Pliocene Pedro Castle Formation due to its lack of internally dipping planes. MacNeil (2001) suggested that tectonic tilting was initiated during deposition of the Pedro Castle Formation, signifying onlap on the west end of Cayman Brac concomitant with subaerial exposure on the east. Tilting ceased prior to deposition of the Pleistocene Ironshore Formation, which unconformably overlies and onlaps the Bluff Group. Given that the lower contact of the Brac Formation with underlying strata has yet to be encountered, the topography of Cayman Brac prior to deposition of the Brac Formation cannot be determined.

The Brac-Cayman Disconformity represents a period of time from the Upper Oligocene to Lower Miocene (~15 Ma) during which sediments of the Brac Formation were subaerially exposed, lithified and eroded to form a karst terrain

(Jones and Hunter, 1994a). On Cayman Brac, the dip of this disconformity ranges from 0.5 to 2º to the west – directionally consistent with the dip of the island. The variable topography on the disconformity is likely due to differential erosion. The same disconformity has been detected in the subsurface on Grand Cayman where it is characterized by as much as 30 m of relief. That relief has been attributed to karst development because there is no indication that Grand Cayman has been tectonically tilted (Jones, *pers. comm*., 2009). The difference between dip angles of the same disconformity on Grand Cayman and Cayman Brac supports the argument that the islands are situated on separate fault blocks (Matley, 1926; Horsfield, 1975) that have undergone independent vertical movement at least since the Oligocene.

4.3 Sea Level During the Oligocene

Eustatic changes in sea level are cyclical but aperiodic processes that operate on a variety of time scales (Van Sickel *et al.*, 2004). The amplitude and timing of sea level fluctuations during the Oligocene are a subject of controversy (Fig. 4.1). The first eustatic sea level curve, presented by Vail *et al.* (1977) at Exxon Production Research Company (EPR), proposed a sea level fall of 400 m in the mid-Oligocene. A decade later, the amplitude of this fall was amended to 140 m (Haq *et al.*, 1987). Recent research indicates that eustatic sea level changes were of considerably smaller magnitude than initial estimates. The maximum amplitude of sea level fall in the Cenozoic is estimated to be 40 to 75 m (Pekar and Miller, 1996; Miller *et al.*, 1998), or approximately half of Haq's estimate (Kominz *et al.*, 1998; Van Sickel *et al.*, 2004). The number and timing, though not the amplitude, of many EPR sea level events were validated by Miller *et al.* (2005), whose estimates of ~30 to 60 m variations in sea level during the Oligocene are at least 2.5 times lower than Haq's.

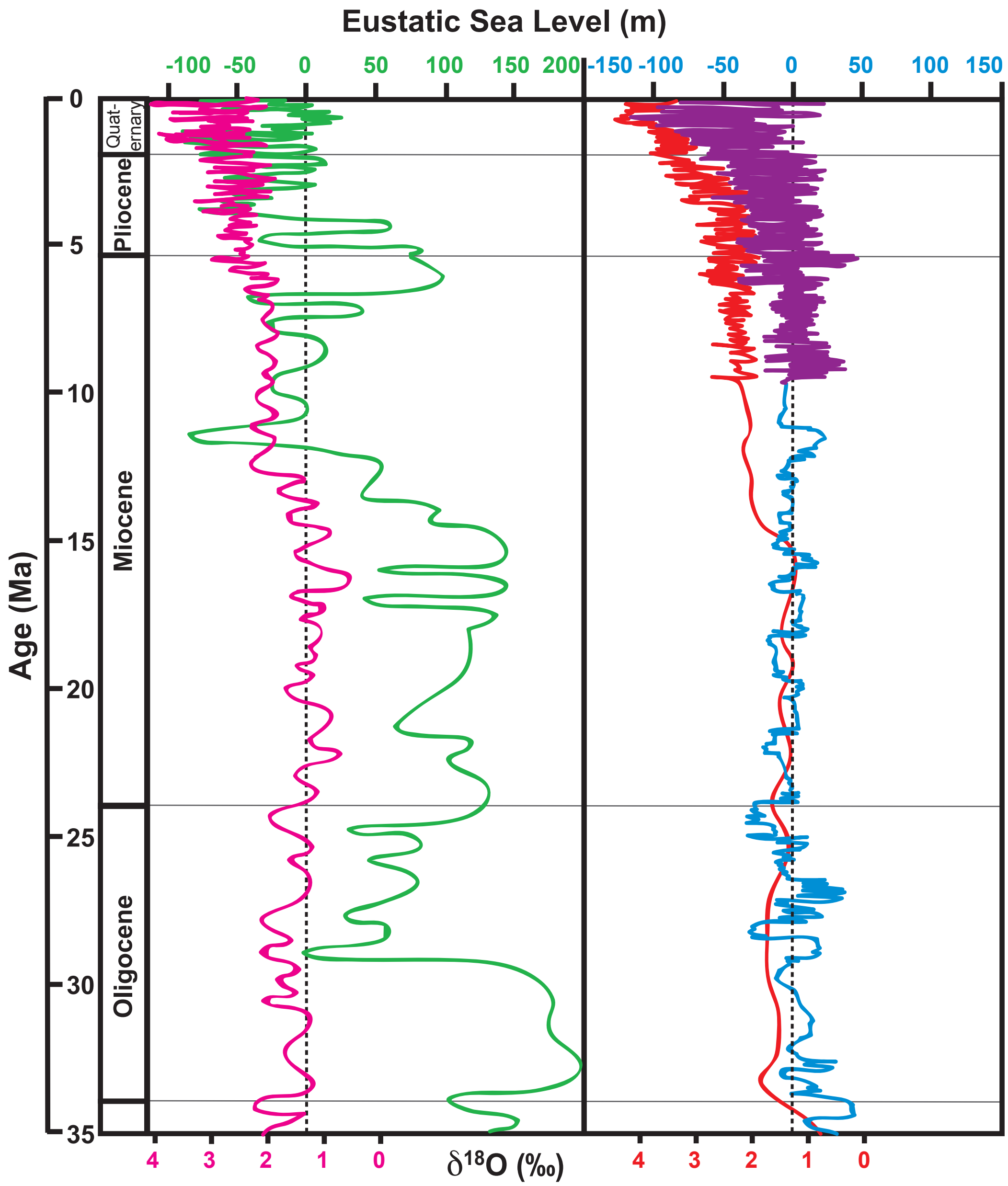

Figure 4.1 Various interpretations of global sea level curves from the Oligocene to present. Third order eustatic curve (green) of Haq *et al.* (1987) based on sequence stratigraphic record recalibrated to more recent biostratigraphic time scales (Abreu and Anderson, 1998); composite oxygen isotope record (pink) based on isotope events identified in DSDP/ODP sites (Abreu and Anderson, 1998). Global sea level (blue) derived from backstripping stratigraphic data; global sea level (purple) derived from $\delta^{18}O$; and benthic foraminiferal $\delta^{18}O$ synthesis (red) shown for comparison (Miller *et al.*, 2005). Backstripped eustatic estimate by Miller *et al.* (2005) indicates that amplitudes of Haq *et al.* (1987) sea level curve are at least 2.5 times too high. Dashed lines represent present-day sea level.

The earliest Oligocene (33 Ma) marked a shift in climate paradigm from a "Greenhouse world" that experienced minor cold snaps to the "Icehouse world" enduring today (Miller *et al.*, 2005). During icehouse periods, growth and decline of continental ice sheets results in high frequency, high-amplitude glacioeustatic sea level fluctuations (Paterson *et al.*, 2006). Evidence of large Cenozoic ice sheets – and thus, an icehouse world – is recorded by Oligocene glaciomarine sediments and high deep-sea $\delta^{18}O$ values (Pekar and Miller, 1996). Fluctuations in sea level from the Oligocene to early Pliocene are attributed to growth and decay of an East Antarctic ice sheet (Abreu and Anderson, 1998; Miller *et al.*, 2005).

Glacioeustatic oscillations cause recurring cycles of platform exposure and flooding, thereby shaping the sedimentary architecture of carbonate platforms. Fourth-order sea level cycles dominate icehouse periods, depositing high-frequency sedimentary packages that alternate with subaerial exposure horizons (Paterson *et al.*, 2006). This relationship is apparent on Cayman Brac, where the unconformity-bounded Brac Formation, Cayman Formation, and Pedro Castle Formation represent three cycles of transgression and regression that controlled Tertiary sedimentation (Jones and Hunter, 1994a).

Although fourth-order sea level cycles can flood carbonate platforms to depths > 45 m during transgression and highstand (Paterson *et al.*, 2006), Cayman Brac was submerged to only ~ 10 m below sea level when sediments of the Brac Formation were deposited (chapter 2). The absence of deep-marine sediments in the Brac Formation indicates that the bank was never drowned (cf. Schlager, 1981). Jones and Hunter (1994a) inferred from the vertical consistency of facies within the Brac Formation that water depth and energy levels were stable during deposition. Geographic zonation between facies and biota provides evidence of local variations in bank morphology during sedimentation, rather than rising or falling sea level. Combined, these observations suggest that the rate of sediment accumulation kept pace with the rate of relative sea level rise. There is no preserved shallowing-upward succession at the top of the Brac Formation that signals the onset of regression and end of sedimentation. A sea level fall of at least 10 m, however, was required to expose the bank and form the overlying disconformity through surface erosion and dissolution. Sediments that recorded the falling stage systems tract could have therefore been lost to karstification (Jones and Hunter, 1994a). The transgressive-regressive cycle that deposited the Brac sediments in the mid-Oligocene ultimately led to their demise with the formation of the Brac-Cayman Disconformity in the late Oligocene.

In the Icehouse world of the past 33 My, variations in ice volume were the primary control on global sea level change (Pekar and Miller, 1996). Glacioeustasy (the growth of continental ice sheets and subsequent sea level fall) thereby drove the formation of global sequence boundaries, which correlate with increases in the deep-sea oxygen isotope record (Pekar and Miller, 1996; Miller *et al.*, 1998; Miller *et al.*, 2005). Pekar and Miller (1996) recognized seven global $\delta^{18}O$ increases in the Oligocene by correlating $\delta^{18}O$ records from deep-sea sites with Oligocene sequence boundaries. $\delta^{18}O$ maxima indicate glacioeustatic falls occurred at 33.5, 32.8, 31.7, 30.3, 28.3, 27.1, and 23.7 Ma. While it cannot be unequivocally determined which sea level fall terminated deposition of the Brac Formation, the event at 23.7 Ma is most probable. This regression is favoured because it is younger than the limestones in the Brac Formation (dated at ~26 Ma on the $^{87}Sr/^{86}Sr$-time curve of McArthur *et al.*, 2001). There is no biostratigraphic evidence to indicate deposition continued beyond the mid-Oligocene, but the uppermost (and therefore youngest) beds in the formation were most likely removed by erosion.

The amplitude of the late Oligocene sea level fall that led to exposure of the Brac Formation is difficult to resolve because of the high variability between global sea level curves (Fig. 4.1). Jones and Hunter (1994a) noted that this drop in sea level corresponds with the 140 m mid-Oligocene regression postulated by Haq *et al.* (1987). However, a major regression of similar amplitude is absent from more recent eustatic curves, and can therefore be discounted due to its extremity. Most Cenozoic sequence boundaries were generated by sea level falls of 30 to 50 m (Abreu and Anderson, 1998). The amplitude of the late Oligocene regression that caused the Brac-Cayman Disconformity is thus interpreted to fall within this range, as there is no evidence that indicates otherwise.

4.4 Paleoenvironmental Setting and Depositional History

The morphology of the Cayman Brac bank prior to sedimentation in the middle Oligocene is not known because the lower contact of the Brac Formation has not yet been encountered (the Brac Formation still being present at the maximum drill depth of ~ 58 m bsl in CRQ#1). The effect of antecedent topography on the bank's evolution is thus unknown. Likewise, the nature of the basal sediments deposited in the Brac Formation remains unresolved, restricting the interpretation of conditions that governed incipient sedimentation.

The sedimentary succession preserved in the Brac Formation records bank aggradation in the euphotic zone, under conditions optimal for rapid production and accumulation of carbonate by photosynthetic organisms. This is analogous to Schlager's (1981) zone of maximum calcium carbonate productivity, in water depths less than 10 m. The rate of bank accretion was probably equal to the rate of relative sea level rise, evidenced by the vertical consistency of skeletal muds and sands throughout the formation. This is substantiated by the absence of peritidal cycles (deposited when bank accumulation outpaces sea level rise) or, conversely, basinal facies that represent platform drowning (deposited when sea level rise outpaces sediment accumulation).

Variations in the lateral distribution of undolomitized facies can be attributed to local variations in topography, physical-energy flux and current levels, and changes in sediment production and transportation (cf. Triffleman *et al*., 1992). The juxtaposition of benthic foraminifera with planktonic forms in the Brac Formation provides evidence for sediment mixing, possibly by deep oceanic currents upwelling along vertical bank margins. Most bank margin variability is produced by variations in the physical energy regime, allowing for lateral facies shifts even along a continuous bank (Hine and Neumann, 1977). A relatively even distribution of skeletal grains across the bank, however, indicates that sedimentation patterns did not differ markedly on the windward versus leeward margins. The lack of data from the west end of Cayman Brac, however, limits this interpretation to the central and eastern parts of the island only. There is no evidence for change in depositional facies from the bank margins to the interior, as no marginal reef was present, although the pervasive recrystallization of CRQ#1 (the most interior well) to finely crystalline dolomite has largely obscured primary textures.

A constant rate of bank aggradation may have produced a dynamic equilibrium profile that resembled Hine and Neumann's (1977) model for leeward, unprotected, buried reefs. Under constant sea level conditions, sand was carried to the bank edge until it reached the marginal escarpment, where it was swept off by cross-bank currents. Sediment carried off the bank margin destroyed reef growth, maintaining a shallow, flat-topped platform profile devoid of a raised rim and bounded by a steeply sloping depositional escarpment (see Fig. 7C of Read, 1985). Bank aggradation likely occurred as sediments became entrained in the roots of sea grass and green algae. Such stabilization of sediments prevented further transport off the bank edge, even without protection from winnowing currents by a fringing reef. Small thickets of branching *Porites* corals may have aided in baffling cross-bank currents, preventing further loss of sediments off the bank margin.

The end of sedimentation in the Oligocene on Cayman Brac was not recorded by a diagnostic facies assemblage that signalled a change in depositional conditions. There is no evidence of a shallowing-upward cycle preserved at the top of the Brac Formation, nor are deep-marine deposits superimposed on top of neritic deposits. However, sediments representing platform emergence or drowning, respectively, were probably lost to successive erosion along the Brac-Cayman disconformity (Jones and Hunter, 1994a). The maximum thickness of the Brac Formation at the time of deposition thus remains unknown. Sedimentation was most likely terminated by a combination of relative sea level fall, tectonic uplift, and sediment accumulation up to sea level.

4.5 Dolomite Genesis

All of the dolomite in the Brac Formation was formed through post-depositional processes. There is no evidence of peritidal cycles and/or associated evaporite minerals, therefore precluding a penecontemporaneous origin. Fabric-retentive replacement textures and void-filling dolomite cements provide evidence for a diagenetic origin (Budd, 1997). Selective, mimetic replacement of grains that were originally composed of high Mg-calcite (e.g., coralline red algae, benthic foraminifera, echinoids) indicates that dolomitization was controlled to some extent by precursor mineralogy (Sibley, 1982; Bullen and Sibley, 1984; Sibley and Gregg, 1987). Rare allochem ghosts of originally aragonitic grains (e.g., *Porites*, bivalves, gastropods) weakly preserve pre-dolomitization textures in sucrosic dolostones, but their original skeletal architecture has been destroyed. Limpid dolomite cement lines biomouldic pores and therefore post-dates dissolution of selected skeletal grains.

The genetic evolution of dolomites formed from limestone precursors in the Brac Formation is summarized by the following sequence of events.

i. **Micritic components of precursor packstones to grainstones were replaced by dolomite.** Lime mud was particularly susceptible to early dolomitization, probably before lithification, because of its (a) high surface area to volume ratio (Sibley, 1982; Sibley and Gregg, 1987); (b) high water-filled microporosity (Choquette and Hiatt, 2007); and (c) metastable aragonite and high Mg-calcite composition (Sibley, 1982; Bullen and Sibley, 1984; Choquette and Hiatt, 2007). These conditions were optimal for dolomitization because they provided a large number of nucleation sites for the growth of incipient dolomite crystals (Sibley, 1982).
ii. **Coarse, aragonitic bioclasts were selectively leached from the matrix.** Dissolved bioclasts (corals, molluscs, *Halimeda*) are represented by fossil mouldic pores in the variably dolomitized groundmass. Micrite envelopes preserve original grain outlines.
iii. **Mimetic dolomite selectively replaced skeletal grains composed of high Mg-calcite.** This late-stage, selective dolomitization of coralline red algae and benthic foraminifera preserved original skeletal architecture. These fossils were preferentially replaced by mimetic dolomite due to the abundance of nucleation sites associated with their cryptocrystalline structure (Bullen and Sibley, 1984) and metastable mineralogy.
iv. **Isopachous, limpid dolomite cement precipitated in available pore-space.** Cement overgrowths formed in optical continuity around existing dolomite crystals. Successive zones of dolomite cement lined and filled pores.

Although genetic relationships can be deciphered between various depositional and diagenetic components, it is impossible to discern the absolute time scale over which dolomitization processes occurred. The variable degrees of diagenesis sustained by samples from different localities in the Brac Formation mean that each stage will not necessarily be evident.

The spatial distribution of dolomite in the Brac Formation is vertically and laterally inconsistent with respect to mineral abundance, chemical composition ($\delta^{18}O$, mol % $CaCO_3$), and texture (crystal size and style of replacement). Although its heterogeneous distribution makes the geometry of the dolomite body difficult to characterize, it appears to diminish from south to north across the island (indicated by its abundance in SCD, APL#1, and CRQ#1 and scarcity in LCB and EOR#1). The general trend of dolomite abundance indicates that dolomitization of the Brac Formation probably proceeded from south to north, possibly due to exposure along a reaction front. Although modified seawater is the most likely fluid to have mediated dolomitization (evidenced by $\delta^{18}O$ data), the dominant fluid-flow mechanism that drove the reaction is not apparent. The reaction front was probably focused along lithological heterogeneities associated with high permeability and/or high reactive surface area (cf. Whitaker *et al.*, 2004), but there is no obvious relationship between depositional facies and style or extent of dolomitization that can be discerned from available data. Small-scale variability in dolomite geochemistry has similarly been recognized in other dolomite bodies (e.g., Jones and Luth, 2002; Budd, 2006). Collectively, these findings provide evidence that the growth of individual dolomite crystals is controlled primarily by small-scale changes in the physiochemical environment rather than large-scale variations in the dolomitizing fluid (Jones and Luth, 2002). Heterogeneous dolomitization of the Brac Formation is therefore interpreted as the result of a complex interplay of growth kinetics at the crystal scale rather than a single, large-scale extrinsic control.

The single largest uncertainty arising from the nature of dolomite distribution in the Brac Formation is why the coarsely crystalline sucrosic dolomite in the Pollard Bay member is different from the finely crystalline dolomite found throughout the strata in the Cayman Formation and Pedro Castle Formation. In addition to its textural contrast with the finely crystalline dolomite, the clustered $\delta^{18}O$ and $\delta^{13}C$ isotope ratios of the sucrosic dolomite help to identify it as a distinct compositional population. This variability could be a function of (a) the availability of active nucleation sites, (b) different stages of textural maturity in response to diagenetic evolution, or (c) different phases of dolomitization. These possibilities are considered herein.

Sibley and Gregg (1987) recognized that dolomitization of a limestone is a genetic process dependent on crystal nucleation and growth kinetics. They suggested that dolomite texture (i.e., crystal size distribution) is a function of competing kinetic processes. Dolomite crystal nucleation is promoted by the availability of numerous active nucleation sites. Thus, if nucleation exceeds the crystal growth rate, a fine-grained aggregate will precipitate. Inversely, a coarser crystal aggregate would develop when the growth rate outpaces nucleation. In addition, polymodal crystal size distributions can result from (a) a heterogeneous distribution of nucleation sites on the precursor substrate; (b) multiple nucleation events; or (c) variable growth rates (Sibley and Gregg, 1987). Following this interpretation, the coexistence of finely crystalline and sucrosic dolomite crystals together in the Brac Formation could signify formation by multiple periods of nucleation or differential nucleation on a heterogeneous substrate. Thus, the finely crystalline dolomite may have formed in response to an abundance of nucleation sites, whereas the sucrosic dolomite would have formed through prolonged growth of fewer crystals as a result of reduced sites available for nucleation. The inability to identify actual crystal nuclei, however, makes it impossible to determine the controls on their density and distribution (Jones, 2005).

The second scenario that could explain the heterogeneous populations of dolomite crystals in the Brac Formation is that dolomitization was a time-transgressive, multiphase process driven by glacio-eustatic events. Recent research indicates that most dolomites are multiphase crystalline rocks that have undergone successive stages of dolomitization (Wheeler *et al.*, 1999; Kyser et al., 2002; Jones and Luth, 2003a; Jones, 2004, 2005, 2007; Choquette and Hiatt, 2007). Indeed, electron microprobe analysis of finely crystalline dolomite in the Brac Formation reveals a complexly interlocking mosaic of HCD and LCD, providing evidence for architectural heterogeneity in individual dolomite crystals as small as 10 μm. These composite crystals record separate phases of dolomite precipitation, and thus provide evidence for multiple episodes of dolomitization (Jones, 2005). It is therefore probable that if separate phases of dolomitization are recorded even within single dolomite crystals, then the coexistence of obviously distinct dolomite populations in the Brac Formation also signifies time-separated dolomitization events.

Choquette and Hiatt (2007) proposed a general pattern of textural maturation in sucrosic dolomites of lime-mud origin that proceeds by (i) coarsening; (ii) induration; and (iii) occlusion of pore systems (their Fig. 17). In this model, sucrosic dolomites represent a more advanced stage of textural evolution (represented by crystal coarsening and cementation) than less pervasively dolomitized, finer crystalline facies. If this model is applied to the Brac Formation, then the co-occurrence of finely crystalline and sucrosic dolomite populations would represent different stages of textural evolution in a multiphase system. The finely crystalline dolomite would therefore express nucleation and cortex growth stages, whereas the sucrosic dolomite would reflect greater development of the subsequent cementation stage. As dolomite texture distribution is likely determined by the porosity and permeability of precursor facies (Wheeler *et al*., 1999), the sucrosic dolomite may represent prolonged exposure along a reaction front controlled by fluid-flow pathways. It is difficult to assess, however, if specific facies with enhanced flow parameters were more conducive to late-stage growth of sucrosic dolomite cements, as the genetic relationship between precursor limestone facies, permeability, and resultant dolomite textures is not evident at this time.

The oxygen isotope data from heterogeneous dolomite populations in the Brac Formation can be construed as evidence for a genetic evolution. The mean $\delta^{18}O$ value of all measured dolomite samples is +1.39‰, indicating that most growth occurred in normal to slightly modified seawater. However, the linear mixing trend of $\delta^{18}O$ values from APL#1 and EOR#1 (wells that contain fabric retentive finely crystalline dolomite, which could reflect the early stage of dolomite cortex growth) may evince some influence from mixed waters. In contrast, the $\delta^{18}O$ values from CRQ#1 (fabric destructive finely crystalline dolomite, in lateral-linkage cement stage) and SCD (sucrosic dolomite, in late pore-filling cement stage) are tightly clustered and more positive, substantiating genesis from normal marine water. A correlation between increasing stages of textual maturity and relative evolution of $\delta^{18}O$ to more positive values may imply that dolomite nucleation began in brackish waters, with later growth and cementation continuing in normal seawater (cf. Kyser *et al.*, 2002; Choquette and Hiatt, 2007). If Brac Formation dolomites did evolve in this manner, then eustatic sea level changes would have driven multiple phases of dolomitization by repeated exposure to fluctuating pore water chemistries in mobile hydrologic zones. Indeed, Wheeler *et al.* (1999) attributed similar observations of alternating limestone and dolomite zones at Niue to vertical oscillations of the meteoric lens in response to glacio-eustatic fluctuations. It is therefore plausible, based on the variability in $\delta^{18}O$ values and dolomite crystal textures, that multiphase dolomites of the Brac Formation evolved through progressive stages of maturity driven by episodic changes in sea level.

The culmination of these observations suggests that it would be an oversimplification to ascribe the complex diagenetic sequence of dolomites in the Brac Formation to a single hydrologic model. Dolomitization of precursor limestones probably occurred through multiple, time-separated nucleation and growth phases driven by eustatic sea level oscillations. Microscale variations in the physiochemical environment immediately surrounding individual dolomite crystals likely produced the textural and geochemical disparities between dolomite populations (cf. Jones and Luth, 2002). Sucrosic dolomite may have formed as a consequence of (a) fewer active nucleation sites than were available in the precursor to finely crystalline dolomite (Sibley and Gregg, 1987); (b) textural maturation of finely crystalline dolomite cement (Choquette and Hiatt, 2007); (c) a separate phase of dolomitization (possibly in modified seawater of a different isotopic composition); or (d) a combination of the factors listed above. Presently, there is not enough evidence to decisively conclude which variable had the greatest effect on the production of texturally and geochemically distinct dolomite populations in the Brac Formation.

4.6 Post-Dolomitization Diagenesis

Following the initial stages of dolomitization, dissolution and cementation processes extensively modified sediments of the Brac Formation. Repeated periods of karst development produced voids ranging in size from tens of μm (interparticle and mouldic pores) to tens of m (solution caverns). Void-filling deposits in the Brac Formation are characterized by complex successions of detrital sediments and precipitates formed in various hydrologic environments in response to glacioeustatic sea level change (Jones, 1992b). The heterogeneous assortment of sediment fills include caymanite, microbreccias, terra rossa, and speleothems (including stalactites, stalagmites, columns, and flowstones).

Pore-occluding cements fill cavities in the Brac Formation, recording a complex diagenetic history involving multiple stages of precipitation from variable pore-water chemistry. The cement succession, though inconsistently developed between individual pores, documents an overall transition from the phreatic zone to the vadose zone. Cementation events are recorded by the sequential precipitation of (i) limpid, isopachous, dolomite cement (consisting of up to 10 bands distinguished by dark, insoluble horizons), (ii) sparry to bladed calcite cement, and (iii) microstalactites composed of mixed calcite and dolomite.

Comparable cement successions found in the dolostones of the Cayman Formation on Grand Cayman were documented by Jones *et al.* (1984), who suggested that the diagenetic regime evolved from the mixing zone to the freshwater phreatic zone and finally to the vadose zone. The preserved cement succession in the Brac Formation is similarly interpreted here to reflect time-separated phases of diagenesis ranging from mixed fresh and marine waters to the freshwater vadose environment. Isopachous dolomite cements may have formed in mixed meteoric-marine waters, where schizohaline conditions are favourable for the precipitation of limpid dolomite crystals (cf. Folk and Siedlecka, 1974; Jones, 2004). The optical clarity and inclusion-free nature of this cement may additionally reflect precipitation from clear pore waters (Kyser *et al.*, 2002; Choquette and Hiatt, 2007). Subsequently, a transition to the freshwater phreatic zone likely caused precipitation of the coarsely crystalline, equant calcite cement (cf. Jones *et al.*, 1984; Ward and Halley, 1985; Humphrey, 1988; Jones, 2004). The microstalactitic cement (found only in outcrop sections exposed on the sea cliffs) was formed during the last phase of cementation in the freshwater vadose zone. The pendant morphology indicates precipitation from water percolating downward through partially air-filled pores. The zoned calcite-dolomite composition of this final cement phase may reflect fluctuations in the Mg/Ca ratio of the groundwater (Jones *et al.*, 1984).

Although similar cement successions have been recorded elsewhere in the Caribbean [e.g., Jamaica (Land, 1973); Yucatan Peninsula (Ward and Halley, 1984); Barbados (Humphrey, 1988); Grand Cayman (Jones *et al.*, 1984)], they probably cannot be attributed to a single eustatic sea level change (Jones, 2004). Rather, the punctuated phases of cementation evident in the Brac Formation, combined with the heterogeneous distribution of pore-filling sediments, likely reflect a complex diagenetic evolution controlled by the upward and downward migration of various hydrologic zones in response to frequent glacioeustatic sea level change.

4.7 Paragenetic Evolution

The timing of deposition and diagenesis in the Brac Formation is difficult to resolve using the $^{87}Sr/^{86}Sr$ geochronometer as a standalone age proxy. The mixed mineralogy, multiple compositional populations of calcite and dolomite, and resetting of $^{87}Sr/^{86}Sr$ isotope ratios through several phases of diagenesis render age estimates for the samples analyzed in this study largely inconclusive. The average $^{87}Sr/^{86}Sr$ ratio of calcite (n=12) is 0.708569, but values range from 0.708033 to 0.709144. Dolomite $^{87}Sr/^{86}Sr$ ratios (n=11) range from 0.708605 to 0.709155, with a mean value of 0.708900. The strontium isotope ratios of calcite in the Brac Formation thus provide a minimum age of deposition of mid-Oligocene, or ~ 28.6 Ma on the $^{87}Sr/^{86}Sr$-time curve of McArthur *et al.* (2001; Look-Up Table Version 4: 08/03). The wide spread in dolomite $^{87}Sr/^{86}Sr$ ratios collected in this study does not allow identification of distinct dolomitization events in the paragenetic evolution of the Brac Formation (Fig. 4.2). This

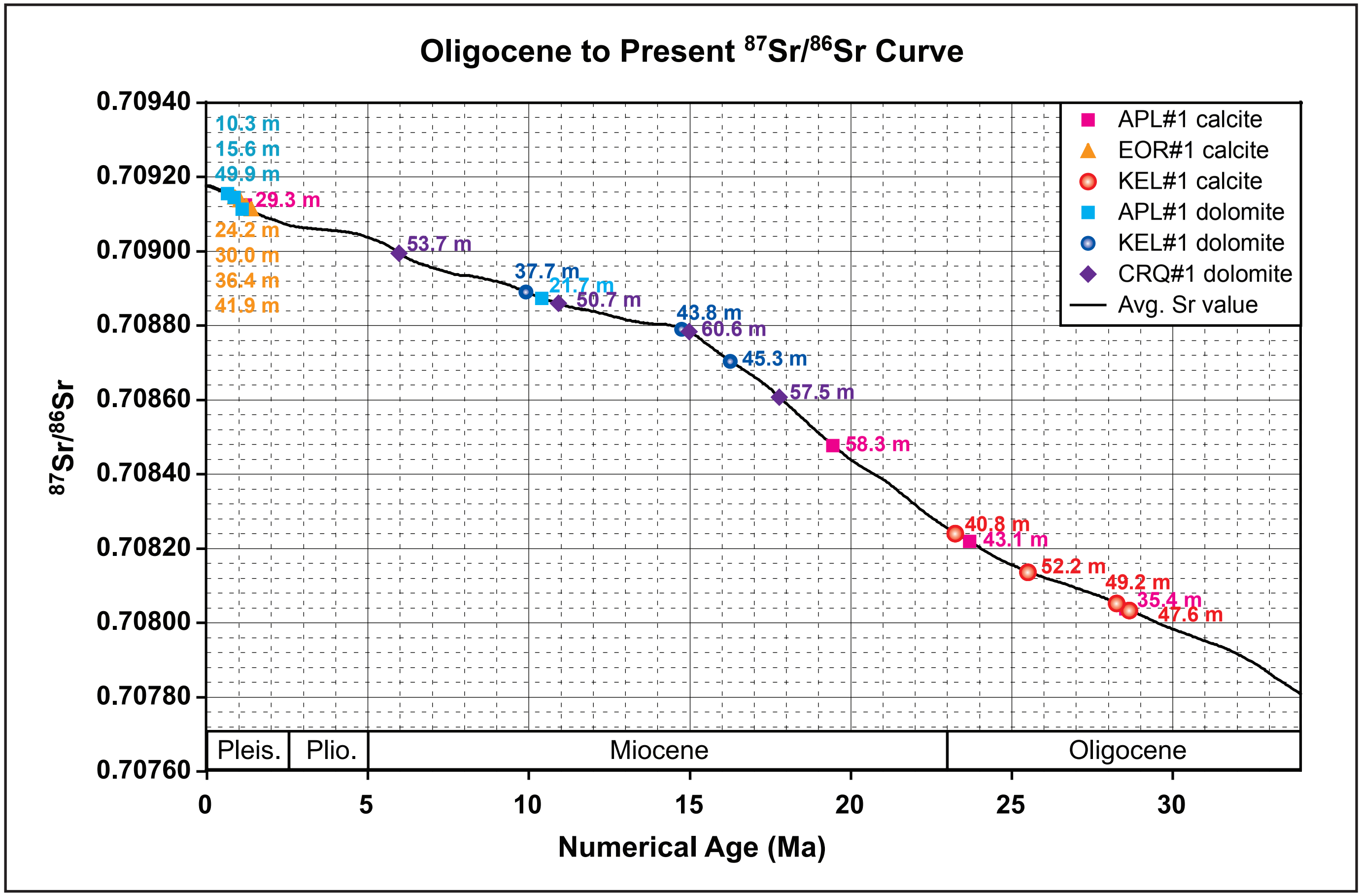

Figure 4.2 Strontium isotope data measured from the Brac Formation (this study; Appendix 1) plotted on the $^{87}Sr/^{86}Sr$-time curve of McArthur *et al*. (2001; Look-Up Table Version 4: 08/03). Sample depths (metres below sea level) are plotted beside data points.

observation is consistent with the interpretation that dolomitization was a time-transgressive process that evolved through multiple stages of crystal growth. The strontium isotope ratios of dolomite do, however, provide a minimum age of ~ 18 Ma (middle Miocene) for the onset of dolomitization.

Jones and Luth (2003a), citing data from Jones *et al.* (1994a), reported average $^{87}Sr/^{86}Sr$ values of 0.708189 and 0.708939 for limestones and dolostones in the Brac Formation, respectively. They interpreted the $^{87}Sr/^{86}Sr$ values from the limestones to indicate an age of ~ 28 Ma, in agreement with the age of deposition derived in this study and verified by age-diagnostic *Lepidocyclina*. Conversely, they interpreted the $^{87}Sr/^{86}Sr$ ratios of dolomite to indicate a late Miocene age, corresponding to the first known phase of dolomitization that altered limestones in the Cayman Islands (Jones and Luth, 2003a).

4.8 Conclusions

A complex sequence of events has refashioned the Brac Formation from the original lime sediments deposited on a shallow bank in the mid-Oligocene into a carbonate unit that is now characterized by a high degree of compositional heterogeneity. The variable lithology, in conjunction with the broad range in geochemical data, is testament to the numerous stages of diagenesis that the rocks have undergone in various hydrologic regimes. Dolomitization of the original limestones was not a single event; rather, it was probably a time-transgressive process driven by eustatic fluctuations in sea level. Oxygen isotope data provide evidence that dolomitization was mediated by normal to slightly modified seawater, producing multiphase dolomite crystals that represent different stages of textural and geochemical maturity. The wide spread in strontium isotope ratios further supports the notion that dolomites were formed through time-separated crystallization events beginning in the middle Miocene. Critical to understanding the paragenetic evolution of the Brac Formation on Cayman Brac is the recognition that diagenesis is continuously modifying the composition of the rocks, even at the present time.

References

Abreu, V.S. and Anderson, J.B., 1998. Glacial eustasy during the Cenozoic: sequence stratigraphic implications. *AAPG Bulletin* **82**, 1385-1400.

Allan, J.R. and Matthews, R.K., 1982. Isotope signatures associated with early meteoric diagenesis. *Sedimentology* **29**, 797-817.

Amirshahkarami, M., Vaziri-Moghaddam, H. and Taheri, A., 2007. Paleoenvironmental model and sequence stratigraphy of the Asmari Formation in southwest Iran. *Historical Biology* **19**, 173-183.

Arts, A., 2000. Sedimentology and stratigraphy of the Pedro Castle Formation, Grand Cayman. Unpublished M.Sc. Thesis, University of Alberta, Edmonton, 107 pp.

Banerjee, A., Yemane, K. and Johnson, A., 2000. Foraminiferal biostratigraphy of Late Oligocene-Miocene reefal carbonates in southwestern Puerto Rico. *Micropaleontology* **46**, 327-342.

Banner, J.L. and Hanson, G.N., 1990. Calculation of simultaneous isotopic and trace element variations during water-rock interaction with applications to carbonate diagenesis. *Geochimica et Cosmochimica Acta* **54**, 3123-3137.

Blanchon, P. and Jones, B., 1995. Marine-planation terraces on the shelf around Grand Cayman: a result of stepped Holocene sea-level rise. *Journal of Coastal Research* **11**, 1-33.

Blanchon, P., Jones, B. and Kalbfleisch, W., 1997. Anatomy of a fringing reef around Grand Cayman: storm rubble, not coral framework. *Journal of Sedimentary Research* **67**, 1-16.

Bosellini, F.R. and Russo, A., 1992. Stratigraphy and facies of an Oligocene fringing reef (Castro Limestone, Salento Peninsula, southern Italy). *Facies* **26**, 145-166.

Budd, D.A., 1997. Cenozoic dolomites of carbonate islands: their attributes and origin. *Earth-Science Reviews* **42**, 1-47.

Budd, D.A., Pranter, M.J. and Reza, Z.A., 2006. Lateral periodic variations in the petrophysical and geochemical properties of dolomite. *Geology* **34**, 373-376.

Bullen, S. and Sibley, D.F., 1984. Dolomite selectivity and mimic replacement. *Geology* **12**, 655-658.

Buxton, M.W.N. and Pedley, H.M., 1989. A standardized model for Tethyan Tertiary carbonate ramps. *Journal of the Geological Society, London* **146**, 746-748.

Chaproniere, G.C.H., 1975. Palaeoecology of Oligo-Miocene larger Foraminiferida, Australia. *Alcheringa* **1**, 37-58.

Choquette, P.W. and Hiatt, E.E., 2008. Shallow-burial dolomite cement: a major component of many ancient sucrosic dolomites. *Sedimentology* **55**, 423-460.

Clayton, R.N. and Degens, E.T., 1959. Use of carbon isotope analysis of carbonates for differentiating fresh-water and marine sediments. *Bulletin of the American Association of Petroleum Geologists* **43**, 890-897.

Cole, W.S., 1961. An analysis of certain taxonomic problems in the larger foraminifera. *Bulletins of American Paleontology* **43**, 373-394.

Coyne, M.K., Jones, B. and Ford, D., 2007. Highstands during Marine Isotope Stage 5: evidence from the Ironshore Formation of Grand Cayman, British West Indies. *Quaternary Science Reviews* **26**, 536-559.

Dixon, T.H., Farina, F., DeMets, C., Jansma, P., Mann, P. and Calais, E., 1998. Relative motion between the Caribbean and North American plates and related boundary zone deformation from a decade of GPS observations. *Journal of Geophysical Research* **103**, 15157-15182.

Dunham, R.J., 1962. Classification of carbonate rocks according to depositional textures. *In* W.E. Ham (ed.), *Classification of Carbonate Rocks*. American Association of Petroleum Geologists Memoir **1**, 108-121.

Emery, K.O. and Milliman, J.D., 1980. Shallow-water limestones from slope off Grand Cayman Island. *Journal of Geology* **88**, 483-488.

Emiliani, C., 1955. Pleistocene paleotemperatures. *Journal of Geology* **63**, 538-578.

Epstein, S., Buchsbaum, R., Lowenstam, H.A., and Urey, H.C., 1953. Revised carbonate-water isotopic temperature scale. *Geological Society of America Bulletin* **64**, 1315-1326.

Epstein, S., Graf, D.L. and Degens, E.T., 1963. Oxygen isotope studies on the origin of dolomites. *In* H. Craig, S.L. Miller, and G.J. Wasserburg (eds.), *Isotopic and Cosmic Chemistry*. North-Holland Pub. Co., Amsterdam, pp. 169-180.

Epstein, S. and Mayeda, T., 1953. Variation of ^{18}O content of waters from natural sources. *Geochimica et Cosmochimica Acta* **4**, 213-224.

Etherington, S., 2004. Sedimentology and depositional architecture of the Cayman (Miocene) and Pedro Castle (Pliocene) formations on western Grand Cayman, British West Indies. Unpublished M.Sc. Thesis, University of Alberta, Edmonton, 122 pp.

Fahlquist, D.A. and Davies, D.K., 1971. Fault-block origin of the western Cayman Ridge, Caribbean Sea. *Deep-Sea Research* **18**, 243-253.

Fenner, D.P., 1993. Some reefs and corals of Roatan (Honduras), Cayman Brac, and Little Cayman. *Atoll Research Bulletin* **388**, 1-30.

Folk, R.L. and Siedlecka, A.A., 1974. The "schizohaline" environment: its sedimentary and diagenetic fabrics as exemplified by late Paleozoic rocks of Bear Island, Svalbard. *Sedimentary Geology* **11**, 1-15.

Fritz, P. and Smith, D.C.W., 1970. The isotopic composition of secondary dolomites. *Geochimica et Cosmochimica Acta* **34**, 1161-1173.

Frost, S.H., Harbour, J.L., Beach, D.K., Realini, M.J. and Harris, M., 1983. Oligocene reef tract development southwestern Puerto Rico. *Sedimenta IX*, Comp. Sed. Lab., Div. Marine Geol. Geoph., RSMAS, Miami, 141 pp.

Frost, S.H. and Langenheim, R.L. Jr., 1974. Cenozoic Reef Biofacies, Northern Illinois University Press, De Kalb, 388 pp.

Gaswirth, S.B., Budd, D.A. and Farmer, G.L., 2007. The role and impact of freshwater-seawater mixing zones in the maturation of regional dolomite bodies within the proto Floridan Aquifer, USA. *Sedimentology* **54**, 1065 1091.

Geel, T., 2000. Recognition of stratigraphic sequences in carbonate platform and slope deposits: empirical models based on microfacies analysis of Palaeogene deposits in southeastern Spain. *Palaeogeography, Palaeoclimatology, Palaeoecology* **155**, 211-238.

Gischler, E., Hauser, I., Heinrich, K. and Scheitel, U., 2003. Characterization of depositional environments in isolated carbonate platforms based on benthic foraminifera, Belize, Central America. *Palaios* **18**, 236-255.

Goldberg, W.M., 1983. Cay Sal Bank, Bahamas: a biologically impoverished physically controlled environment. *Atoll Research Bulletin* **271**, 1-23.

Gonzalez, L.A., Ruiz, H.M., Taggart, B.E., Budd, A.F. and Monell, V., 1997. Geology of Isla de Mona, Puerto Rico, in: H.L. Vacher and T. Quinn (Eds.), *Geology and Hydrogeology of Carbonate Islands. Developments in Sedimentology* **54**, 327-358.

Haig, D.W., 1985. *Lepidocyclina* associated with Early Miocene planktic foraminiferids from the Fairfax Formation, Papua New Guinea. *Spec. Publ., S. Aust. Dept. Mines and Energy* **5**, 117-131.

Hallock, P. and Glenn, E.C., 1986. Larger foraminifera: a tool for paleoenvironmental analysis of Cenozoic carbonate depositional facies. *Palaios* **1**, 55-64.

Haq, B.U., Hardenbol, J. and Vail, P.R., 1987. Chronology of fluctuating sea levels since the Triassic. *Science* **235**, 1156-1167.

Hardie, L.A., 1987. Dolomitization: a critical view of some current views. *Journal of Sedimentary Petrology* **57**, 166-183.

Hine, A.C. and Neumann, A.C., 1977. Shallow carbonate-bank-margin growth and structure, Little Bahama Bank, Bahamas. *The American Association of Petroleum Geologists Bulletin* **61**, 376-406.

Holcombe, T.L., Ladd, J.W., Westbrook, G.K., Edgar, N.T. and Bowland, C.L., 1990. Caribbean marine geology; ridges and basins of the plate interior. *In* G. Dengo and J.E. Case (eds.), *The Caribbean Region*. *The Geology of North America* **H**, 231-260.

Horsfield, W.T., 1975. Quaternary vertical movements in the Greater Antilles. *Geological Society of America Bulletin* **86**, 933-938.

Humphrey, J.D., 1988. Late Pleistocene mixing zone dolomitization, southeastern Barbados, West Indies. *Sedimentology* **35**, 327-348.

Humphrey, J.D., 2000. New geochemical support for mixing-zone dolomitization at Golden Grove, Bahamas. *Journal of Sedimentary Research* **70**, 1160-1170.

Hunter, I.G. and Jones, B., 1996. Coral associations of the Pleistocene Ironshore Formation, Grand Cayman. *Coral Reefs* **15**, 249-267.

James, N.P. and Choquette, P.W., 1984. Diagenesis 9. – Limestones – the meteoric diagenetic environment. *Geoscience Canada* **11**, 161-194.

Jones, B., 1989. Syntaxial overgrowths on dolomite crystals in the Bluff Formation, Grand Cayman, British West Indies. *Journal of Sedimentary Petrology* **59**, 839-847.

Jones, B., 1992a. Caymanite, a cavity-filling deposit in the Oligocene-Miocene Bluff Formation of the Cayman Islands. *Canadian Journal of Earth Science* **29**, 720-736.

Jones, B., 1992b. Void-filling deposits in karst terrains of isolated oceanic islands: a case study from Tertiary carbonates of the Cayman Islands. *Sedimentology* **39**, 857-876.

Jones, B., 2004. Petrography and significance of zoned dolomite cements from the Cayman Formation (Miocene) of Cayman Brac, British West Indies. *Journal of Sedimentary Research* **74**, 95-109.

Jones, B., 2005. Dolomite crystal architecture: genetic implications for the origin of the Tertiary dolostones of the Cayman Islands. *Journal of Sedimentary Research* **75**, 177-189.

Jones, B., 2007. Inside-out dolomite. *Journal of Sedimentary Research* **77**, 537-551.

Jones, B. and Hunter, I.G., 1989. The Oligocene-Miocene Bluff Formation on Grand Cayman. *Caribbean Journal of Earth Science* **25**, 71-85.

Jones, B. and Hunter, I.G., 1990. Pleistocene paleogeography and sea levels on the Cayman Islands, British West Indies. *Coral Reefs* **9**, 81-91.

Jones, B. and Hunter, I.G., 1994a. Evolution of an isolated carbonate bank during Oligocene, Miocene and Pliocene times, Cayman Brac, British West Indies. *Facies* **30**, 25-50.

Jones, B. and Hunter, I.G., 1994b. Messinian (Late Miocene) karst on Grand Cayman, British West Indies: an example of an erosional sequence boundary. *Journal of Sedimentary Research* **B64**, 531-541.

Jones, B., Hunter, I.G., and Kyser, K., 1994a. Stratigraphy of the Bluff Formation (Miocene - Pliocene) and the newly defined Brac Formation (Oligocene), Cayman Brac, British West Indies. *Caribbean Journal of Science* **30**, 30-51.

Jones, B., Hunter, I.G., and Kyser, K., 1994b. Revised stratigraphic nomenclature for Tertiary strata of the Cayman Islands, British West Indies. *Caribbean Journal of Science* **30**, 53-68.

Jones, B., Lockhart, E.B. and Squair, C., 1984. Phreatic and vadose cements in the Tertiary Bluff Formation of Grand Cayman Island, British West Indies. *Bulletin of Canadian Petroleum Geology* **32**, 382-397.

Jones, B. and Luth, R.W., 2002. Dolostones from Grand Cayman, British West Indies. *Journal of Sedimentary Research* **72**, 559-569.

Jones, B. and Luth, R.W., 2003a. Temporal evolution of Tertiary dolostones on Grand Cayman as determined by $^{87}Sr/^{86}Sr$. *Journal of Sedimentary Research* **73**, 187-205.

Jones, B. and Luth, R.W., 2003b. Petrography of finely crystalline Cenozoic dolostones as revealed by backscatter electron imaging: case study of the Cayman Formation (Miocene), Grand Cayman, British West Indies. *Journal of Sedimentary Research* **73**, 1022-1035.

Jones, B., Luth, R.W. and MacNeil, A.J., 2001. Powder X-ray diffraction analysis of homogeneous and heterogeneous sedimentary dolostones. *Journal of Sedimentary Research* **71**, 790-799.

Jones, B., Ng, K.-C. and Hunter, I.G., 1997. Geology and hydrogeology of the Cayman Islands, in: H.L. Vacher and T. Quinn (Eds.), *Geology and Hydrogeology of Carbonate Islands. Developments in Sedimentology* **54**, 299-326.

Jones, B., Pleydell, S.M., Ng, K.-C. and Longstaffe, F.J., 1989. Formation of poikilotopic calcite-dolomite fabrics in the Oligocene-Miocene Bluff Formation of Grand Cayman, British West Indies. *Bulletin of Canadian Petroleum Geology* **37**, 255-265.

Kim, S.-T. and O'Neil, J.R., 1997. Equilibrium and nonequilibrium oxygen isotope effects in synthetic carbonates. *Geochimica et Cosmochimica Acta* **61**, 3461-3475.

Kominz, M.A., Miller, K.G. and Browning, J.V., 1998. Long-term and short-term global Cenozoic sea-level estimates. *Geology* **26**, 311-314.

Kyser, K.T., 1987. Equilibrium fractionation factors for stable isotopes, in: K.T. Kyser (Ed.), *Stable Isotope Geochemistry of Low Temperature Processes. Mineralogical Association of Canada Short Course Handbook* **13**, pp. 1-84.

Kyser, T.K., James, N.P. and Bone, Y., 2002. Shallow burial dolomitization and dedolomitization of Cenozoic cool-water limestones, southern Australia: geochemistry and origin. *Journal of Sedimentary Research* **72**, 146-157.

Ladd, J.W., Holcombe, R.L., Westbrook, G.K. and Edgar, N.T., 1990. Caribbean marine geology; active margins of the plate boundary. *In* G. Dengo and J.E. Case (eds.), *The Caribbean Region. The Geology of North America* **H**, 261-290.

Land, L.S., 1973. Contemporaneous dolomitization of middle Pleistocene reefs by meteoric water, north Jamaica. *Bulletin of Marine Science* **23**, 64-92.

Land, L.S., 1980. The isotopic and trace element geochemistry of dolomite: the state of the art, in: D.H. Zenger, J.B. Dunham, and R.L. Ethington (Eds.), *Concepts and Models of Dolomitization. Spec. Publs Soc. Econ. Paleont. Mineral* **28**, pp. 87-110.

Land, L.S., 1983. The application of stable isotopes to studies of the origin of dolomite and to problems of diagenesis of clastic sediments, in: M.A. Arthur, T.F. Anderson, I.R. Kaplan, J. Veizer and L.S. Land (Eds.), *Stable Isotopes in Sedimentary Geology. SEPM Short Course Notes*, **10**, pp. 4 1–4-22.

Land, L.S., 1985. The origin of massive dolomite. *Journal of Geological Education* **33**, 112-125.

Land, L.S., 1992. The dolomite problem: stable and radiogenic isotope clues, in: N. Clauer and S. Chaudhuri (Eds.), *Isotopic Signatures and Sedimentary Records. Lecture Notes in Earth Science* **43**, pp. 49-68.

Lawrence, J.R., 1998. Isotopic spikes from tropical cyclones in surface waters: opportunities in hydrology and paleoclimatology. *Chemical Geology* **144**, 153-160.

Lawrence, J.R., Gedzelman, S.D., Gamache, J. and Black, M., 2002. Stable isotope ratios: Hurricane Olivia. *Journal of Atmospheric Chemistry* **41**, 67 82.

Li, C. and Jones, B., 1997. Comparison of foraminiferal assemblages in sediments on the windward and leeward shelves of Grand Cayman, British West Indies. *Palaios* **12**, 12-26.

Li, C., Jones, B. and Kalbfleisch, W.B.C., 1998. Carbonate sediment transport pathways based on foraminifera: case study from Frank Sound, Grand Cayman, British West Indies. *Sedimentology* **45**, 109-120.

Lohmann, K.C., 1988. Geochemical patterns of meteoric diagenetic systems and their application to studies of paleokarst, in: P.W. Choquette and N.P. James (Eds.), *Paleokarst.* Springer-Verlag, New York, pp. 55-80.

MacDonald, K.C. and Holcombe, T.L., 1978. Inversion of magnetic anomalies and sea-floor spreading in the Cayman Trough. *Earth and Planetary Science Letters* **40**, 407-414.

Machel, H.G., 2000. Dolomite formation in Caribbean islands – driven by plate tectonics?! *Journal of Sedimentary Research* **70**, 977-984.

Machel, H.G., 2004. Concepts and models of dolomitization: a critical reappraisal, in: C.J.R. Braithwaite, G. Rizzi, and G. Darke (Eds.), *The Geometry and Petrogenesis of Dolomite Hydrocarbon Reservoirs. Geological Society, London, Special Publications* **235**, 7-63.

Machel, H.G. and Mountjoy, E.W., 1986. Chemistry and environments of dolomitization – a reappraisal. *Earth Science Reviews* **23**, 175-222.

MacNeil, A.J., 2001. Sedimentology, diagenesis, and dolomitization of the Pedro Castle Formation on Cayman Brac, British West Indies. Unpublished M.Sc. Thesis, University of Alberta, Edmonton, 128 pp.

MacNeil, A. and Jones, B., 2003. Dolomitization of the Pedro Castle Formation (Pliocene), Cayman Brac, British West Indies. *Sedimentary Geology* **162**, 219-238.

Manfrino, C., Riegl, B., Hall, J.L. and Graifman, R., 2003. Status of the coral reefs of Little Cayman, Grand Cayman and Cayman Brac, British West Indies, in 1999 and 2000 (Part 1: stony corals and algae). *In* J.C. Lang (ed.), *Status of the Coral Reefs of the Western Atlantic: Results of the Initial Survey, Atlantic and Gulf Rapid Reef Assessment (AGRRA) Program. Atoll Research Bulletin* **496**, 204-225.

Matley, C.A., 1924a. Reconnaissance geological survey of Cayman Islands, British West Indies. *Pan-Amer. Geol.* **42**, 313-315.

Matley, C.A., 1924b. Report of a reconnaissance geological survey of the Cayman Islands. Supplement to the Jamaica Gazette, June 13, 1924, pp. 69-73.

Matley, C.A., 1925a. Report of a reconnaissance geological survey of the Cayman Islands. Jamaica, Annual General Report for 1923, pp. 41-45.

Matley, C.A., 1925b. Reconnaissance geological survey of the Cayman Islands, British West Indies. *British Assoc. Adv. Sci., Rept*. 92nd Meeting (Toronto), pp. 392-393.

Matley, C.A., 1926. The geology of the Cayman Islands (British West Indies) and their relation to the Bartlett Trough. *Quarterly Journal of the Geological Society of London* **82**, 352-387.

Matthews, A. and Katz, A., 1977. Oxygen isotope fractionation during the dolomitization of calcium carbonate. *Geochimica et Cosmochimica Acta* **41**, 1431-1438.

McArthur, J.M. and Howarth, R.J., 2004. 7: Strontium isotope stratigraphy. *In* F.M Gradstein, J.G. Ogg and A.G. Smith (eds.), *A Geologic Time Scale 2004*. Cambridge University Press, 610 pp.

McArthur, J.M., Howarth, R.J. and Bailey, T.R., 2001. Strontium isotope stratigraphy: LOWESS version 3. Best fit to the marine Sr-isotope curve for 0-509 Ma and accompanying look-up table for deriving numerical age. Look-up table version 4: 08/03. *Journal of Geology* **109**, 155-170.

McCrea, J.M., 1950. On the isotopic chemistry of carbonates and a paleotemperature scale. *Journal of Chemical Physics* **18**, 849-857.

Melim, L.A., Swart, P.K. and Eberli, G.P., 2004. Mixing zone diagenesis in the subsurface of Florida and the Bahamas. *Journal of Sedimentary Research* **74**, 904-913.

Miller, D.L., Mora, C.I., Grissino-Mayer, H.D., Mock, C.J., Uhle, M.E. and Sharp, Z., 2006. Tree-ring isotope records of tropical cyclone activity. *PNAS* **103**, 14294-14297.

Miller, K.G., Kominz, M.A., Browning, J.V., Wright, J.D., Mountain, G.S., Katz, M.E., Sugarman, P.J., Cramer, B.S., Christie-Blick, N. and Pekar, S.F., 2005. The Phanerozoic record of global sea-level change. *Science* **310**, 1293-1298.

Miller, K.G., Mountain, G.S., Browning, J.V., Kominz, M., Sugarman, P.J., Christie-Blick, N., Katz, M.E. and Wright, J.D., 1998. Cenozoic global sea level, sequences, and the New Jersey Transect: results from coastal plain and continental slope drilling. *Reviews of Geophysics* **36**, 569-601.

Ng, K.-C., 1990. Diagenesis of the Oligocene-Miocene Bluff Formation of the Cayman Islands. Unpublished Ph.D. Thesis, University of Alberta, Edmonton, 344 pp.

Ng, K.-C., Jones, B. and Beswick, R., 1992. Hydrogeology of Grand Cayman, British West Indies: a karstic dolostone aquifer. *Journal of Hydrology* **134**, 273-295.

Northrop, D.A. and Clayton, R.N., 1966. Oxygen-isotope fractionation in systems containing dolomite. *Journal of Geology* **74**, 174-196.

O'Neil, J.R. and Epstein, S., 1966. Oxygen isotope fractionation in the system dolomite-calcite-carbon dioxide. *Science* **152**, 198-201.

Oslick, J.S., Miller, K.G., Feigenson, M.D. and Wright, J.D., 1994. Oligocene-Miocene strontium isotopes: stratigraphic revisions and correlations to an inferred glacioeustatic record. *Paleoceanography* **9**, 427-443.

Paterson, R.J., Whitaker, F.F., Jones, G.D., Smart, P.L., Waltham, D. and Felce, G., 2006. Accommodation and sedimentary architecture of isolated icehouse carbonate platforms: insights from forward modeling with CARD3D. *Journal of Sedimentary Research* **76**, 1162-1182.

Pekar, S. and Miller, K.G., 1996. New Jersey Oligocene "Icehouse" sequences (ODP Leg 150X) correlated with global $\delta^{18}O$ and Exxon eustatic records. *Geology* **24**, 567-570.

Pemberton, S.G. and Jones, B., 1988. Ichnology of the Pleistocene Ironshore Formation, Grand Cayman Island, British West Indies. *Journal of Paleontology* **62**, 495-505.

Perfit, M.R. and Heezen, B.C., 1978. The geology and evolution of the Cayman Trench. *Geological Society of America Bulletin* **89**, 1155-1174.

Pleydell, S.M., Jones, B., Longstaffe, F.J. and Baadsgaard, H., 1990. Dolomitization of the Oligocene-Miocene Bluff Formation on Grand Cayman, British West Indies. *Canadian Journal of Earth Science* **27**, 1098-1110.

Quinn, T.M., 1991. Meteoric diagenesis of Plio-Pleistocene limestones at Enewetak Atoll. *Journal of Sedimentary Petrology* **61**, 681-703.

Read, J.F., 1985. Carbonate platform facies models. *The American Association of Petroleum Geologists Bulletin* **69**, 1-21.

Riegl, B., 2001. Inhibition of reef framework by frequent disturbance: examples from the Arabian Gulf, South Africa, and the Cayman Islands. *Palaeogeography, Palaeoclimatology, Palaeoecology* **175**, 79-101.

Rigby, J.K. and Roberts, H.H., 1976. Geology, reefs and marine communities of Grand Cayman Island, B.W.I. *Brigham Young Univ., Geology Studies, Spec. Publ.* **4,** 122 pp.

Salamy, K.A. and Zachos, J.C., 1999. Latest Eocene-Early Oligocene climate change and Southern Ocean fertility: inferences from sediment accumulation and stable isotope data. *Palaeogeography, Palaeoclimatology, Palaeoecology* **145**, 61–77.

Schlager, W., 1981. The paradox of drowned reefs and carbonate platforms. *Geological Society of America Bulletin* **92**, 197-211.

Schmidt, M., Xeflide, S., Botz, R., and Mann, S., 2005. Oxygen isotope fractionation during synthesis of CaMg-carbonate and implications for sedimentary dolomite formation. *Geochimica et Cosmochimica Acta* **69**, 4665-4674.

Scholle, P.A. and Ulmer-Scholle, D.S., 2003. A color guide to the petrography of carbonate rocks: grains, textures, porosity, diagenesis. American Association of Petroleum Geologists Memoir 77, 474 pp.

Sheppard, S.M.F. and Schwarcz, H.P., 1970. Fractionation of carbon and oxygen isotopes and magnesium between metamorphic calcite and dolomite. *Contributions to Mineralogy and Petrology* **26**, 161-198.

Sibley, D.F., 1982. The origin of common dolomite fabrics: clues from the Pliocene. *Journal of Sedimentary Petrology* **52**, 1087-1100.

Sibley, D.F. and Gregg, J.M., 1987. Classification of dolomite rock textures. *Journal of Sedimentary Petrology* **57**, 967-975.

Tarhule-Lips, R.F.A. and Ford, D.C., 1998. Condensation corrosion in caves on Cayman Brac and Isla de Mona. *Journal of Cave and Karst Studies* **60**, 84-95.

Tarutani, T., Clayton, R.C. and Mayeda, T.K., 1969. The effect of polymorphism and magnesium substitution on oxygen isotope fractionation between calcium carbonate and water. *Geochimica et Cosmochimica Acta* **33**, 987-996.

ten Brink, U.S., Coleman, D.F. and Dillon, W.P., 2002. The nature of the crust under Cayman Trough from gravity. *Marine and Petroleum Geology* **19**, 971-987.

Triffleman, N.J., Hallock, P. and Hine, A.C., 1992. Morphology, sediments, and depositional environments of a small carbonate platform: Serranilla Bank, Nicaraguan Rise, southwest Caribbean Sea. *Journal of Sedimentary Petrology* **62**, 591-606.

Vahrenkamp, V.C. and Swart, P.K., 1994. Late Cenozoic dolomites of the Bahamas: metastable analogues for the genesis of ancient platform dolomites. *Spec. Publs. Int. Ass. Sediment.* **21**, 133-153.

Vail, P.R., Mitchum, R.M., Jr., Todd, R.G., Widmier, J.M., Thompson, S. III, Sangree, J.B., Bubb, J.N. and Hatlelid, W.G., 1977. Seismic stratigraphy and global changes of sea level, *in*: C.E. Payton (Ed.), *Seismic stratigraphy – Applications to hydrocarbon exploration. American Association of Petroleum Geologists Memoir* ***26***, 49-212.

Van Sickel, W.A., Kominz, M.A., Miller, K.G. and Browning, J.V., 2004. Late Cretaceous and Cenozoic sea-level estimates: backstripping analysis of borehole data, onshore New Jersey. *Basin Research* **16**, 451-465.

Vasconcelos, C., McKenzie, J.A., Warthmann, R., and Bernasconi, S.M., 2005. Calibration of the $\delta^{18}O$ paleothermometer for dolomite precipitated in microbial cultures and natural environments. *Geology* **33**, 317-320.

Vaughan, T.W., 1926. Species of *Lepidocyclina* and *Carpentaria* from the Cayman Islands, and their geological significance. *Quarterly Journal of the Geological Society of London* **82**, 388-400.

Vaziri-Moghaddam, H., Kimiagari, M. and Taheri, A., 2006. Depositional environment and sequence stratigraphy of the Oligo-Miocene Asmari Formation in SW Iran. *Facies* **52**, 41-51.

Vézina, J., Jones, B. and Ford, D., 1999. Sea-level highstands over the last 500,000 years: evidence from the Ironshore Formation on Grand Cayman, British West Indies. *Journal of Sedimentary Research* **69**, 317-327.

Vecsei, A., 2000. Database on isolated low-latitude carbonate banks. *Facies* **43**, 205-222.

Walters, L.J., Claypool, G.E. and Choquette, P.W., 1972. Reaction rates and $\delta^{18}O$ variation for the carbonate-phosphoric acid preparation method. *Geochimica et Cosmochimica Acta* **36**, 129-140.

Ward, W.C. and Halley, R.B., 1985. Dolomitization in a mixing-zone of near-normal seawater composition, late Pleistocene, northeastern Yucatan Peninsula. *Journal of Sedimentary Petrology* **55**, 407-420.

Wheeler, C., Aharon, P. and Ferrell, R.E., 1999. Successions of Late Cenozoic platform dolomites distinguished by texture, geochemistry, and crystal chemistry: Niue, South Pacific. *Journal of Sedimentary Research* **69**, 239 255.

Whitaker, F.F., Smart, P.L. and Jones, G.D., 2004. Dolomitization: from conceptual to numerical models, *in:* C.J.R. Braithwaite, G. Rizzi and G. Darke (Eds.), *The Geometry and Petrogenesis of Dolomite Hydrocarbon Reservoirs. The Geological Society of London, Special Publications* **235**, 99-139.

Wignall, B.W. 1995. Sedimentology and diagenesis of the Cayman (Miocene) and Pedro Castle (Pliocene) Formations at Safe Haven, Grand Cayman, British West Indies. Unpublished M.Sc. Thesis, University of Alberta, Edmonton, 110 pp.

Willson, E.A., 1998. Depositional and diagenetic features of the Middle Miocene Cayman Formation, Roger's Wreck Point, Grand Cayman, British West Indies. Unpublished M.Sc. Thesis, University of Alberta, Edmonton, 104 pp.

Woodroffe, C.D., Stoddart, D.R., Harmon, R.S. and Spencer, T., 1983. Coastal Morphology and Late Quaternary History, Cayman Islands, West Indies. *Quaternary Research* **19**, 64-84.

Zachos, J.C., Stott, L.D., and Lohmann, K.C., 1994. Evolution of early Cenozoic marine temperatures. *Paleoceanography* **9**, 353-387.

Zachos, J.C., Quinn, T.M. and Salamy, K.A., 1996. High-resolution (10^4 years) deep-sea foraminiferal stable isotope records of the Eocene-Oligocene climate transition. *Paleoceanography* **11**, 251-266.

APPENDIX 1: SAMPLE DATA

1. All data are from the Brac Formation on Cayman Brac.
2. Sections WOJ-2 and WOJ-7 are the combined equivalent of section SCD.
3. Heights of measured sections are measured in metres above sea level.
4. Drilling depths are measured in feet, where depth is below the present-day surface.
5. All dolomite oxygen and carbon isotopes are expressed as PDB normalized to NBS-18. Raw oxygen data is not corrected for any fractionation factor with phosphoric acid.
6. The percent calcium [%Ca = (molar Ca/(Ca + Mg) x 100)] in dolomite was determined by powder X-ray diffraction analysis using the peak-fitting technique (PF-XRD) of Jones *et al.* (2001). Values are reported as weighted averages of low-Ca calcium dolomite (LCD < 55 mol % $CaCO_3$) and high-Ca calcium dolomite (HCD > 55 mol % $CaCO_3$) in each sampled interval.

Appendix 1 Data

Well/ Section	Depth (ft)	Depth (m)	% Cal.	% Dol.	%Ca in Dol.	Calcite (‰ PDB)		Dolomite (‰ PDB)		$^{87}Sr/^{86}Sr$
						$\delta^{13}C$	$\delta^{18}O$	$\delta^{13}C$	$\delta^{18}O$	
APL#1	28.75	8.76	81.5	18.5	60.05	-3.64	-3.32	-2.86	-0.72	
APL#1	31.25	9.53	72.1	27.9	55.11	-4.82	-5.10	1.98	1.20	
APL#1	33.75	10.29	0.0	100.0	54.78	-	-	2.70	1.41	0.709155 +/- 0.000025
APL#1	36.25	11.05	100.0	0.0	-	-2.50	-2.75	-0.74	-0.67	
APL#1	38.75	11.81	49.7	50.3	56.01	-3.39	-4.20	2.35	1.69	
APL#1	41.25	12.57	61.2	38.8	57.12	-4.63	-4.36	1.11	0.90	
APL#1	43.75	13.34	45.5	54.6	56.93	-2.05	-3.79	2.70	1.87	
APL#1	46.25	14.10	29.8	70.2	56.58	-1.36	-0.66	2.71	2.27	
APL#1	48.75	14.86	90.9	9.1	59.51	-6.60	-4.84	-3.20	-0.72	
APL#1	51.25	15.62	0.0	100.0	52.17	-	-	3.02	1.62	0.709145 +/- 0.000019
APL#1	53.75	16.38	76.4	23.6	59.17	-5.81	-3.37	-1.66	0.12	
APL#1	56.25	17.15	81.6	18.4	57.46	-6.42	-4.44	-0.37	0.50	
APL#1	58.75	17.91	89.6	10.4	56.91	-1.50	-1.34	0.62	2.87	
APL#1	61.25	18.67	41.9	58.1	55.94	-5.03	-3.88	2.50	2.02	
APL#1	63.75	19.43	30.0	70.0	56.08	-6.48	-4.32	2.57	2.55	
APL#1	66.25	20.19	6.7	93.3	57.05	-1.96	-0.51	2.65	2.59	
APL#1	68.75	20.96	12.2	87.8	56.98	-3.81	-1.86	2.32	2.28	
APL#1	71.25	21.72	0.0	100.0	57.07	-	-	2.63	1.33	0.708873 +/- 0.000021
APL#1	73.75	22.48	41.9	58.1	57.49	-5.94	-3.69	1.27	1.88	
APL#1	76.25	23.24	59.0	41.0	56.49	-6.49	-4.68	2.04	2.06	
APL#1	78.75	24.00	43.9	56.1	57.00	-5.94	-4.24	2.96	2.38	
APL#1	81.25	24.77	11.4	88.6	56.63	-2.26	-0.62	1.82	1.78	
APL#1	83.75	25.53	23.2	76.8	57.49	-3.06	-1.46	2.02	2.52	
APL#1	86.25	26.29	36.8	63.2	56.49	-4.35	-1.94	1.62	2.76	
APL#1	88.75	27.05	79.6	20.4	57.31	-2.11	-1.00	1.04	2.27	
APL#1	91.25	27.81	62.1	37.9	57.30	-6.05	-3.74	1.74	2.43	
APL#1	93.75	28.58	71.4	28.6	56.92	-2.69	-1.53	2.37	2.49	
APL#1	96.25	29.34	70.7	29.3	57.36	-0.72	-0.63	1.79	0.43	0.709124 +/- 0.000020
APL#1	98.75	30.10	86.4	13.6	57.84	-3.02	-2.67	0.24	1.16	
APL#1	101.25	30.86	89.1	10.9	60.65	-3.96	-3.13	-2.57	-0.39	
APL#1	103.75	31.62	62.0	38.0	56.83	-4.45	-3.31	1.76	2.11	
APL#1	106.25	32.39	62.0	38.0	56.79	-0.41	-0.40	2.36	2.82	
APL#1	108.75	33.15	74.0	26.0	55.59	-4.82	-3.44	0.69	1.51	
APL#1	112.50	34.29	90.0	10.0	56.38	-1.33	-1.59	3.80	4.73	
APL#1	116.25	35.43	100.0	0.0	-	-1.62	-1.99	-	-	0.708037 +/- 0.000015
APL#1	118.75	36.20	51.3	48.7	57.30	-0.70	-1.16	2.36	2.81	
APL#1	121.25	36.96	56.8	43.2	56.85	-0.69	-0.61	0.95	2.60	
APL#1	123.75	37.72	60.8	39.2	56.92	-1.75	-1.31	0.65	2.76	
APL#1	126.25	38.48	36.8	63.2	57.00	-2.47	-1.64	0.26	2.42	
APL#1	128.75	39.24	87.9	12.1	56.84	-3.63	-2.50	0.20	1.68	
APL#1	131.25	40.01	100.0	0.0	-	-1.48	-1.33	-	-	

Well/ Section	Depth (ft)	Depth (m)	% Cal.	% Dol.	%Ca in Dol.	Calcite (‰ PDB)		Dolomite (‰ PDB)		$^{87}Sr/^{86}Sr$
						$\delta^{13}C$	$\delta^{18}O$	$\delta^{13}C$	$\delta^{18}O$	
APL#1	133.75	40.77	87.6	12.4	57.42	-1.98	-1.60	0.45	2.21	
APL#1	136.25	41.53	80.4	19.6	57.74	-1.03	-1.16	1.43	1.43	
APL#1	138.75	42.29	84.1	15.9	56.58	-0.54	-0.75	1.72	2.22	
APL#1	141.25	43.05	77.2	22.8	56.64	-0.58	-0.73	0.81	2.77	0.708218 +/- 0.000018
APL#1	143.75	43.82	93.7	6.3	57.73	-0.98	-0.97	-0.46	-1.43	
APL#1	146.25	44.58	100.0	0.0	-	-1.12	-1.05	-	-	
APL#1	148.75	45.34	92.5	7.5	57.38	-1.64	-1.32	0.07	-0.21	
APL#1	151.25	46.10	73.6	26.4	58.07	-0.97	-2.62	-0.38	-0.29	
APL#1	153.75	46.86	54.8	45.2	57.84	-4.67	-2.46	-0.57	1.71	
APL#1	156.25	47.63	82.9	17.1	57.26	-2.03	-1.13	-1.27	-0.80	
APL#1	158.75	48.39	72.6	27.4	57.12	-4.89	-2.92	0.08	-0.48	
APL#1	161.25	49.15	81.2	18.8	58.36	-1.32	-1.14	-0.53	-1.37	
APL#1	163.75	49.91	51.5	48.5	56.25	-2.97	-1.90	1.40	0.05	0.709113 +/- 0.000014
APL#1	166.25	50.67	80.9	19.1	57.45	-0.99	-1.15	1.41	-0.83	
APL#1	168.75	51.44	92.6	7.4	57.77	-1.33	-2.28	-2.09	-2.32	
APL#1	171.25	52.20	68.9	31.1	58.13	-6.49	-3.68	-1.19	0.50	
APL#1	173.75	52.96	75.8	24.2	57.22	-2.90	-1.59	-4.53	-0.50	
APL#1	176.25	53.72	92.3	7.7	55.57	-0.28	-0.81	1.05	-0.17	
APL#1	178.75	54.48	69.5	30.5	56.09	-0.39	-0.69	2.07	1.46	
APL#1	181.25	55.25	88.4	11.6	56.19	0.10	-0.50	0.95	3.43	
APL#1	183.75	56.01	95.6	4.4	56.91	-0.18	-0.50	1.90	2.82	
APL#1	186.25	56.77	66.2	33.9	57.47	-0.91	-1.28	0.87	0.94	
APL#1	188.75	57.53	93.5	6.5	56.89	-0.34	-1.06	0.87	0.39	
APL#1	191.25	58.29	60.0	40.0	56.41	-0.10	-0.98	1.52	-0.59	0.708476 +/- 0.000015
APL#1	193.75	59.06	94.3	5.7	57.88	-2.36	-2.20	-1.13	-0.05	
APL#1	196.25	59.82	95.3	4.7	57.06	-0.48	-0.83	2.03	2.11	
APL#1	198.75	60.58	79.6	20.4	57.56	-1.62	-1.50	0.68	1.16	
EOR#1	72.5	22.10	72.1	27.9	58.65	-2.80	-2.69	1.48	1.30	
EOR#1	74.0	22.56	66.9	33.1	58.67	-1.86	-1.84	1.29	1.31	
EOR#1	76.5	23.32	70.9	29.1	58.52	-2.39	-4.22	-2.62	-4.64	
EOR#1	79.5	24.23	94.7	5.3	58.47	-3.80	-3.27	-2.76	-3.34	0.709144 +/- 0.000025
EOR#1	82.5	25.15	86.9	13.1	58.69	-2.01	-1.73	-0.23	0.13	
EOR#1	85.5	26.06	89.1	10.9	58.74	-0.66	-1.13	0.15	0.61	
EOR#1	88.5	26.97	82.0	18.0	58.95	-2.53	-1.85	0.67	1.36	
EOR#1	91.5	27.89	76.1	23.9	58.83	-2.33	-2.03	0.28	0.42	
EOR#1	94.5	28.80	63.0	37.0	58.39	-2.30	-1.44	1.98	2.06	
EOR#1	96.5	29.41	74.0	26.0	57.61	-2.70	-1.90	1.40	1.70	
EOR#1	98.5	30.02	91.8	8.2	59.11	-3.80	-3.82	-1.25	-2.61	0.709136 +/- 0.000015
EOR#1	101.5	30.94	60.5	39.5	58.71	-3.17	-1.90	1.32	1.59	
EOR#1	104.5	31.85	73.5	26.5	58.64	-1.31	-0.87	0.61	0.52	
EOR#1	107.5	32.77	67.3	32.7	58.25	-2.45	-1.97	0.19	0.18	

Well/ Section	Depth (ft)	Depth (m)	% Cal.	% Dol.	%Ca in Dol.	Calcite (‰ PDB)		Dolomite (‰ PDB)		$^{87}Sr/^{86}Sr$
						$\delta^{13}C$	$\delta^{18}O$	$\delta^{13}C$	$\delta^{18}O$	
EOR#1	110.5	33.68	60.5	39.5	59.04	-2.05	-1.89	1.18	1.36	
EOR#1	113.5	34.59	73.9	26.1	58.57	-0.61	-0.38	1.77	1.69	
EOR#1	116.5	35.51	71.2	28.8	58.48	-1.44	-1.21	1.59	1.67	
EOR#1	119.5	36.42	72.7	27.3	58.87	-2.75	-2.54	0.12	0.13	0.709112 +/- 0.000019
EOR#1	121.3	36.97	63.0	37.0	58.56	-1.02	-1.09	1.65	1.57	
EOR#1	122.8	37.43	74.4	25.6	58.18	-1.61	-1.63	1.41	1.63	
EOR#1	125.5	38.25	73.9	26.1	58.51	-1.67	-1.22	1.57	1.87	
EOR#1	128.5	39.17	73.5	26.5	58.09	-2.08	-1.37	1.53	1.72	
EOR#1	131.5	40.08	81.2	18.8	58.77	-0.86	-0.96	0.17	0.18	
EOR#1	134.5	41.00	82.3	17.7	58.85	-2.03	-2.98	0.48	0.07	
EOR#1	137.5	41.91	100.0	0.0	-	-2.72	-3.49	-	-	0.709120 +/- 0.000023
EOR#1	140.0	42.67	96.6	3.4	58.17	-3.33	-4.48	-1.85	-2.61	
KEL#1	123.75	37.72	10.9	89.1	56.94	0.70	1.09	2.60	2.24	0.70889 +/- 0.000013
KEL#1	126.25	38.48	81.3	18.7	56.29	-1.82	-1.06	0.69	1.78	
KEL#1	128.75	39.24	59.9	40.1	56.84	-1.79	-1.05	1.29	2.27	
KEL#1	131.25	40.01	83.2	16.8	56.73	-1.55	-0.86	0.98	1.95	
KEL#1	133.75	40.77	84.4	15.6	57.2	-0.51	-0.87	2.43	1.70	0.70824 +/- 0.000011
KEL#1	136.25	41.53	81.2	18.8	56.8	-1.09	-0.51	1.24	1.92	
KEL#1	138.75	42.29	42.9	57.1	56.87	-0.84	-1.30	2.71	2.27	
KEL#1	141.25	43.05	36.1	63.9	57.04	-0.38	-0.74	2.74	2.07	
KEL#1	143.75	43.82	13.9	86.1	56.56	0.28	-0.01	2.18	1.97	0.70879 +/- 0.000017
KEL#1	146.25	44.58	36.5	63.5	56.69	0.57	0.50	2.68	1.99	
KEL#1	148.75	45.34	10.0	90.0	56.71	-1.18	-0.82	2.18	1.54	0.708704 +/- 0.000016
KEL#1	151.25	46.10	62.1	37.9	57.15	-1.03	-1.65	2.25	1.89	
KEL#1	153.75	46.86	55.5	44.5	57.7	-0.51	-0.50	2.08	1.52	
KEL#1	156.25	47.63	94.2	5.8	57.13	-1.85	-1.93	0.73	0.65	0.708033 +/- 0.000010
KEL#1	158.75	48.39	84.3	15.7	57.42	-1.57	-1.46	2.02	1.30	
KEL#1	161.25	49.15	100.0	0.0	-	-1.03	-1.17	-	-	0.708052 +/- 0.000008
KEL#1	163.75	49.91	77.7	22.3	56.99	-1.51	-1.57	0.86	0.64	
KEL#1	166.25	50.67	29.3	70.7	56.81	-0.23	-0.71	2.46	2.11	
KEL#1	168.75	51.44	52.1	47.9	56.54	-0.99	-0.76	1.91	2.35	
KEL#1	171.25	52.20	89.6	10.4	57.01	-1.27	-1.22	1.87	1.53	0.708136 +/- 0.000080
KEL#1	173.75	52.96	54.6	45.4	57.43	-1.61	-1.58	1.71	1.46	
CRQ#1	163.75	49.91	0	100	55.55	-	-	2.50	2.50	
CRQ#1	166.25	50.67	0	100	55.44	-	-	2.10	2.62	0.708857 +/- 0.000014
CRQ#1	168.75	51.44	42.1	57.9	54.98	-3.38	-1.56	2.30	2.55	
CRQ#1	171.25	52.20	15.6	84.4	56.34	-3.45	-1.44	1.73	2.48	
CRQ#1	173.75	52.96	13.0	87.0	56.97	-1.23	0.07	2.15	2.53	

Well/ Section	Depth (ft)	Depth (m)	% Cal.	% Dol.	%Ca in Dol.	Calcite (‰ PDB)		Dolomite (‰ PDB)		$^{87}Sr/^{86}Sr$
						$\delta^{13}C$	$\delta^{18}O$	$\delta^{13}C$	$\delta^{18}O$	
CRQ#1	176.25	53.72	8.1	91.9	55.77	-1.94	-0.55	2.18	2.74	0.708992 +/- 0.000014
CRQ#1	178.75	54.48	7.4	92.6	56.22	-1.03	0.70	2.11	2.74	
CRQ#1	181.25	55.25	32.4	67.6	56.76	-2.10	-1.18	1.95	2.49	
CRQ#1	183.75	56.01	48.3	51.7	57.52	-2.35	-1.79	1.88	2.50	
CRQ#1	186.25	56.77	27.1	72.9	57.00	-1.91	-1.07	1.56	2.22	
CRQ#1	188.75	57.53	28.3	71.7	56.92	-2.30	-1.64	1.93	2.45	0.708605 +/- 0.000016
CRQ#1	191.25	58.29	76.7	23.3	56.92	-4.43	-2.95	1.53	2.19	
CRQ#1	193.75	59.06	25.4	75.6	56.44	-3.79	-2.53	2.38	2.51	
CRQ#1	196.25	59.82	39.6	60.4	56.99	-1.60	-1.30	2.37	2.23	
CRQ#1	198.75	60.58	16.0	84.0	56.53	-0.26	0.01	2.26	2.26	0.708781 +/- 0.000015
WOJ-2	-	7.6	0.0	100.0	56.33	-	-	2.95	1.76	
WOJ-2	-	8.5	0.0	100.0	55.64	-	-	3.13	1.85	
WOJ-2	-	10.1	0.0	100.0	56.43	-	-	2.78	1.96	
WOJ-2	-	11.6	5.7	94.3	57.19	1.16	0.91	3.13	1.85	
WOJ-2	-	13.1	0.0	100.0	56.82	-	-	2.85	1.88	
WOJ-2	-	14.6	0.0	100.0	56.49	-	-	2.21	1.68	
WOJ-2	-	15.8	0.0	100.0	56.70	-	-	2.12	1.69	
WOJ-2	-	16.1	100.0	0.0	-	-6.03	-3.28	-	-	
WOJ-2	-	17.7	47.7	52.3	57.36	-8.42	-4.97	1.48	0.58	
WOJ-2	-	19.2	0.0	100.0	56.77	-	-	2.09	1.43	
WOJ-2	-	19.2	0.0	100.0	56.91	-	-	1.40	0.75	
WOJ-2	-	20.7	5.1	94.9	56.68	0.95	1.24	2.04	1.66	
WOJ-2	-	22.2	5.6	94.4	57.07	0.34	0.76	2.25	1.95	
WOJ-2	-	23.7	59.5	40.5	56.62	-4.77	-3.03	0.17	0.81	
WOJ-2	-	23.7	6.2	93.8	57.12	0.12	0.82	1.46	1.66	
WOJ-2	-	25.0	40.1	59.9	57.08	-5.07	-3.10	0.96	1.44	
WOJ-2	-	25.2	100.0	0.0	-	-2.89	-2.49	-	-	
WOJ-2	-	25.4	100.0	0.0	-	-3.98	-3.14	-	-	
WOJ-2	-	26.1	100.0	0.0	-	-2.33	-2.34	-	-	
WOJ-2	-	26.7	100.0	0.0	-	-2.69	-2.51	-	-	
WOJ-2	-	26.7	100.0	0.0	-	-10.68	-6.11	-	-	
WOJ-2	-	27.0	0.0	100.0	55.50	-	-	2.74	1.89	
WOJ-2	-	27.1	0.0	100.0	56.98	-	-	2.46	1.56	
WOJ-2	-	27.6	0.0	100.0	56.65	-	-	3.09	1.68	
WOJ-2	-	28.6	0.0	100.0	56.00	-	-	3.15	1.67	
WOJ-2	-	30.2	0.0	100.0	55.33	-	-	2.76	1.77	
WOJ-7	-	0.0	0.0	100.0	56.62	-	-	2.29	1.94	
WOJ-7	-	0.9	0.0	100.0	56.43	-	-	2.47	2.08	
WOJ-7	-	3.4	0.0	100.0	56.26	-	-	2.79	2.03	
WOJ-7	-	4.3	0.0	100.0	56.61	-	-	2.92	1.90	
WOJ-7	-	5.2	0.0	100.0	56.36	-	-	3.07	2.00	

Well/ Section	Depth (ft)	Depth (m)	% Cal.	% Dol.	%Ca in Dol.	Calcite (‰ PDB)		Dolomite (‰ PDB)		$^{87}Sr/^{86}Sr$
						$\delta^{13}C$	$\delta^{18}O$	$\delta^{13}C$	$\delta^{18}O$	
WOJ-7	-	6.1	0.0	100.0	56.79	-	-	2.70	1.88	
WOJ-7	-	7.0	0.0	100.0	56.97	-	-	2.28	1.88	
WOJ-7	-	7.9	0.0	100.0	56.38	-	-	2.53	1.82	
WOJ-7	-	8.8	0.0	100.0	56.58	-	-	2.90	1.62	
WOJ-7	-	9.8	0.0	100.0	56.73	-	-	1.89	1.85	
WOJ-7	-	10.7	0.0	100.0	56.19	-	-	2.77	1.75	